**Article:**
MacDonald, Jed, Logemann, Kai, Krainski, Elias et al. (5 more authors) (2017) Can collective memories shape fish distributions? A test, linking space-time occurrence models and population demographics. Ecography. pp. 1-59. ISSN 1600-0587

https://doi.org/10.1111/ecog.03098

ECOGRAPHY

# Can collective memories shape fish distributions? A test, linking space-time occurrence models and population demographics



| | |
|---|---|
| Journal: | *Ecography* |
| Manuscript ID | ECOG-03098.R2 |
| Wiley - Manuscript type: | Research |
| Date Submitted by the Author: | 14-Jun-2017 |
| Complete List of Authors: | Macdonald, Jed; Haskoli Islands, Faculty of Life and Environmental Sciences; Hafrannsoknastofnun; The University of Melbourne, School of BioSciences<br>Logemann, Kai; Haskoli Islands, Faculty of Life and Environmental Sciences; Helmholtz Zentrum Geesthacht, Institute of Coastal Research<br>Krainski, Elias; The Norwegian University for Science and Technology, Department of Mathematical Sciences; Universidade Federal do Parana, Departamento de Estatística<br>Sigurðsson, Þorsteinn; Hafrannsoknastofnun<br>Beale, Colin; University of York, Department of Biology<br>Huse, Geir; Havforskningsinstituttet<br>Hjøllo, Solfrid; Havforskningsinstituttet<br>Marteinsdóttir, Guðrún ; Haskoli Islands, Faculty of Life and Environmental Sciences |
| Keywords: | collective behaviour, environmental effects, fishery management, INLA, schooling fishes, spatial memory, temperature, traditions |





| | |
|---|---|
| Abstract: | Social learning can be fundamental to cohesive group living, and schooling fishes have proven ideal test subjects for recent work in this field. For many species, both demographic factors, and inter- (and intra-) generational information exchange are considered vital ingredients in how movement decisions are reached. Yet key information is often missing on the spatial outcomes of such decisions, and questions concerning how migratory traditions are influenced by collective memory, density-dependent and density-independent processes remain open. To explore these issues, we focused on Atlantic herring (Clupea harengus), a long-lived, dense-schooling species of high commercial importance, noted for its unpredictable shifts in winter distribution, and developed a series of Bayesian space-time occurrence models to investigate wintering dynamics over 23 years, using point-referenced fishery and survey records from Icelandic waters. We included covariates reflecting local-scale environmental factors, temporally-lagged prey biomass and recent fishing activity, and through an index capturing distributional persistence over time, derived two proxies for spatial memory of past wintering sites. The previous winter's occurrence pattern was a strong predictor of the present pattern, its influence increasing with adult population size. Although the |

| | |
|---|---|
| | mechanistic underpinnings of this result remain uncertain, we suggest that a 'wisdom of the crowd' dynamic may be at play, by which navigational accuracy towards traditional wintering sites improves in larger and/or denser, better synchronized schools. Wintering herring also preferred warmer, fresher, moderately stratified waters of lower velocity, close to hotspots of summer zooplankton biomass, our results indicative of heightened environmental sensitivity in younger cohorts. Incorporating spatiotemporal correlation structure and time-varying regression coefficients improved model performance, and validation tests on independent observations one-year ahead illustrate the potential of uniting demographic information and non-stationary models to quantify both the strength of collective memory in animal groups and its relevance for the spatial management of populations. |
| | |

# Can collective memories shape fish distributions? A test, linking space-time occurrence models and population demographics

Jed. I. Macdonald[1,2,3], Kai Logemann[1,4], Elias T. Krainski[5,6], Þorsteinn Sigurðsson[2], Colin M. Beale[7], Geir Huse[8], Solfrid S. Hjøllo[8], Guðrún Marteinsdóttir[1]

[1]Faculty of Life and Environmental Sciences, University of Iceland, Askja, Sturlugötu 7, 101 Reykjavík, Iceland

[2]Marine Research Institute, Skulagötu 4, 121 Reykjavík, Iceland

[3]School of BioSciences, The University of Melbourne, Parkville, Victoria 3010, Australia

[4]Institute of Coastal Research, Helmholtz Zentrum Geesthacht, Geesthacht, Germany

[5]Department of Mathematical Sciences, The Norwegian University for Science and Technology, Trondheim, Norway

[6]Departamento de Estatística, Universidade Federal do Paraná, Curitiba, Brazil

[7]University of York, Department of Biology, Heslington, York YO10 5DD, UK

[8]Institute of Marine Research and Hjort Centre for Marine Ecosystem Dynamics, P.O. Box 1870 Nordnes, NO-5817 Bergen, Norway

**Corresponding author:** Jed I. Macdonald, Faculty of Life and Environmental Sciences, University of Iceland, Askja, Sturlugötu 7, 101 Reykjavík, Iceland. E-mail: jedimacdonald@gmail.com

**Abstract**

Social learning can be fundamental to cohesive group living, and schooling fishes have proven ideal test subjects for recent work in this field. For many species, both demographic factors, and inter- (and intra-) generational information exchange are considered vital ingredients in how movement decisions are reached. Yet key information is often missing on the spatial outcomes of such decisions, and questions concerning how migratory traditions are influenced by collective memory, density-dependent and density-independent processes remain open. To explore these issues, we focused on Atlantic herring (*Clupea harengus*), a long-lived, dense-schooling species of high commercial importance, noted for its unpredictable shifts in winter distribution, and developed a series of Bayesian space-time occurrence models to investigate wintering dynamics over 23 years, using point-referenced fishery and survey records from Icelandic waters. We included covariates reflecting local-scale environmental factors, temporally-lagged prey biomass and recent fishing activity, and through an index capturing distributional persistence over time, derived two proxies for spatial memory of past wintering sites. The previous winter's occurrence pattern was a strong predictor of the present pattern, its influence increasing with adult population size. Although the mechanistic underpinnings of this result remain uncertain, we suggest that a 'wisdom of the crowd' dynamic may be at play, by which navigational accuracy towards traditional wintering sites improves in larger and/or denser, better synchronized schools. Wintering herring also preferred warmer, fresher, moderately stratified waters of lower velocity, close to hotspots of summer zooplankton biomass, our results indicative of heightened environmental sensitivity in younger cohorts. Incorporating spatiotemporal correlation structure and time-varying regression coefficients improved model performance, and validation tests on independent observations one-year ahead illustrate the potential of uniting demographic

information and non-stationary models to quantify both the strength of collective memory in animal groups and its relevance for the spatial management of populations.

**Key words:** collective behaviour, environmental effects, fishery management, INLA, schooling fishes, spatial memory, temperature, traditions

## Introduction

Although notions of the 'animal mind' remain equivocal (Dawkins 2001) there is now widespread acceptance that sociality, learning and memory can play important roles in determining migration patterns and space use in group-living animals (Kao et al. 2014, Merkle et al. 2014). In animal groups, decisions about when to migrate, where to feed, or how best to escape from predators are often made collectively, as a result of some consensus being reached among individuals' preferences (Conradt and Roper 2005). Such preferences are thought to arise through relatively simple interactions among close neighbours, with individuals trading-off aspects of their own experience and behavioural state with those of others (Berdahl et al. 2013).

Fishes have proved useful models on which to explore these ideas (Brown 2015 and references therein), and much empirical and theoretical research effort has been devoted to understanding the seemingly complex individual behaviours required to maintain school cohesion and coordinate large-scale migration (Parrish et al. 2002, Berdahl et al. 2016). Within fish schools, neighbouring individuals are usually not closely related, and hence self-interest may shape the nature of group-level movement decisions in which the majority opinion is often adopted (Couzin et al. 2011). In now rather famous experiments on groups of three-spined sticklebacks (*Gasterosteus aculeatus*), Ward et al. (2008) and Sumpter et al. (2008) showed that collective movement decisions can follow non-linear quorum rules, in

which the probability of an individual fish choosing a certain route increases abruptly beyond a threshold number of neighbours that have recently chosen that same route. Through simulations, and in later experimental work (Ward et al. 2011), these authors also demonstrated that quorum responses increase decision accuracy, and that larger fish shoals, in general, make better, faster decisions; *sensu* 'the wisdom of crowds' (Surowiecki 2004). These patterns appear to emerge across a wide range of taxa and ecological functions (Sumpter and Pratt 2009, but see Kao and Couzin 2014), and for fish, can manifest in improved navigation and capacity to sense dynamic environmental gradients, among other benefits (Berdahl et al. 2013, 2016).

Quorum responses may also be initiated, and consensus achieved, through leadership by a minority of more 'experienced' individuals, or those with strongly held preferences (Reebs 2000, Huse et al. 2002). Often, only a knowledgeable few are needed to produce highly accurate movement decisions (Reebs 2000); however, a complete absence of such leaders may result in poor navigational accuracy or lack of directionality (Helfman and Schultz 1984). These observations, in conjunction with growing recognition of the cognitive abilities of group-living fishes (Hotta et al. 2015), give credence to theories purporting the existence of spatial learning and tradition formation in some species (see Brown 2015 for a review), in which information on previously-used migration routes is thought to be passed down from older, experienced fish to younger, naïve ones, communicated within cohorts and remembered (Corten 1993). Further support for such ideas derives from evidence for time-place learning in fishes (e.g. Brännäs 2014), and experimental demonstrations of highly accurate short- and long-term memory (Brown 2001, Hotta et al. 2015).

These phenomena may be particularly relevant for long-lived, schooling species like Atlantic herring (*Clupea harengus*, hereafter 'herring') (Wynne-Edwards 1962). Herring are widely distributed across the North Atlantic Ocean and support several important commercial

fisheries. The species is characterized by complex population dynamics (Iles and Sinclair 1982, Huse 2016) perhaps best described by a metapopulation model (McQuinn 1997), with individuals within local populations forming densely-packed, mixed-age schools for much of the year and undertaking large-scale migrations between spawning, feeding and overwintering areas for which strong fidelity is exhibited in most, but not all years (Fernö et al. 1998, Langård et al. 2014). Several hypotheses have been advanced to explain this fluctuating 'conservatism' in migratory strategies (Jakobsson 1969, Corten 2002), with a particular focus in recent times on the striking shifts in winter distribution observed occasionally (Óskarsson et al. 2009, Huse et al. 2010). Current thinking favours aspects of McQuinn's 'adopted migrant hypothesis' (McQuinn 1997) akin to Petitgas et al.'s 'entrainment hypothesis' (Petitgas et al. 2006). When tuned to wintering herring, these hypotheses contend that naïve, first-time winterers (i.e. age 3) learn about traditional wintering areas by schooling with older, experienced winterers (i.e. age 4 and older, hereafter age 4+), typically returning to these same areas subsequently (Höglund 1955). However, when the learning process is disrupted during a stock collapse, when age classes are segregated, or when strong recruitment leads to numerical domination by naïve fish, dramatic shifts in winter distribution may occur, suggesting a break in tradition when teachers are few (Corten 1999, 2002, Huse et al. 2002, 2010). Understanding *why* and *when* distribution shifts might occur is clearly interesting for ecologists, fishers and fisheries managers alike. However, spatially-resolved information on the outcomes of such shifts (i.e. resultant spatial distribution patterns) is currently lacking – a situation that hinders development of spatial management strategies that maximize economic and conservation benefits. Specifically, two longstanding questions remain: 1) can we predict *where* herring decide to spend the winter, and 2) does tradition and/or spatial memory drive these decisions, or are other factors at play?

We attempt to answer these questions here. First, we derive a spatial similarity index (SSI) to quantify the persistence or transience in spatial distribution between one year *t*, and the previous year *t*-1, and demonstrate its utility in describing the recent wintering patterns of Icelandic summer spawning (ISS) herring. In our example, the SSI operates at the scale of the entire wintering population, and we consider it a proxy for the level of geographic attachment to, or spatial memory for, areas occupied previously. Next, using the variables created through the SSI (and others), we develop a series of space-time regression models for wintering ISS herring spanning a 23-year time series of fishery and acoustic survey data. We are particularly interested in the role of spatial memory in shaping distribution patterns, and present a Bayesian mixed-modelling framework based on stochastic partial differential equations (SPDE) (Lindgren et al. 2011) to disentangle its influence from factors representing the dynamic and static environment, prey availability during the pre-wintering feeding period, the magnitude of recent fishing effort and density-dependence.

Our specific hypotheses are as follows. 1) We predict that spatial memory for previous wintering areas would be a key driver of occurrence patterns in the present winter, and that its relative influence across the time series may have a demographic basis. That is, spatial memory would be strongest in years where more experienced individuals are present in the wintering population, or when overall adult population size is large. 2) As our study region is near a range edge for herring, we also expect that environmental gradients (e.g. temperature, salinity) would be influential. 3) Moreover, when population size is small, or naïve fish outnumber experienced adults, we hypothesize that environmental and/or other density-independent processes (e.g. prey availability, fishing pressure) may become unmasked, contributing more to shaping occurrence patterns. In addressing these hypotheses, we explore evidence for temporal non-stationarity in model parameters, and test if these

dynamics can be harnessed to accurately predict winter occurrence patterns, both within the time series, and to held-out observations one-year ahead.

## Material and methods

*Fishery and acoustic survey data*

We use two point-referenced datasets comprising $T = 23$ years of fishery and acoustic survey records for our analysis. Logbook data from the autumn/winter purse seine fishery for ISS herring were collated over the period 1991_1992 to 2013_2014. The fishery is highly selective for adult herring (i.e. age 3+), with effort centred on the wintering grounds between October and January each year. We refer to this period as a fishing 'year'. At the outset of each fishing year, extensive searches for wintering schools are made by the fishing fleet of ~ 15 vessels, covering the full (known) distribution of the stock (see Supplementary material Appendix 1 for a discussion of sampling coverage). Our logbook dataset provides information on each fishing event, defined here as an individual purse seine net shot, including the date, location, and biomass of herring captured $c$ (tonnes) per shot. Due to the dependence of $c$ on factors such as fisher behaviour and vessel capabilities (Thorlindsson 1988), we simplified the biomass information to occurrence/non-occurrence records, and retained only confirmed occurrences (i.e. where $c > 0$ tonnes). Although several instances of zero catch were observed, we excluded these records as $c = 0$ is often a function of gear failure, and not the absence of herring *per-se* (authors' personal observation).

We augmented the logbook data with fishery-independent acoustic survey records from annual cruises conducted by the Marine Research Institute (MRI), Reykjavík, between 1991_1992 and 2013_2014. Surveys were targeted towards wintering herring and ran between October and January each year, spanning the full wintering phase and matching the timing of fishing activities. Survey tracks were not consistent across years; however, spatial

coverage was typically broad (see Supplementary material Appendix 1 for details). Herring biomass estimates $s$ (tonnes), as calculated from echosounder backscatter strength measurements, were aggregated at 2 km resolution, forming a single survey event, referenced by date and location.

Data on age-class structure per fishing/survey event were unavailable. Hence, our models focused on the entire adult component of the stock (i.e. age 3+) which form mixed-age schools on the wintering grounds. This also meant that we could not determine which age classes contributed to $s$, estimates of which were likely influenced by a substantial, and unknown proportion of juveniles (i.e. age 0 to 2) in some regions. For this reason, we extracted only zero biomass records from the survey data (i.e. $s = 0$) and consider these true absences. Detection for both fishery and survey datasets is essentially perfect, notwithstanding potential recording errors (see Supplementary material Appendix 1). Our dataset, comprising $n = 48{,}724$ occurrence/absence records, is visualized in Fig. 1. Wintering patterns showed marked stability spatially across several consecutive years throughout the 23-year time series, interspersed by occasional, dramatic distributional shifts (Fig. 1a–c). Occurrence records were characterized by strong spatial structuring within years (explored through correlograms), and dense clustering east, west and south of Iceland (Fig. 1d).

*Capturing shifting distributions: a spatial similarity index (SSI)*

To more formally quantify the spatial and temporal patterns of wintering we constructed the SSI, a metric that unlike those designed for standardized survey data (see Woillez et al. 2007) is most useful when fishing/survey locations are inconsistent in space and time, and/or when abundance data are not available (or uncertain), as was the case here. Calculation is based around two georeferenced variables that map 1) the area of occurrence, denoted $\text{distrib}_t$, and 2) the density of occurrences, denoted $\text{counts}_t$, in a given year $t$, with

comparisons made with maps of these variables generated for the previous year (i.e. $distrib_{t-1}$, $counts_{t-1}$). We refer readers to Fig. 2a–e and Supplementary material Appendix 2.1, 2.2 for calculation details, and Appendix 2.3 for R code).

*Modelling winter occurrence patterns*

*Covariates for estimation and prediction*

We took a hypothesis-driven approach to the inclusion of covariates that capture the strength of spatial memory for previous wintering areas (i.e. spatially-explicit representations of the SSI), features of the dynamic and static environment, the magnitude of recent fishing activity and prey availability during the previous summer (see Table 1 for details, and Supplementary material Appendix 3 for derivation). Covariates were either constructed, computed from the CODE ocean model (Logemann et al. 2013) or extracted from other databases (GEBCO, <www.gebco.net>) at varying spatial and temporal scales (Table 1). Given the importance of scale in drawing conclusions about ecological systems (Levin 1992), we balanced ecological knowledge with model resolution in an attempt to select scales for each covariate that best match the processes acting on individual herring schools at the time of capture or survey (Mackinson et al. 1999, see also Table 1 and Supplementary material Appendix 3). Rasters of each covariate were created at the desired scales (see Supplementary material Appendix 3, Fig. A1–A5 for examples), and data for each occurrence or absence record extracted for use in model fitting. To facilitate interpretation of regression coefficients, all continuous inputs were centred and scaled to have mean = 0, sd = 0.5 prior to analysis, with binary inputs centred to have mean = 0 (Gelman 2008). To avoid issues related to collinearity (Dormann et al. 2013), we visualized covariate associations through scatterplots and calculated pairwise correlation coefficients (Pearson's $r$). If $|r| > 0.7$, we prioritized ecological reasoning in deciding which covariate to retain. Only bottom_depth and

dist_to_shore were highly collinear ($r$ = -0.78). As bathymetric features may act directly to structure herring school distribution (Maravelias et al. 2000a), we chose to remove dist_to_shore from all further analyses. Prior to model fitting, all covariates were screened graphically for potentially influential values, and data tabulated to test for any separation issues (Zorn 2005). The distributions of fish_magnitude and counts$_{t-1}$ were characterized by many zeros and some high values. Each of these values was checked and found to be measured accurately, and as no clear outliers were detected, all records were retained for modelling.

*Model specification*

As residual correlation patterns were of direct interest, we considered models that incorporate these patterns explicitly. Let $c_{e,i,t}$ be the total catch (tonnes), and $s_{e,i,t}$ the estimated biomass (tonnes) of an individual fishing/survey event respectively, $e$, at location $i$, in year $t$. We define a new variable, $y_{e,i,t}$ representing observed herring occurrence for each event, location and year (Eq. 1).

$$y_{e,i,t} = \begin{cases} 1, & \text{if } c_{e,i,t} > 0 \text{ tonnes} \\ 0, & \text{if } s_{e,i,t} = 0 \end{cases} \qquad (1)$$

As detection probability equals one, $y_{e,i,t}$ also represents the true occurrence state for each observation. Our interest was in estimating the probability of herring occurrence $\psi$, for event $e$, at location $i$, in year $t$, so we treated each event as an independent trial and modelled $\psi_{e,i,t}$ with a binomial generalized linear mixed model (GLMM) and logit link (Eq. 2, 3).

$$y_{e,i,t} \sim \text{Bernoulli}(\psi_{e,i,t}) \qquad \text{for } e = 1, \ldots, n_t;\ i = 1, \ldots, n_t;\ t = 2, \ldots, T \qquad (2)$$

$$\text{logit}(\psi_{e,i,t}) = \alpha + \text{spatial memory} + \text{dynamic environment} + \text{static environment}$$

$$+ \text{predators} + \text{prey} + \beta_{12}\text{year}_t + \omega_{i,t} \qquad (3)$$

$$\text{spatial memory} = \beta_1\text{distrib}_{i,t\text{-}1} + \beta_2\text{counts}_{i,t\text{-}1}$$

$$\text{dynamic environment} = \beta_3\text{SST}_{e,i,t} + \beta_4\text{SSS}_{e,i,t} + \beta_5\text{PEA}_{e,i,t} + \beta_6\text{change}_{e,i,t} + \beta_7\text{current\_vel}_{e,i,t}$$

$$\text{static environment} = \beta_8\text{bottom\_depth}_i + \beta_9\text{slope}_i$$

$$\text{predators} = \beta_{10}\text{fish\_magnitude}_{e,i,t}$$

$$\text{prey} = \beta_{11}\text{CF\_Aug}_{i,t}$$

Eq. 3 represents the full *stationary* model, where all regression coefficients are static in space and time, $\alpha$ is the intercept and the $\beta$'s quantify the linear effects of covariates reflecting spatial memory, the dynamic and static environment, predators and prey on $\psi$ (see Table 1). For models with no spatiotemporal random field (i.e. 'no-space' and 'time-indep' forms of $\omega_{i,t}$ – see *Spatiotemporal random effects* for details) we included a fixed factor for year. This categorical term captures the overall temporal pattern, common to all locations, and allows for year-to-year fluctuation in occurrence probabilities without assuming a predictable trend among time points.

To explore potential non-linearity in covariate effects, we fitted models that 1) assume linear trends for all covariates, 2) include quadratic terms for all environmental covariates, and 3) treat each environmental covariate as a smooth term, represented by a penalized regression spline with two knots (Crainiceanu et al. 2005, see Supplementary material Appendix 4 for R code). These specifications form a gradient of increasing flexibility in occurrence-covariate relationships, whilst maintaining ecologically realistic functional forms. To control against overfitting, yet maximize biological inference on our hypotheses, we offset this flexibility by specifying additive terms only, and not considering first- or higher-order interactions in our models.

*Spatiotemporal random effects*

In Eq. 3, $\omega_{i,t}$ is the spatiotemporal random effect, which accounts for residual spatial (and temporal) patterns not explained by the covariates. This term is spatially explicit and estimated for each location *i*. Three forms of $\omega_{i,t}$ were tested: 1) where $\omega_{i,t} = 0$ (i.e. the 'no-space' case); 2) where $\omega_{i,t}$ is a temporally independent realization of the spatial field for each year (i.e. the 'time-indep' case); and 3) where $\omega_{i,t}$ follows a 1st order autoregressive (ar1) process allowing correlation between years (i.e. the 'time-corr' case) (Eq. 4),

$$\omega_{i,t} = a\,\omega_{i,t-1} + \xi_{i,t} \qquad \xi_{i,t} \overset{iid}{\sim} N(0, \Sigma) \qquad \text{for } t = 2, \ldots, T \qquad (4)$$

where the *a* coefficient denotes the temporal dependence in $\omega_{i,t}$, with $|a| < 1$. When $a = 0$, $\xi_{i,t}$ is the sole representation of the spatial field for year *t* (i.e. the 'time-indep' case – see Ono et al. (2016) for a similar approach). If $a \neq 0$, the spatiotemporal field in *t* depends on the intensity and pattern of the field in *t*-1 (i.e. the 'time-corr' case – see Ward et al. (2015) for an example). In this latter instance, the realization of the spatial process for $t = 1$, $\omega_{i,1}$, is derived from the stationary distribution $N(0, \Sigma/(1-a^2))$ (see Cameletti et al. 2013 for details).

In both time_indep and time_corr cases, $\xi_{i,t}$ is a zero mean Gaussian random field assumed to be independent in time and defined by a Matérn covariance function (Eq. 5).

$$\mathrm{Cov}\left[\xi_{i,t}, \xi_{i',t'}\right] = \begin{cases} 0, & \text{if } t \neq t' \\ \Sigma_{i,i'}, & \text{if } t = t' \end{cases} \qquad (5)$$

where $i \neq i'$ and,

$$\Sigma_{i,i'} = \frac{\sigma_\omega^2}{\Gamma(v)2^{v-1}}(\kappa\|i\text{-}i'\|)^v K_v(\kappa\|i\text{-}i'\|) \qquad (6)$$

This is a representation of a Gaussian Markov random field (GMRF). In Eq. 6, $\Sigma_{i,i'}$ is the covariance between locations $i$ and $i'$. $\Gamma$ is the gamma function and $v$ is a smoothing parameter equal to $\alpha - d/2$, where $\alpha$ governs the smoothness of the random field, and $d$ is the number of dimensions in the model. We set $\alpha = 2$ and $d = 2$, hence $v = 1$. $\kappa$ is a scaling parameter associated with the practical range $\rho = \frac{\sqrt{8}}{\kappa}$, which represents the distance at which spatial correlation reduces to ~ 0.13, and $K_v$ is the modified Bessel function of the second order. With these parameter values set, the marginal variance of the GMRF, $\sigma_\omega^2$ is given by:-

$$\sigma_\omega^2 = \frac{1}{4\pi\kappa^2\tau^2} \qquad (7)$$

where $\tau$ in Eq. 7 is the local variance parameter.

*General approach*

First, we considered a suite of *stationary* models that assume that the response of the herring population to each covariate is static across the time series (see Eq. 3). We began with full models including all covariates, specified as linear, quadratic or spline terms, a fixed year effect and all forms of the spatiotemporal random component $\omega_{i,t}$ (i.e. models s1–s15, Table 2). This approach allowed us to evaluate different random-effect structures, whilst gaining an initial picture of the nature and magnitude of covariate effects (Zuur et al. 2009). After accounting for the overall spatial and temporal trends, the $\text{distrib}_{t\text{-}1}$ covariate was found to be strongly influential, exhibiting positive associations with $\psi$ in all cases (see Fig. 3, Supplementary material Appendix 7, Table A1). As abrupt shifts in herring winter

distribution occurred periodically, interrupting phases of spatial continuity (Fig. 1, 2), we considered that the relative importance of $distrib_{t-1}$ may also vary in time and be a key indicator of the degree of temporal correlation in winter occurrence patterns. We explored this possibility by fitting a series of *partly non-stationary* models (i.e. models part_ns1–part_ns9, Table 2), allowing regression coefficients for $distrib_{t-1}$ to be represented by a time-ordered vector with elements that vary by year according to 1st order random walk (rw1) dynamics. The rw1 models were defined by a Gaussian distribution N(0, *prec***R**), where *prec* is the precision parameter assigned a Gamma(1, 5e-05) prior, and **R** is a fixed structure matrix (see Supplementary material Appendix 5 for details on alternative model and prior specifications considered). Finally, we fitted a series of *fully non-stationary* models in which coefficients for all fixed effects could vary annually with the same rw1 specification (i.e. models full_ns1–full_ns9, Table 2). These *non-stationary* models enabled us to explore associations between covariate influence and changes in population demographics in the ISS herring stock over time, whilst naturally handling temporal dependence among adjacent years (see Supplementary material Appendix 4 for R code).

*Model fitting details*

Models were fitted in R-INLA (Rue et al. 2009) using the SPDE approach (Lindgren et al. 2011). We grouped models by stationarity level for ease of explanation, and summarize key details in Table 2 and Supplementary material Appendix 7, Table A2. Prior to fitting, we created a triangulated mesh upon which to build the GMRFs, covering a spatial domain that encompassed all of our observations (see Krainski et al. 2016 for details, and Supplementary material Appendix 4 for R code). We initially used a Gaussian approximation strategy to enable fast model comparison. We then refitted all models using simplified Laplace approximation – providing a compromise between correcting the Gaussian approximation for

errors in location and/or skewness (Rue et al. 2009) whilst retaining good computational properties. Vague normal priors were assigned to all fixed effects N(0, 1000), and the intercept N(0, ∞). To assess sensitivity to prior choice, we refitted all *stationary* 'no-space' models using weakly informative Cauchy priors with mean = 0 and scale = 2.5 for the fixed effects, and 10 for the intercept using the 'bayesglm' function in the 'arm' package in R (Gelman et al. 2008). Both prior specifications produced stable, highly congruent posterior estimates, so we proceeded using normal priors only. Priors for the SPDE model hyper-parameters ($a$, $\kappa$, $\tau$), the latter two defining $\rho$ and $\sigma^2_\omega$, are provided in Supplementary material Appendix 5.

*Assessing fit and predictive performance*

We calculated the deviance information criterion (DIC) (Spiegelhalter et al. 2002) and a series of metrics based on the conditional predictive ordinate (CPO) (Pettit 1990) to check model fit and assess predictive performance. For each model, we used the $CPO_{e,i,t}$ given by $\pi(y_{e,i,t}|y_{-(e,i,t)})$, which represents the cross-validated (cv) 'leave-one-out' predictive density at observation $y_{e,i,t}$ with the $y_{e,i,t}$th observation removed, to derive the mean logarithmic (log) score (Gneiting and Rafferty 2007), a measure of predictive quality, and the cv Brier score (i.e. mean prediction error), a measure of model goodness-of-fit reflecting both discriminatory ability and calibration that evaluates the degree of correspondence between fitted probabilities and observed binary outcomes (Schmid and Griffith 2005, Roos and Held 2011). Lower values on both scores reflect a better model, with Brier scores interpreted in relation to reference values that are a function of sampling prevalence (see Held et al. 2012 for an example). As an additional calibration check for out-of-sample predictions, we examined histograms of probability integral transform (PIT) values for departures from uniformity (Dawid 1984, Gneiting et al. 2007, Held et al. 2010). Despite its known

deficiencies (Lobo et al. 2008), given perfect detection in our data, the similarity in both geographic and environmental space in model fitting and prediction domains, and the explicit consideration of spatiotemporal error structure in our modelling approach, we also calculated the AUC for each model.

*Covariate importance and model selection*

After comparing full models using the aforementioned criteria and determining an optimal structure for $\omega_{i,t}$, we used the best-performing full *stationary* model (including the fixed year effect and $\omega_{i,t}$) to estimate covariate importance and find an appropriate fixed-effect structure. We first examined parameter estimates and 95% credible intervals (CIs) for each covariate. Next, we dropped one covariate at a time from the full model (i.e. single-term deletion) and compared the DIC, mean log score and Brier score of the reduced models with the full model, and a baseline model comprising only an intercept, $\text{year}_t$ and the optimal structure for $\omega_{i,t}$ (see Illian et al. 2013 for a similar approach).

*Correlation among covariates and demographic parameters*

To examine associations between covariate importance and population demographics, we calculated Pearson's *r* coefficients between time series of posterior means for the linear term for influential covariates (i.e. those with 95% CIs not overlapping 0 in at least one year) in the best *non-stationary* models, and nine demographic parameters for the ISS stock derived from annual stock assessments coordinated by The International Council for the Exploration of the Sea (ICES). Calculations were made on the first 18, 19, 20, 21, and 22 years of data. Demographic parameters considered include three ratios of the numbers (millions) of naïve, first-time winterers to older, experienced individuals (i.e. age3:age4to7, age3:age8to13, age3:age4+), spawning stock biomass (SSB – '000 tonnes), spawning stock numbers (SSN –

millions), numbers (millions) of young experienced individuals (*n* age4to7), old experienced individuals (*n* age8to13), and all experienced individuals (*n* age4+), and mean age (years) of the spawning stock (mean age).

*Spatial prediction and validation*

An area of interest for spatial prediction was defined within the extent of the fishery and survey data, covering the entire distributional range of ISS herring. The area, spanning 62.475 to 67.975°N and 9.008 to 28.008°W, was divided into 0.1° longitude × 0.05° latitude (~5 × 5 km) grid cells, matching the resolution of several covariates used in model building and providing a scale useful for fishery management (see Supplementary material Appendix 3, 6). Our interest was in predicting herring occurrence probability on an annual time-step. Hence, maps were created for each covariate based on mean grid cell values calculated across each year. The range of covariate values in the prediction space was monitored, and closely matched the values used for model fitting (Table 1).

The different classes of models we built have different utility regarding prediction. The *stationary* models are very general, making them well suited for predictions to randomly selected data within the time series or for long-term forecasts. By contrast, the *fully non-stationary* models, with their annually-varying coefficients, are less flexible, but useful in mapping occurrence probabilities for specific years within the time series. The task of short-term forecasting (e.g. to $t$+1) befits the *partly non-stationary* models, which occupy a middle ground in terms of generality. For these reasons, we used the best performing *fully non-stationary* model to generate annual prediction maps within the time series. Predictions were made for the last 22 years (i.e. 1992_93 to 2013_14), but we present results for four years (i.e. 1994_95, 2001_02, 2007_08, 2013_14) representative of the different wintering phases. Implementation is straightforward in R-INLA (see Supplementary material Appendix 4 for R

code). For predictions to $t$+1 we used the best *partly non-stationary* specification. We ran validation tests on held-out observations by building models for the first 18, 19, 20 and 21 years of data, and testing how well the predicted probabilities of occurrence match the observations in the 19th, 20th, 21st, and 22nd years, respectively. For this, we needed to estimate the $distrib_{t-1}$ regression coefficient for $t$+1. We reasoned that if strong correlations exist between the $distrib_{t-1}$ regression coefficients and one or more demographic parameters, and we can estimate these demographic parameter(s) for $t$+1, then prediction of the $distrib_{t-1}$ regression coefficient in $t$+1 may be possible. We summarize the main findings in the Results section, but provide full annotated R code (see Supplementary material Appendix 4) and explanatory notes in Appendix 6. All analyses were run in R version 3.2.2 (R Development Core Team), and datasets and code are available from the Dryad Digital Repository <http://datadryad.org/>.

## Results

*Spatial similarity across years*

The SSI accurately reproduced the temporal dynamics of wintering patterns across our time series. The spatial persistence of the distribution during the 'East' phase (Fig. 1a) was reflected in relatively high SSI values, with the northward shift witnessed between 1994_95 and 1997_98 forcing a gradual reduction in the index (Fig. 2). SSI values were lower over the following decade. This is a result of a patchier distribution during these years (Fig. 1b), although year-to-year consistency was sometimes observed (e.g. between 2001_02 and 2002_03). From 2007_08 until 2012_13, the majority of the adult population wintered inshore, in fjords on Iceland's west coast (Fig. 1c). Strong fidelity to these fjords was observed during this period, resulting in high SSI values. The SSI dropped in 2013_14, as

younger cohorts established a new wintering area off the southeast coast (Óskarsson and Reynisson 2014).

*Model performance*

Our models generally fitted the data well and showed low mean prediction error, with cross-validated Brier scores falling below the prevalence-based reference value of 0.138 for all models incorporating spatiotemporal random structure (Table 2). Discriminatory ability was high, with AUC values > 0.9 in all cases, and Gaussian and simplified Laplace approximation strategies were in full agreement regarding the best-performing models (Table 2, Supplementary material Appendix 7, Table A2). The inclusion of spatial and temporal structure was beneficial, and results from the *stationary* models suggest that independent realizations of the spatial random field (i.e. time-indep $\omega_{i,t}$) and a fixed year effect (i.e. year$_t$) more appropriately describe the data than a smooth year-to-year transition in either of these processes (i.e. time-corr $\omega_{i,t}$) (Table 2). Allowing fixed effect parameters to vary in time through the *non-stationary* models improved goodness-of-fit and predictive capacity over the *stationary* cases, and there was stronger support for models allowing some non-linearity in occurrence-covariate relationships (i.e. quadratic terms for environmental covariates) (Table 2).

*Covariate importance and model selection*

The addition of covariates improved model performance. Although posterior 95% CIs overlapped 0 in some cases (Supplementary material Appendix 7, Table A1), backwards selection on the best *stationary* model (s9) indicated that most covariates added some information and none detrimentally affected predictive capacity (Supplementary material

Appendix 7, Table A3). Hence, all covariates were retained, and full models used for further inference.

*Nature of occurrence-covariate relationships*

Positive associations were found between distrib$_{t\text{-}1}$ and $\psi$ in all models - this pattern persisting when spatially and temporally structured terms were included (Fig. 3, Supplementary material Appendix 7, Table A1). This result supports the existence of a strong connection with previously-used wintering sites in most years. The best *partly non-stationary* model (part_ns5) outperformed s9 (Table 2), suggesting that the predictive ability of the distrib$_{t\text{-}1}$ covariate may vary in time. Posterior mean estimates for distrib$_{t\text{-}1}$ in the part_ns5 model were always positive however, and 95% CIs never overlapped 0 (Fig. 3f). This model also assumes that the response of the wintering population to all other covariates is static in time. We visualized the nature of these associations by plotting the marginal effect for covariates with posterior 95% CIs that did not overlap 0 (Fig. 3a–e, see Supplementary material Appendix 7, Fig. A7 for plots of all other covariates).

Several local-scale environmental variables were found to be important. Occurrence probability increased in warmer, fresher and moderately stratified waters (Fig. 3a–c), in lower velocity zones (Fig. 3d), and in areas near high zooplankton (i.e. adult *C. finmarchicus*) biomass in the August preceding wintering (Fig. 3e). Notably, dependence on the density of occurrence records from the previous year, as captured by counts$_{t\text{-}1}$, was low. Similarly, the vertical temperature gradient, bathymetric features, and the magnitude of recent fishing activity all had little impact (Fig. A7, see Supplementary material Appendix 7, Table A1).

These patterns were further investigated in the full_ns5 model – the best model overall – in which all fixed effects could vary by year. Again, distrib$_{t\text{-}1}$ was influential; however, the increased number of random effects in the full_ns5 model acted to dampen its

effect (Fig. 3g–i). The importance of SST, SSS and PEA shifted in time, with these covariates' influence increasing during the early to mid-2000s when the wintering population was patchily distributed around Iceland (Fig. 1, 3h). Estimates for fish_magnitude were generally small, with large variance (Fig. 3i). Covariates describing bathymetric features showed no strong trends over time, and CF_Aug exhibited a small positive association with $\psi$ in some years (Fig. 3i).

*Correlations among covariates and demographic parameters*

The importance of the distrib$_{t-1}$ covariate was found to increase most strongly with adult population size (SSN) in both the part_ns5 and full_ns5 models, with positive associations also observed with *n* age4to7, *n* age 4+ and SSB (Table 3). Focussing on the full_ns5 model, a stronger positive effect of SST was detected when the ratio of naïve : older, experienced individuals (age3:age8to13) increased (Table 3). The posterior mean estimates for SSS decreased as SSN and SSB increased, and coefficients for PEA were negatively associated with *n* age8to13. All other correlations were non-significant.

*Spatial prediction within the time series*

Spatial predictions of occurrence probabilities derived from the full_ns5 model showed high concordance with the observations (Fig. 4). The model accurately predicted the occurrence patterns in years when the wintering population was confined to small regions of the prediction space (e.g. 2007_08), when it was spread out (e.g. 1994_95), when it was patchily distributed (e.g. 2001_02), and during distributional shifts (e.g. 2007_08, 2013_14) (Fig. 4a). For the four representative years considered here, model predictions were well calibrated, with small mean squared differences between predicted probabilities and actual observations (Brier score: 1994_95 = 0.162, 2001_02 = 0.132, 2007_08 = 0.152, 2013_14 =

0.168, all below reference values), and showed near-perfect discrimination between observed occurrences and absences (AUC: 1994_95 = 0.998, 2001_02 = 0.994, 2007_08 = 0.999, 2013_14 = 0.999).

Data were scarce in some years (e.g. 1994_95, 2013_14), with large areas of the prediction space containing few observations. The SPDE approach handles this by evaluating the continuous spatial or spatiotemporal random effects as discretely indexed GMRFs, allowing predictions to be made to unsampled locations whilst robustly estimating the uncertainty of these predictions. The sd of $\psi$ was highest in areas where occurrence and absence records were close in geographic space (Fig. 4b), likely due to difficulties in resolving such a steep gradient of probabilities over such short spatial scales. Variance was low and uniform in unsampled regions.

Inclusion of spatiotemporal random effects ($\omega$) improved model fit and predictive performance (Table 2), indicating that the covariate components were not overfitted, but also that factors important in shaping $\psi$ have been missed, and/or were occurring at scales that our models could not resolve. The patterns in $\omega$ (Fig. 4c) reveal the presence of spatial dependence at relatively large scales (i.e. 100's of km), confirmed by the posterior estimates for the practical range $\rho$ (Table 3), and likely reflect rapid changes in school shape, size and structure that our models did not capture (Pitcher et al. 1996, Nøttestad and Axelson 1999, Makris et al. 2009). The trends observed in the random field sd's are a function of data coverage, with uncertainty increasing with distance from the observations (Fig. 4d).

*Predicting occurrence patterns in t+1*

We found strong positive correlations between time series of SSN and posterior mean estimates of the $distrib_{t-1}$ covariate in the *partly non-stationary* models (i.e. part_ns5 specification) fitted to the first 18, 19, 20 and 21 years of data (Pearson's *r* mean = 0.623, sd

= 0.127) (Fig. 5). Given this degree of correlation, we then were able to predict the posterior mean estimate for $distrib_{t-1}$ in $t$+1 from the estimate of SSN in $t$+1 (obtained from MRI surveys – Óskarsson and Reynisson 2014). This allowed us to validate our models on withheld observations one-year ahead, and assess prediction accuracy for the last four years of the time series (see Supplementary material Appendix 6 for details). Predictive performance was high in three out of the four years (19$^{th}$ year: Brier score = 0.142, AUC = 0.961; 20$^{th}$ year: Brier score = 0.137, AUC = 0.976; 21$^{st}$ year: Brier score = 0.128, AUC = 0.976), but dropped sharply in the last year (22$^{nd}$ year: Brier score = 0.194, AUC = 0.588) concurrent with a reduction in correlation strength between time series of SSN and $distrib_{t-1}$ coefficients (Fig. 5).

**Discussion**

Our study on ISS herring heeds recent calls for a greater focus on the role of collective learning in shaping animal distributions (Keith and Bull 2017), whilst demonstrating that social cues may not necessarily act alone. Consistent with our expectations, we found that the $distrib_{t-1}$ covariate, describing the previous winter's occurrence pattern, imparted strong influence on the present pattern, the magnitude of its effect increasing with adult population size. Moreover, we showed that local-scale environmental and temporally-lagged prey-related factors were sometimes important; our results suggesting a heightened sensitivity of younger age classes to some environmental effects (e.g. SST). Importantly, the accuracy of our predictions to $t$+1 highlights the potential of combining demographic time series with non-stationary models in exploring evidence for collective memory in fishes and other group-living animals, and in guiding spatial management decisions.

*The multiple drivers of spatial distribution*

A variety of intrinsic and extrinsic controls, often working synergistically, are known to structure marine fish distributions (Planque et al. 2011). For example, the use of visual stimuli to locate landmarks is well documented (Silveira et al. 2015), whilst geomagnetic and olfactory cues provide important compasses for migrating salmon (Putman et al. 2013). Furthermore, environmental gradients, predators, competitors and prey, population demographics and spatial memory can all be influential (Perry et al. 2005, Rindorf and Lewy 2006, Loots et al. 2010). Many of these factors appear relevant to herring, and work spanning many decades has demonstrated the importance of bottom-up (e.g. climate, local-scale environment, zooplankton biomass), top-down (e.g. predation) and demographic processes in structuring the species' population dynamics (e.g. Lindegren et al. 2011, see Huse 2016 for a review). Despite these efforts, the question of what governs where herring spend the winter, a non-feeding period during which schools are heavily targeted by commercial fisheries, has remained largely unresolved. We think that this may be a consequence of three factors. 1) High environmental flexibility in wintering populations (see Fig. 3a–d, Supplementary material Appendix 7, Fig. A6) – a trait potentially explaining the marked geographic plasticity in wintering locations observed previously (Óskarsson et al. 2009, Huse et al. 2010). 2) The lack of proximate feeding and spawning cues, or competitive forces acting during the winter months – making underlying mechanisms difficult to pinpoint, and 3) mismatches between the true scale of processes acting on wintering populations and the scales captured by previous studies.

In designing our study, we felt that progress could be made by viewing the realized winter distribution as the result of two behavioural states: (state 1) migrating to, and colonizing wintering areas; and (state 2) living within these areas following colonization; and that herring may be tuned to different stimuli in each. In state 1, decisions must be made on

the directionality of migration. Such decisions are thought to have a demographic origin; the probability of following previously-used routes increasing with the proportion of experienced individuals present in the stock, and contingent upon information-sharing opportunities among cohorts during some period preceding wintering. These ideas, supported now by both theory and empirical work (McQuinn 1997, Corten 2002, Huse et al. 2010) have advanced our capacity for predicting when populations are likely to follow suit, returning to traditional grounds, or break tradition and disperse to new areas.

*Capturing spatial memory*

Through construction of the SSI and in our models, we extend these ideas in a spatially-explicit manner by linking observations from the previous year's distribution to the present year's, and considering demographic parameters as potential mechanisms influencing spatial persistence from year-to-year. In effect, our approach simultaneously tests for geographic attachment to certain wintering areas (*sensu* Loots et al. 2010) – a well-known herring trait (Höglund 1955), while inclusion of the demographic components allows for an exploration, albeit correlative, of evidence for spatial memory and/or tradition-formation in the species. The strong effect of $distrib_{t-1}$ on $\psi$ in both the *stationary* (Supplementary material Appendix 7, Table A1) and *non-stationary* models (Fig. 3f–i), combined with the correlation observed between time series of the $distrib_{t-1}$ coefficients and SSN (Table 3) suggests that although the proportion of naïve : experienced individuals appears fundamental to how decisions on directionality of winter migration are reached (state 1 – Huse et al. (2010)), population size may determine if these decisions are honoured. The mechanisms underpinning these observations remain unclear, but may relate to some form of wisdom through numbers (Surowiecki 2004), or the 'many wrongs principle' (Simons 2004) by which navigational accuracy increases in larger and/or denser schools through pooling many

individual directional estimates. Makris et al. (2009) found direct evidence for this in herring. These authors demonstrated that a threshold density of individuals (i.e. 0.2 fish $m^{-2}$) promoted extremely rapid school-formation and growth at dusk, initiated by joining of small leading groups, and resulting in coordinated spawning migrations towards Georges Bank in the Gulf of Maine. If such processes also operate during the winter migration period, our results suggest that recolonizing previously-used wintering areas is sometimes deemed a good decision by the majority, or at least by some threshold number of influential leaders, and that adherence to these decisions may be stronger when the population is large.

*Influence of prey resources and summer feeding distribution*

Whilst important, the $distrib_{t-1}$ covariate did not explain all the variation in our observations. We had also speculated that where herring feed during summer might influence winter migration trajectories (Fernö et al. 1998), and used August biomass estimates for the zooplankter *C. finmarchicus* to test this hypothesis. Wintering areas were often geographically quite close to summer prey patches (Table 3, Fig. 3e) – a situation that could advantage herring approaching wintering grounds, as energy conserved through minimizing dispersal away from profitable feeding areas would be highly valued during the subsequent non-feeding period. Georeferenced data on the summer feeding distribution in addition to empirical measures of *C. finmarchicus* biomass would permit a deeper examination of this idea; first, by providing a validation (in Icelandic waters) of the *C finmarchicus* IBM used to derive our biomass layers (Hjøllo et al. 2012); and second, by allowing the degree of herring-zooplankton prey overlap to be estimated. Such information would provide useful insights into the importance of pre-wintering actions in general, and where they occur, on subsequent wintering behaviour. We argue that this may be especially relevant to the summer feeding

period when several age classes mix (Libungan et al. 2015), offering a perfect arena for decision-making on the nature of the upcoming winter migration.

*Wintering and density-dependence*

Following settlement in wintering areas (i.e. state 2), herring hardly feed (Slotte 1999), and minimizing metabolic costs is likely prioritized. The absence of competition for food at this time removes a key mechanism thought to promote positive relationships between population abundance and occupied area, now demonstrated for several fish species (e.g. Fisher and Frank 2004) and predicted under most models of marine fish spatial dynamics (e.g. the 'basin model' – MacCall (1990)) through 'ideal free distribution' theory (Fretwell and Lucas 1969). Such positive associations are commonly taken as evidence for density-dependent habitat selection (DDHS), although they may also arise via density-independent means (Shepherd and Litvak 2004).

We found no support for any abundance-area association in our data (see Supplementary material Appendix 8, Fig. A8), and no evidence for an effect of $counts_{t\text{-}1}$, a conservative surrogate for local herring density in $t$-1, on the occurrence pattern in $t$ (Table 3, Fig. 3g, Supplementary material Appendix 7, Fig. A7a). In light of these results, we propose that DDHS is probably not a strong guiding force driving large-scale wintering patterns. Indeed, as the dense schooling behaviour typical of this phase may impart some fitness benefits in terms of predator evasion (Nøttestad and Axelsen 1999), the lack of an abundance-area association, as we found here, might reflect a distribution that is near ideal and free. This idea requires further testing, as density-dependent mechanisms are known to influence feeding and spawning migrations in the species (see Ciannelli et al. 2013), and to structure schooling dynamics at micro- (i.e. cm to m) and meso-scales (i.e. 10's of m to 10's of km) (Pitcher et al. 1996, Mackinson et al. 1999).

*Environmental effects*

Given the nature of our dataset (i.e. 48,724 observations over 23 winters), we suggest that our models provide a broad, yet robust picture of environmental preferences of wintering ISS herring over the time period considered. We found that several local-scale dynamic variables influenced estimates of $\psi$ (Fig. 3, Supplementary material Appendix 7, Tale A1). Whilst we cannot pinpoint the mechanistic basis of these relationships, we contend that this environmental sensitivity can be framed as a balance between maximizing individual fitness and fidelity to traditional wintering sites. Temperature (i.e. SST), the most influential environmental factor in our models, is a pervasive force shaping marine fish distributions (Perry et al. 2005), and although adult herring can tolerate a wide array of temperatures (Nøttestad et al. 2007), studies at the range margins suggest that physiological barriers may exist (e.g. < ~ 2°C) which are rarely crossed (Jakobsson 1969, Misund et al. 1997). We observed this here. Wintering ISS herring were never encountered in SST < 1.5°C, and were rarely captured north of 67°N, a region under the influence of cold East Icelandic Current water (Logemann et al. 2013) (Fig. 1, 3a, Supplementary material Appendix 7, Fig. A6a). This is indicative of a lower bound of thermal tolerance below which individual fitness may be compromised. If this is the case, then persistence of SST's far colder than 1.5°C off much of Iceland's north coast during winter, in conjunction with winter SST's in the study region approaching 10°C (see Supplementary material Appendix 3, Fig. A2), may neatly explain the monotonic positive trend detected between SST and $\psi$ (Fig. 3a). Even though residence in warmer waters likely involves higher energetic demands, given the species' flexibility in temperature preferences within the ~ 4 to 9°C range as seen here (Fig. 3a, Supplementary material Appendix 7, Fig. A6a), and its capacity to tolerate far higher temperatures elsewhere

(Maravelias and Reid 1997) we suggest that our upper temperature bound would not be physiologically constraining.

These findings, in conjunction with pronounced drops in both median SSS and PEA values observed in wintering areas in the latter part of the time series (Supplementary material Appendix 7, Fig. A6b, c), add weight to Huse et al.'s suggestion that winter habitat selection in herring may not be precisely optimized (Huse et al. 2010). However, the consistency in SSS and PEA values seen across several consecutive years; the uniformly low current velocity characteristic of all wintering areas (Supplementary material Appendix 7, Fig. A6d) and the significant relationships detected between $\psi$ and SST, SSS, PEA and current_vel (Fig. 3) indicate a degree of environmental control in wintering site selection, at least in some years (see Supplementary material Appendix 7 for a further discussion).

*Temporal non-stationarity*

One of the most interesting results of this study came through considering that the response of herring populations to intrinsic and extrinsic factors may alter through time. We found evidence for temporal non-stationarity in some cases (i.e. $distrib_{t-1}$, SST, SSS, PEA) (Fig. 3h); in addition to the $distrib_{t-1}$ – SSN relationship, we showed that the relative influence of SST increased with the proportion of first-time winterers compared with older, age 8 to 13 individuals in the population (Table 3). This may reflect a heightened sensitivity of younger cohorts to environmental forcing, in combination with an increased tendency to follow traditions as fish get older, as suggested by Corten (2002) (*explanation 1*). At the population level, such a scenario would manifest in environmental factors, such as temperature, becoming unmasked as strong drivers of wintering area selection when there are fewer older fish to provide guidance.

If we make the assumption that the population truly responds differently to some environmental variables in different years, then our results could also stem from flexibility in population-wide environmental preferences during winter, as suggested by Óskarsson et al. (2009) and Huse et al. (2010) (*explanation 2*), or from age- or size-related variation in habitat preferences (e.g. Bailey et al. 1998, Bartolino et al. 2011) that would act to shape the population's collective reaction dependent on age-class structure (see results for SSS and PEA – Table 3) (*explanation 3*).

A fourth alternative involves the presence of interactions between density-dependent and environmental factors (*explanation 4*) (see Ciannelli et al. 2012 for an example). No clear density-dependent environmental responses were observed in our study, a finding in agreement with Maravelias et al. (2000a, b), who reported marked stability in relationships between occurrence, abundance and ambient environmental conditions across a four-year period of population decline in North Sea herring. Our inference is limited to fishery records, but the addition of spatially-consistent survey information would allow a more rigorous exploration of how biomass and environmental factors might interact to influence range size during wintering. Finally, the trends we observed may in part reflect the nature of our datasets (*explanation 5*). Fishing and survey coverage varied across years; a function of fisher behaviour, catch efficiency, funding and/or time availability and possibly other unknown, annually-varying factors our models did not capture directly (see Supplementary material Appendix 1). The $\text{year}_t$ term in the *stationary* models accounts for year-to-year variation in the outcome of such processes, yet with regard to the *non-stationary* models, tests including or omitting this term, or a temporal component in $\omega_{i,t}$, left parameter estimates essentially unchanged, suggesting that the time-varying patterns we see are not strongly dependent on data availability in a given year, and likely have some other basis.

This list of explanations is not exhaustive; all are plausible, and not necessarily mutually exclusive. However, we propose *explanation 1* and/or *3* as most likely on empirical and theoretical grounds (Corten 1993, 2002). Opportunities for fine-tuning the dynamics of connections through time based on ecological or physiological knowledge are emerging through continued advancements in process-based models (see Teal et al. in press), and ongoing work on penalized complexity (PC) priors (Simpson et al. 2015). By combining such approaches, and using outputs from models like those presented here to guide parameterization, we see great potential for identifying the mechanistic fundaments of non-stationarity in ecological time series like ours (see also Supplementary material Appendix 9).

*Fishing and predation*

The direct impact of fishing on commercially harvested species, including herring, can be immense (Jackson et al. 2001, Dickey-Collas et al. 2010). It is increasingly recognized, however, that intense exploitation can reduce resilience to environmental change, and that fishing and climate can interact to influence long-term distribution patterns (Engelhard et al. 2011) and spatial structure (Ciannelli et al. 2013). In our models, we attempted to capture the impact of recent purse-seine fishing activity whilst considering local-scale environmental variables as additive factors only. This decision reflects an attempt to balance model complexity with meaningful ecological inference (Merow et al. 2014), and although this reduced our power to detect fishing-environment interactions directly, our expectation that increased fish_magnitude would act to reduce $\psi$ at nearby locations in the following week was not met (Supplementary material Appendix 7, Fig. A7e, Table A1). This was surprising, given the known disruptive effects of fishing and vessel activity on the behaviour of pelagic species like herring (Vabø et al. 2002). As herring schools can show incredibly fast predator-evasion responses (Pitcher et al. 1996), we proffer that the weekly

window we chose for fish_magnitude was too long, and the 5 × 5 km grid cell dimensions too large to capture the complexity in fleet dynamics (Branch et al. 2006), or the patchiness and speed of fishing-herring interactions and their cumulative effects over time. Investigating the scale-dependence of harvesting impacts, induced both by fishers and other predators (Similä 1997, Overholtz and Link 2007, Samarra and Foote 2015, Supplementary material Appendix 10) might provide insight into the trade-offs herring and other fishes face in adhering to migratory traditions, whilst avoiding predation in a previously risky arena.

*Spatial prediction: implications for fishery management and fisheries*

Our space-time models generated predictions that closely matched the observed occurrence patterns of wintering ISS herring. Whilst noting the limitations inherent in fishery and non-standardized survey datasets (Supplementary material Appendix 1, 9), by incorporating time-varying effects, and simultaneously considering spatially- and temporally-structured processes in our analysis, we were able to robustly estimate $\psi$ and its uncertainty across our spatial domain, both within the time series (see Fig. 4) and to held-out observations one-year ahead (Supplementary material Appendix 6, 9).

The capacity to predict distribution patterns in $t$+1 has important implications for the spatial management of herring stocks throughout the North Atlantic, and for other species exhibiting some homing tendency, for which our models could be easily adapted. In our example, predictive accuracy depended upon the strength of association between SSN and posterior mean estimates for $\text{distrib}_{t\text{-}1}$, estimated by the part_ns5 model (Table 3, Supplementary material Appendix 6). In three out of four years tested, correlation was strong, models were well calibrated and AUC values exceeded 0.95. Accuracy for the final year – 2013_14, fell dramatically however, due most likely to two unusual mass-mortality events in

a small fjord on Iceland's west coast that forced the 2012_13 stock assessment estimate of SSN down, despite marked overlap in the area fished in 2011_12 and 2012_13 (Fig. 2, 5).

Although preliminary in nature, these results do highlight the potential of temporally non-stationary models in predicting states at one time point based on states at nearby time points. With rapid improvements in uncertainty estimation in stock assessment models for data-poor fish stocks (e.g. Kokkalis et al. 2017) coupled with the abundance of information-rich, point-referenced fishery datasets available, the time is ripe for further investigation into the demographic influences on migratory behaviour in other less-studied, commercially-important species. We believe the modelling framework outlined here is a solid starting point for such work.

*Conclusions*

Despite growing recognition of social learning as a key element in shaping collective movement behaviour, the evolutionary consequences of, and the mechanisms giving rise to, this phenomenon remain unclear for many taxa. Using wintering ISS herring for illustration, we searched for pattern in these behaviours by building space-time models for multi-year, point-referenced fishery and survey datasets and linking model output with time series of demographic parameters. Though we cannot pry too deeply into the 'fish mind', at least at present, our findings lend correlative support to the existence of collective memory in this long-lived, schooling species (Fernö et al 1998, Corten 2002), and suggest that wintering site selection may be tuned to population size and age-class structure, in concert with local-scale environmental factors and temporally-lagged prey distribution. The accuracy of our model predictions implies that considering such processes explicitly in spatiotemporal models could benefit spatial management strategies for fishes and other group-living animals that display a degree of conservatism in migratory behaviour.

**Acknowledgements**

This work was supported by the Nordic Centre for Research on Marine Ecosystems and Resources Under Climate Change (NorMER), through the Norden Top-Level Research Initiative subprogram 'Effect Studies and Adaptation to Climate Change', and research grant 'Rannsóknarsjóðs síldarútvegsins 2013', awarded to J. Macdonald and G. Marteinsdóttir from the Icelandic Association of Herring Fisheries. We thank V. Gunnarsson for his efforts in administering this latter fund. We are indebted to the skippers and crews of the vessels from which our data came, and in particular, G. Jóhannsson and the crew aboard w/w Dröfn RE-35. Thanks to P. Reynisson for providing access to acoustic survey data and reports, and to H. Rue for hosting J. Macdonald at NTNU in Trondheim. We are grateful to D. Ramsey, M. Scroggie and R. Critchlow for suggestions on the statistical approach, I. and K. Macdonald for advice on figure layout and M. Mörsdorf, G. Heard, W. Butler, Z. Cságoly, D. Eme, and S. Campana for stimulating discussions on ecological theory that shaped the direction of this paper. Comments from the Subject Editor and two reviewers greatly improved a previous version.

**References**

Bailey, M. C. et al. 1998. Changes in the spatial distribution of autumn spawning herring (*Clupea harengus* L.) derived from annual acoustic surveys during the period 1984-1996. – ICES J. Mar. Sci. 55: 545–555.

Bartolino, V. et al. 2011. Ontogenetic and sex-specific differences in density-dependent habitat selection of a marine fish population. – Ecology 92: 189–200.

Berdahl, A. et al. 2013. Emergent sensing of complex environments by mobile animal groups. – Science 339: 574–576.

Berdahl, A. et al. 2016. A collective navigation hypothesis for homeward migration in anadromous salmonids. – Fish Fish. 17: 525–542.

Branch, T. A. et al. 2006. Fleet dynamics and fishermen behaviour: lessons for fisheries managers. – Can. J. Fish. Aquat. Sci. 63: 1647–1668.

Brännäs, E. 2014. Time-place learning and leader-follower relationships in Arctic charr *Salvelinus alpinus*. – J. Fish Biol. 84: 133–144.

Brown, C. 2001. Familiarity with the test environment improves escape responses in the crimson spotted rainbowfish, *Melanotaenia duboulayi*. – Anim. Cogn. 4: 109–113.

Brown, C. 2015. Fish intelligence, sentience and ethics. – Anim. Cogn. 18: 1–17.

Cameletti, M. et al. 2013. Spatio-temporal modeling of particulate matter concentration through the SPDE approach. – AStA Adv. Stat. Anal. 97: 109–131.

Ciannelli, L. et al. 2012. Non-additive and non-stationary properties in the spatial distribution of a large marine fish population. – Proc. R. Soc. B 279: 3635–3642.

Ciannelli, L. et al. 2013. Theory, consequences and evidence of eroding population spatial structure in harvested marine fishes: a review. – Mar. Ecol. Prog. Ser. 480: 227–243.

Conradt, L. and Roper, T. J. 2005. Consensus decision making in animals. – Trends Ecol. Evol. 20: 449–456.

Corten, A. 1993. Learning processes in herring migrations. ICES Document C.M. 1993/H:18 Pelagic Fish Committee, Copenhagen, Denmark.

Corten, A. 1999. A proposed mechanism for the Bohuslan herring periods. – ICES J. Mar. Sci. 56: 207–220.

Corten, A. 2002. The role of "conservatism" in herring migrations. – Rev. Fish Biol. Fisher. 11: 339–361.

Couzin, I. D. et al. 2011. Uninformed individuals promote democratic consensus in animal groups. – Science 334: 1578–1580.

Crainiceanu, C. M. et al. 2005. Bayesian analysis for penalized spline regression using WinBUGS. – J. Stat. Softw. 14: 1–24.

Dawid, A. 1984. Statistical theory: the prequential approach (with discussion). – J. R. Stat. Soc. A 147: 278–292.

Dawkins, M. 2001. Who needs conciousness? Anim. Welfare 10: 19–29.

Dickey-Collas, M. et al. 2010. Lessons learned from stock collapse and recovery of North Sea herring: a review. – ICES J. Mar. Sci. 67: 1875–1886.

Dormann, C. F. et al. 2013. Collinearity: a review of methods to deal with it and a simulation study evaluating their performance. – Ecography 36: 27–46.

Engelhard, G. H. et al. 2011. Nine decades of North Sea sole and plaice distribution. – ICES J. Mar. Sci. 68: 1090–1104.

Fernö, A. T. et al. 1998. The challenge of the herring in the Norwegian sea: making optimal collective spatial decisions. – Sarsia 83: 149–167.

Fisher, J. and Frank, K. 2004. Abundance-distribution relationships and conservation of exploited marine fishes. – Mar. Ecol. Prog. Ser. 279: 201–213.

Fretwell, S. D. and Lucas, H. L. J. 1969. On territorial behaviour and other factors influencing habitat distribution in birds. – Acta Biotheor. 19: 16–36.

Gelman, A. 2008. Scaling regression inputs by dividing by two standard deviations. Statist. Med. – 27: 2865–2873.

Gelman, A. et al. 2008. A weakly informative default prior distribution for logistic and other regression models. – Ann. Appl. Stat. 2: 1360–1383.

Gneiting, T. and Raftery, A. E. 2007. Strictly proper scoring rules, prediction, and estimation. – J. Am. Stat. Assoc. 102: 359–378.

Gneiting, T. et al. 2007. Probabilistic forecasts, calibration and sharpness. – J. R. Stat. Soc. B 69: 243–268.

Held, L. et al. 2010. Posterior and cross-validatory predictive checks: a comparison of MCMC and INLA. – In: Kneib, T. and Tutz, G. (eds), Statistical modelling and regression structures. Springer, pp. 91–110.

Held, U. et al. 2012. Validating and updating a risk model for pneumonia - a case study. – BMC Med. Res. Methodol. 12: 99.

Helfman, G. S. and Schultz, E. T. 1984. Social transmission of behavioural traditions in a coral reef fish. – Anim. Behav. 32: 379–384.

Hjøllo, S. S. et al. 2012. Modelling secondary production in the Norwegian Sea with a fully coupled physical/primary production/individual-based *Calanus finmarchicus* model system. – Mar. Biol. Res. 6: 508–526.

Höglund, H. 1955. Swedish herring tagging experiments, 1949-1953. – Rapports et procès-verbaux des réunions/Conseil permanent international pour l'exploration de la mer 40: 19–29.

Hotta, T. et al. 2015. The use of multiple sources of social information in contest behaviour: testing the social cognitive abilities of a cichlid fish. – Front. Ecol. Evol. 3: 1–9.

Huse, G. 2016. A spatial approach to understanding herring population dynamics. – Can. J. Fish. Aquat. Sci. 73: 177–188.

Huse, G. et al. 2010. Establishment of new wintering areas in herring co-occurs with peaks in the "first time/repeat spawner" ratio. – Mar. Ecol. Prog. Ser. 409: 189–198.

Huse, G. et al. 2002. Modelling changes in migration pattern of herring: collective behaviour and numerical domination. – J. Fish Biol. 60: 571–582.

Iles, T. D. and Sinclair, M. 1982. Atlantic herring: stock discreteness and abundance. – Science 215: 627–633.

Illian, J. B. et al. 2013. Fitting complex ecological point process models with integrated nested Laplace approximation. – Methods Ecol. Evol. 4: 305–315.

Jackson, J. B. C. et al. 2001. Historical overfishing and the recent collapse of coastal ecosystems. – Science 293: 629–638.

Jakobsson, J. 1969. Síld og sjávarhiti. – In: Einarsson, M. Á. (ed.), Hafásinn. Reykjavík, Iceland, pp. 497–511.

Kao, A. B. and Couzin, I. D. 2014. Decision accuracy in complex environments is often maximized by small group sizes. – Proc. R. Soc. B 81: 20133305.

Kao, A. B. et al. 2014. Collective learning and optimal consensus decisions in social animal groups. – PLoS Comput. Biol. 10:e1003762.

Keith, S. A. and Bull, J. W. 2017. Animal culture impacts species' capacity to realise climate-driven range shifts. – Ecography 40: 296–304.

Kokkalis, A. et al. 2017. Estimating uncertainty of data limited stock assessments. – ICES J. Mar. Sci. 74: 69–77.

Krainski, E. T. et al. 2016. The R-INLA tutorial on SPDE models. – Norwegian University of Science and Technology, Trondheim, Norway.

Langård, L. et al. 2014. State-dependent spatial and intra-school dynamics in pre-spawning herring *Clupea harengus* in a semi-enclosed ecosystem. Mar. Ecol. Prog. Ser. 501: 251–263.

Levin, S. 1992. The problem of pattern and scale in ecology. – Ecology 73: 1943–1967.

Libungan, L. A. et al. 2015. Otolith shape: a population marker for Atlantic herring *Clupea harengus*. – J. Fish Biol. 86: 1377–1395.

Lindegren, M. et al. 2011. Interacting trophic forcing and the population dynamics of herring. – Ecology 92: 1407–1413.

Lindgren, F. et al. 2011. An explicit link between Gaussian fields and Gaussian Markov random fields: the stochastic partial differential equation approach. – J. R. Stat. Soc. B 73: 423–498.

Lobo, J. M. et al. 2008. AUC: A misleading measure of the performance of predictive distribution models. – Global Ecol. Biogeogr. 17: 145–151.

Logemann, K. et al. 2013. The circulation of Icelandic waters – a modelling study. – Ocean Sci. 9: 931–955.

Loots, C. et al. 2010. What controls the spatial distribution of the North Sea plaice spawning population? Confronting ecological hypotheses through a model selection framework. – ICES J. Mar. Sci. 67: 244–257.

MacCall, A. D. 1990. Dynamic geography of marine fish populations. – University of Washington Press.

Mackinson, S. et al. 1999. Cross-scale observations on distribution and behavioural dynamics of ocean feeding Norwegian spring-spawning herring (*Clupea harengus* L.). – ICES J. Mar. Sci. 56: 613–626.

Makris, N. C. et al. 2009. Critical population density triggers rapid formation of vast oceanic fish shoals. – Science 323: 1734–1737.

Maravelias, C. D. and Reid, D. G. 1997. Identifying the effects of oceanographic features and zooplankton on prespawning herring abundance using generalized additive models. – Mar. Ecol. Prog. Ser. 147: 1–9.

Maravelias, C. D. et al. 2000a. Seabed substrate, water depth and zooplankton as determinants of the prespawning spatial aggregation of North Atlantic herring. – Mar. Ecol. Prog. Ser. 195: 249–259.

Maravelias, C. D. et al. 2000b. Modelling spatio-temporal effects of environment on Atlantic herring, *Clupea harengus*. – Environ. Biol. Fish. 58: 157–172.

McQuinn, I. 1997. Metapopulations and the Atlantic herring. – Rev. Fish Biol. Fisher. 7:297–329.

Merkle, J. A. et al. 2014. A memory-based foraging tactic reveals an adaptive mechanism for

restricted space use. – Ecol. Lett. 17: 924–931.

Merow, C. et al. 2014. What do we gain from simplicity versus complexity in species distribution models? – Ecography 37: 1267–1281.

Misund, O. et al. 1997. Migration behaviour of Norwegian spring spawning herring when entering the cold front in the Norwegian Sea. – Sarsia 82: 107–112.

Nøttestad, L. and Axelsen, B. E. 1999. Herring schooling manoeuvres in response to killer whale attacks. – Can. J. Fish. Aquat. Sci. 77: 1540–1546.

Nøttestad, L. et al. 2007. Herring at the Arctic front: influence of temperature and prey on their spatio-temporal distribution and migration. – Mar. Ecol. 28: 123–133.

Ono, K. et al. 2016. Space-time investigation of the effects of fishing on fish populations. – Ecol. Appl. 26: 392–406.

Óskarsson, G. J. and Reynisson, P. 2014. Results of acoustic measurements of Icelandic summer-spawning herring in the winter 2013/2014. – Working Document No. 20, ICES North Western Working Group, 24 April - 1 May 2014, Copenhagen, Denmark.

Óskarsson, G. J. et al. 2009. Variation in spatial distribution and migration of Icelandic summer-spawning herring. – ICES J. Mar. Sci. 66: 1762–1767.

Overholtz, W. J. and Link, J. S. 2007. Consumption impacts by marine mammals, fish, and seabirds on the Gulf of Maine – Georges Bank Atlantic herring (*Clupea harengus*) complex during the years 1977-2002. – ICES J. Mar. Sci. 64: 83–96.

Parrish, J. K. et al. 2002. Self-organized fish schools: an examination of emergent properties. – Biol. Bull. 202: 296–305.

Perry, A. et al. 2005. Climate change and distribution shifts in marine fishes. – Science 308: 1912–1915.

Petitgas, P. et al. 2006. The entrainment hypothesis: an explanation for the persistence and innovation in spawning migrations and life cycle spatial patterns. – ICES Document

C.M. 2006/B:07, Copenhagen, Denmark.

Pettit, L. 1990. The conditional predictive ordinate for the Normal distribution. – J. R. Stat. Soc. B 52: 175–184.

Pitcher, T. J. et al. 1996. Adaptive behaviour of herring schools in the Norwegian Sea as revealed by high-resolution sonar. – ICES J. Mar. Sci. 53: 449–452.

Planque, B. et al. 2011. Understanding what controls the spatial distribution of fish populations using a multi-model approach. – Fish. Oceanogr. 20: 1–17.

Putman, N. F. et al. 2013. Evidence for geomagnetic imprinting as a homing mechanism in pacific salmon. – Curr. Biol. 23: 312–316.

Reebs, S. 2000. Can a minority of informed leaders determine the foraging movements of a fish shoal? – Anim. Behav. 59: 403–409.

Rindorf, A. and Lewy, P. 2006. Warm, windy winters drive cod north and homing of spawners keeps them there. J. Appl. Ecol. 43:445–453.

Roos, M. and Held, L. 2011. Sensitivity analysis in Bayesian generalized linear mixed models for binary data. – Bayesian Anal. 6: 259–278.

Rue, H. et al. 2009. Approximate Bayesian inference for latent Gaussian models by using integrated nested Laplace approximations. – J. R. Stat. Soc. B 71: 319–392.

Samarra, F. I. P. and Foote, A. D. 2015. Seasonal movements of killer whales between Iceland and Scotland. – Aquat. Biol. 24: 75–79.

Schmid, C. H. and J. L. Griffith. 2005. Multivariate classification rules: calibration and discrimination. Pages 3491–3497 *in* P. Armitage, and T. Colton, editors. Encyclopedia of biostatistics, second edition. John Wiley & Sons, London, UK.

Shepherd, T. D. and Litvak, M. K. 2004. Density-dependent habitat selection and the ideal free distribution in marine fish spatial dynamics: considerations and cautions. – Fish Fish. 5: 141–152.

Silveira, M. M. et al. 2015. Dusky damselfish *Stegastes fuscus* relational learning: evidences from associative and spatial tasks. – J. Fish Biol. 86: 1109–1120.

Similä, T. 1997. Sonar observations of killer whales (*Orcinus orca*) feeding on herring schools. – Aquat. Mamm. 23: 119–126.

Simons, A. 2004. Many wrongs: the advantage of goup navigation. – Trends Ecol. Evol. 19: 453–455.

Simpson, D. P. et al. 2015. Penalising model component complexity: A principled, practical approach to constructing priors. – arXiv 1403.4630.

Slotte, A. 1999. Differential utilization of energy during wintering and spawning migration in Norwegian spring-spawning herring. – J. Fish. Biol. 54: 338–355.

Spiegelhalter, D. J. et al. 2002. Bayesian measures of model complexity and fit. – J. R. Stat. Soc. B 64: 583–639.

Sumpter, D. J. T. and Pratt, S. C. 2009. Quorum responses and consensus decision making. – Phil. Trans. R. Soc. B 364: 743–53.

Sumpter, D. J. T. et al. 2008. Consensus decision making by fish. – Curr. Biol. 18: 1773–1777.

Surowiecki, J. 2004. The wisdom of crowds. – Random House.

Teal, L. R. et al. in press. Physiology-based modelling approaches to characterize fish habitat suitability: their usefulness and limitations. – Estuar. Coast. Shelf Sci. doi: 10.1016/j.ecss.2015.11.014.

Thorlindsson, T. 1988. The skipper effect in the Icelandic herring fishery. – Hum. Organ. 47: 199–212.

Vabø, R. et al. 2002. The effect of vessel avoidance of wintering Norwegian spring spawning herring. – Fish. Res. 58: 59–77.

Ward, A. J. et al. 2011. Fast and accurate decisions through collective vigilance in fish

shoals. – Proc. Natl Acad. Sci. USA 108: 2312–2315.

Ward, E. J. et al. 2015. Using spatiotemporal species distribution models to identify temporally evolving hotspots of species co-occurrence. – Ecol. Appl. 25: 2198–2209.

Woillez, M. et al. 2007. Indices for capturing spatial patterns and their evolution in time, with application to European hake (*Merluccius merluccius*) in the Bay of Biscay. – ICES J. Mar. Sci. 64: 537–550.

Wynne-Edwards, V. C. 1962. Animal dispersion in relation to social behaviour. – Oliver & Boyd.

Zorn, C. 2005. A solution to separation in binary response models. – Polit. Anal. 13: 157–170.

Zuur, A. et al. 2009. Mixed effects models and extensions in ecology with R. – Springer.

Supplementary material (Appendix EXXXXX at <www.oikosoffice.lu.se/appendix>).

Appendix 1–10.

Table 1. Covariates considered in space-time regression models for wintering ISS herring (see Supplementary material Appendix 3 for details on their calculation, hypotheses behind their selection, the spatial and temporal scales considered, and examples of raster layers for each covariate used for spatial predictions). F and P represent the range of values used in model fitting and spatial prediction respectively. Scales for estimation vary by covariate; however spatial predictions are made to a common 0.1° longitude × 0.05° latitude (i.e. ~5 × 5 km) grid at an annual time-step. ↑, ↓ denote hypothesized directions of the occurrence-covariate relationships, and ↓↑ indicates that the direction of the occurrence-covariate relationship is uncertain. References relate either to the data source, the expected relationship with $\psi$, or papers contributing to the selection of this covariate for modelling (see Supplementary material Appendix 3 for the full reference list).

| Covariate | Abbreviation | Description | Units & derivation | Range (min, max) | Spatial scales for fitting | Temporal scales for fitting | Expected relationship with $\psi$ | Source | References |
|---|---|---|---|---|---|---|---|---|---|
| *Spatial memory* | | | | | | | | | |
| Occurrence in previous year | $distrib_{t-1}$ | Using the $distrib_t$ layers created for the spatial similarity index (SSI), we selected the layer for *t*-1 to capture the occurrence pattern one-year earlier. | 1 = occurrence in same cell in *t*-1<br><br>0 = absence in same cell in *t*-1 | F (0, 1)<br>P (0, 1) | 0.1° longitude × 0.05° latitude (i.e. ~5 × 5 km) | Annual | ↑, with stronger ↑ influence in years when more 'experienced' individuals are present and/or stock size is large. | Fishery logbooks | Jakobsson 1969, Corten 1993, 2000, 2002, McQuinn 1997, Fernö et al. 1998, Huse et al. 2002, 2010 |
| Density of occurrences in previous year | $counts_{t-1}$ | Similar to $distrib_{t-1}$, we used the $counts_t$ layers (created during SSI derivation) and selected the layer for *t*-1 to capture the density of occurrences one-year earlier. | % (see Eq. A1 in for derivation) | F (0, 43.67)<br>P (0, 45.19) | 0.1° × 0.05° | Annual | As above | As above | As above |
| *Dynamic environment* | | | | | | | | | Logemann et al. 2013 (for all dynamic variables) |
| Sea surface temperature | SST | Temperature at 1.25 m depth. | °C | F (-1.76, 9.68)<br>P (-1.36, 9.38) | 1 × 1<br>4 × 4<br>8 × 8 km | Day of record, mean of 7 days previous | ↑, but influence of SST and all other covariates may change with stock demographics. | CODE | Blaxter 1985, Maravelias 1997, Misund et al. 1997, 1998, Maravelias et al. 2000a, Toresen and Østvedt 2000, Corten 2001, Nøttestad et al. 2007, Bartolino et al. 2014 |
| Sea surface salinity | SSS | Salinity at 1.25 m depth. | practical salinity unit (psu) | F (31.51, 35.38)<br>P (33.00, 35.24) | 1 × 1<br>4 × 4<br>8 × 8 km | Day of record, mean of 7 d previous | ↓ | CODE | Blaxter 1985, Maravelias and Reid 1995, 1997, Lindegren et al. 2011 |
| Potential energy anomaly | PEA | Energy needed to instantaneously homogenize the water column with a given density stratification. Calculated here as a function of temperature and salinity. | $kg\ m^{-1}\ s^{-2}$<br>$\frac{1}{H}\int_{-h}^{\eta}(\bar{\rho}-\rho)gz\ dz$ | F (0, 55.19)<br>P (0, 54.99) | 1 × 1<br>4 × 4<br>8 × 8 km | Day of record, mean of 7 d previous | ↓↑ | CODE | Simpson 1981, Huse and Korneliussen 2000, Maravelias and Reid 1997, Maravelias et al. 2000b, Planque et al. 2006, de Boer et al. 2008, Burchard and Hofmeister 2008, Huret et al. 2013 |
| Difference between SST and bottom temperature | change | SST - temperature at 1.25 m above the sea floor. | °C | F (-8.16, 5.05)<br>P (-4.77, 4.16) | 1 × 1<br>4 × 4<br>8 × 8 km | Day of record, mean of 7 d previous | ↓ | CODE | Maravelias and Reid 1997, Maravelias et al. 2000b |
| Current velocity | current_vel | Mean of the absolute values of the U and V flow vectors at 1.25 m depth. | $m\ s^{-1}$ | F (0, 0.64)<br>P (3.25e-04, 2.20) | 1 × 1<br>4 × 4<br>8 × 8 km | Day of record, mean of 7 d previous | ↓ | CODE | Corten and van de Kamp 1992, Corten 1999a,b |
| *Static environment* | | | | | | | | | |
| Water depth | bottom_depth | Depth of the water column. | m | F (-2290, -11)<br>P (-2560, 0) | 30 arcsec | - | ↓↑ | GEBCO <www.gebco.net> | Maravelias et al. 2000a, Nøttestad et al. 2007, echosounder data (this study) |
| Bottom slope | slope | Slope of the sea floor. | ° | F (0, 25.37)<br>P (1.44e-02, 0.12) | 30 arcsec | - | ↓ | GEBCO | Maravelias et al. 2000a, echosounder data (this study) |
| Distance to shore | dist_to_shore | Distance from each occurrence/absence record to the nearest landmass. | km | F (0.01, 334.31)<br>P (0, 344.71) | Exact | - | ↓↑ | Fishery logbooks, 'geo' R package | R package 'geo', MRI, Reykjavík, Iceland <https://r-forge.r-project.org/R/?group_id=945> |
| *Predators* | | | | | | | | | |
| Fishing magnitude | fish_magnitude | Product of no. of successful fishing events and total landings in tonnes in the week preceding each occurrence/absence record. | tonnes | F (0, 6.15e05)<br>P (0, 7.06e06) | 0.1° × 0.05° | Weekly | ↓ | Fishery logbooks | Olsen 1971, Vabø et al. 2002, Ona et al. 2007, Doksæter et al. 2009, Lindegren et al. 2011 |
| *Prey* | | | | | | | | | |
| Zooplankton biomass | CF_Aug | Biomass estimates for adult *Calanus finmarchicus* (i.e. C4, C5, C6 stages) averaged for the August preceding wintering each year. | $\mu g\ C\ m^{-2}$ | F (0, 1.32e07)<br>P (0, 9.62e06) | 20 × 20 km | Annual, but simulation covers 1995-2007 only | ↑ | Hjøllo et al. 2012. IBM for *C. finmarchicus* | Bainbridge and Forsyth 1972, Holst et al. 1997, Maravelias and Reid 1997, Corten 1999*b*, Maravelias et al. 2000*b*, Gislason and Astthorsson 2002, Prokopchuk and Sentyabov 2006, Nøttestad et al. 2007, Hjøllo et al. 2012, Utne et al. 2012 |

Table 2. Structure and performance of candidate space-time occurrence models for wintering Atlantic herring. Each model contains all covariates (full), and results are shown for fitting using simplified Laplace approximation (see Supplementary material Appendix 7, Table A2 for results based on a Gaussian approximation strategy). s1-s15, *stationary* models; part_ns1-part_ns9, *partly non-stationary* models; full_ns1-full_ns9, *fully non-stationary* models. Covariate form refers to models that include linear terms only (linear), and quadratic terms (quadratic) or penalized regression spline terms for environmental covariates (spline). Space/time structure describes the form of the spatiotemporal random effect $\omega_{i,t}$, and if a fixed factor for year ($year_t$) was included; no-space/no-time, no spatially or temporally structured effects; time_indep, independent realization of the spatial random field at each $t$; time_corr, temporal correlation (ar1) is considered in the realization of the spatial random field at each $t$. The best-performing model within each stationarity class is shown in bold.

| Model | Covariate form | Structure | DIC | mean log score | Brier score | AUC |
|---|---|---|---|---|---|---|
| *Stationary* | | | | | | |
| s1 | linear | full (no-space/no-time) | 49104.2 | 0.504 | 0.157 | 0.934 |
| s2 | linear | full + $year_t$ | 48353.6 | 0.496 | 0.154 | 0.974 |
| s3 | linear | full + time_indep $\omega_{i,t}$ | 41872.1 | 0.429 | 0.123 | 0.993 |
| s4 | linear | full + $year_t$ + time_indep $\omega_{i,t}$ | 41811.9 | 0.429 | 0.122 | 0.993 |
| s5 | linear | full + time_corr $\omega_{i,t}$ | 41877.0 | 0.429 | 0.123 | 0.992 |
| s6 | quadratic | full (no-space/no-time) | 48917.2 | 0.502 | 0.156 | 0.943 |
| s7 | quadratic | full + $year_t$ | 48059.1 | 0.493 | 0.152 | 0.981 |
| s8 | quadratic | full + time_indep $\omega_{i,t}$ | 41732.1 | 0.428 | 0.122 | 0.994 |
| **s9** | **quadratic** | **full + $year_t$ + time_indep $\omega_{i,t}$** | **41629.0** | **0.427** | **0.122** | **0.995** |
| s10 | quadratic | full + time_corr $\omega_{i,t}$ | 41733.0 | 0.428 | 0.122 | 0.993 |
| s11 | spline | full (no-space/no-time) | 49232.2 | 0.505 | 0.158 | 0.917 |
| s12 | spline | full + $year_t$ | 48365.1 | 0.496 | 0.154 | 0.973 |
| s13 | spline | full + time_indep $\omega_{i,t}$ | 41907.0 | 0.430 | 0.123 | 0.993 |
| s14 | spline | full + $year_t$ + time_indep $\omega_{i,t}$ | 41833.3 | 0.429 | 0.123 | 0.993 |
| s15 | spline | full + time_corr $\omega_{i,t}$ | 41908.3 | 0.430 | 0.123 | 0.992 |
| *Partly non-stationary* | | | | | | |
| part_ns1 | linear | full (no-space/no-time) | 48953.2 | 0.502 | 0.157 | 0.952 |
| part_ns2 | linear | full + time_indep $\omega_{i,t}$ | 41733.4 | 0.428 | 0.122 | 0.993 |
| part_ns3 | linear | full + time_corr $\omega_{i,t}$ | 41742.0 | 0.428 | 0.122 | 0.992 |
| part_ns4 | quadratic | full (no-space/no-time) | 48725.5 | 0.500 | 0.155 | 0.960 |
| **part_ns5** | **quadratic** | **full + time_indep $\omega_{i,t}$** | **41621.5** | **0.427** | **0.122** | **0.994** |
| part_ns6 | quadratic | full + time_corr $\omega_{i,t}$ | 41625.5 | 0.427 | 0.122 | 0.994 |
| part_ns7 | spline | full (no-space/no-time) | 49080.7 | 0.504 | 0.157 | 0.943 |

| | | | | | | |
|---|---|---|---|---|---|---|
| part_ns8 | spline | full + time_indep $\omega_{i,t}$ | 41780.0 | 0.428 | 0.122 | 0.993 |
| part_ns9 | spline | full + time_corr $\omega_{i,t}$ | 41785.5 | 0.428 | 0.122 | 0.992 |
| *Fully non-stationary* | | | | | | |
| full_ns1 | linear | full (no-space/no-time) | 47330.3 | 0.486 | 0.148 | 0.989 |
| full_ns2 | linear | full + time_indep $\omega_{i,t}$ | 41334.7 | 0.424 | 0.120 | 0.996 |
| full_ns3 | linear | full + time_corr $\omega_{i,t}$ | 41342.3 | 0.424 | 0.120 | 0.995 |
| full_ns4 | quadratic | full (no-space/no-time) | 46756.0 | 0.480 | 0.146 | 0.995 |
| **full_ns5** | **quadratic** | **full + time_indep $\omega_{i,t}$** | **41047.1** | **0.421** | **0.119** | **0.997** |
| full_ns6 | quadratic | full + time_corr $\omega_{i,t}$ | 41055.3 | 0.421 | 0.119 | 0.997 |
| full_ns7 | spline | full (no-space/no-time) | 46972.0 | 0.482 | 0.147 | 0.993 |
| full_ns8 | spline | full + time_indep $\omega_{i,t}$ | 41219.1 | 0.422 | 0.119 | 0.996 |
| full_ns9 | spline | full + time_corr $\omega_{i,t}$ | 41226.4 | 0.423 | 0.119 | 0.996 |

Table 3. Mean (1 sd) Pearson's *r* coefficients calculated between time series of demographic parameters (Demo.) for the ISS herring stock and posterior mean estimates for influential covariates (Cov.) in the best *non-stationary* models. Mean and sd were calculated from correlations made for five time series incorporating the first 18, 19, 20, 21 and 22 years of data. Demographic parameters are age3:age4to7, age3:age8to13, age3:age4+, three ratios of numbers of naïve, first-time winterers to young experienced, old experienced, and all experienced individuals respectively; SSB, spawning stock biomass; SSN, spawning stock numbers; *n* age4to7, number of young experienced individuals; *n* age8to13, number of old experienced individuals; *n* age4+, number of all experienced individuals; mean age, average age of the spawning stock.

| Cov. \ Demo. | age3: age4to7 | age3: age8to13 | age3: age4+ | SSB | SSN | *n* age4to7 | *n* age8to13 | *n* age4+ | mean age |
|---|---|---|---|---|---|---|---|---|---|
| *Partly non-stationary* model (part_ns5) | | | | | | | | | |
| distrib$_{t-1}$ | 0.101 | 0.418 | 0.178 | 0.471 | 0.575 | 0.520 | 0.044 | 0.479 | -0.328 |
| | (0.047) | (0.128) | (0.066) | (0.061) | (0.125) | (0.107) | (0.021) | (0.089) | (0.126) |
| *Fully non-stationary* model (full_ns5) | | | | | | | | | |
| distrib$_{t-1}$ | 0.120 | 0.106 | 0.113 | 0.455 | 0.489 | 0.372 | 0.320 | 0.446 | -0.040 |
| | (0.036) | (0.107) | (0.040) | (0.055) | (0.125) | (0.129) | (0.047) | (0.104) | (0.118) |
| SST | 0.113 | 0.481 | 0.213 | 0.404 | 0.415 | 0.404 | -0.220 | 0.324 | -0.354 |
| | (0.014) | (0.020) | (0.016) | (0.006) | (0.014) | (0.011) | (0.022) | (0.008) | (0.026) |
| SSS | -0.118 | -0.375 | -0.187 | -0.454 | -0.501 | -0.435 | 0.028 | -0.405 | 0.257 |
| | (0.007) | (0.008) | (0.007) | (0.003) | (0.007) | (0.005) | (0.015) | (0.005) | (0.016) |
| PEA | -0.008 | 0.156 | 0.030 | -0.386 | -0.362 | -0.265 | -0.481 | -0.362 | -0.164 |
| | (0.030) | (0.049) | (0.024) | (0.027) | (0.071) | (0.076) | (0.023) | (0.060) | (0.062) |
| current_vel | -0.134 | -0.009 | -0.104 | 0.056 | 0.101 | 0.154 | -0.011 | 0.124 | -0.131 |
| | (0.019) | (0.034) | (0.026) | (0.004) | (0.017) | (0.012) | (0.021) | (0.010) | (0.032) |
| CF_Aug | -0.256 | -0.444 | -0.324 | -0.317 | -0.405 | -0.294 | 0.088 | -0.256 | 0.385 |
| | (0.007) | (0.027) | (0.010) | (0.002) | (0.017) | (0.016) | (0.013) | (0.010) | (0.029) |

**Figure legends**

Figure 1. Winter distribution of ISS herring during the period 1991_92 to 2013_14. Panels (a–c) illustrate the spatial shifts in landings by the autumn/winter purse seine fishery through time. We identified three major wintering phases over the 23 years of our time series, and aggregated the landings data within each phase: (a) 'East' - 1991_92 to 1997_98; (b) 'Eastwest' - 1998_99 to 2006_07; and (c) 'West' – 2007_08 to 2013_14 (see Óskarsson et al. 2009). Note the differences in color bar scales. (d) Twenty-three years of fishery occurrence and survey absence records. Grey lines denote 200 m and 500 m isobaths.

Figure 2. Calculation of the spatial similarity index (SSI). We defined an area of interest inclusive of all occurrence records in our dataset, divided this into 0.1° longitude × 0.05° latitude grid cells, and, for each year $t = 1, 2, \ldots, T$, coded each cell as 1 if herring were captured within it during year $t$, or 0 if they were not. This resulted in a $\text{distrib}_t$ layer for each year. For each $t = 2, 3, \ldots, T$, we then calculated the percentage of cells occupied in both $t$-1 and $t$, out of the number of cells occupied in $t$-1 or $t$ (a–c). Next, we weighted this value by the change (km) in the center of gravity (ΔCOG) of the stock between $t$-1 and $t$. Using the $\text{counts}_t$ layers that were constructed based on Eq. A1 (see Supplementary material Appendix 2 for details), we then calculated Pearson's $r$ between $\text{counts}_{t\text{-}1}$ and $\text{counts}_t$ and added this value (d, e). Data are presented for 1994_95 ($t$-1) and 1995_96 ($t$), with the SSI value for 1995_96 circled.

Figure 3. (a–e) Marginal effect plots for influential covariates in the part_ns5 model (see Table 1 for covariate codes), and (f) time series of posterior mean estimates (red line) and 95% credible intervals (CIs) (red-shaded region) for the $\text{distrib}_{t\text{-}1}$ covariate. In (a–e), black lines are median estimates of 1000 draws from the posterior distribution for a sequence of

100 values across the full range of each covariate, and grey-shaded regions are 95% CIs. Tick marks denote the percentile distribution of raw data for each covariate for occurrence records (top of plots) and absence records (bottom of plots). Plots (a–c) represent quadratic effects, and (d, e) the linear effect of the covariate. (g–h) Time series of posterior mean estimates for the linear term (circles) and 95% CIs (vertical lines) for all covariates from the full_ns5 model. Symbols are offset slightly, and results for the $distrib_{t-1}$ covariate plotted as a red line (posterior mean) and red-shaded region (95% CIs) in panel (g).

Figure 4. Spatial predictions of occurrence probability for four representative winters of the time series as derived from the full_ns5 model. For each year, (a) is the mean occurrence probability ($\psi$) and (b) the sd of $\psi$ (expressed as log-odds) for each grid cell. (c) is the mean intensity of the temporally-independent realization of the spatial random field ($\omega$), and (d) is the sd of $\omega$. Observed occurrences (black circles) and absences (grey crosses) for each year are overlaid in (a).

Figure 5. Time series of posterior mean estimates for $distrib_{t-1}$ derived from *partly non-stationary* models (i.e. part_ns5 specification) fitted to the first 18, 19, 20 and 21 years of data (solid lines), and estimates of adult population size for the ISS herring stock, represented by spawning stock numbers (SSN – in millions) (dashed line). Pearson's *r* values reflect the degree of correlation between each model time series and SSN in the years included in that model (see Supplementary material Appendix 6 for further details).

Figure 1

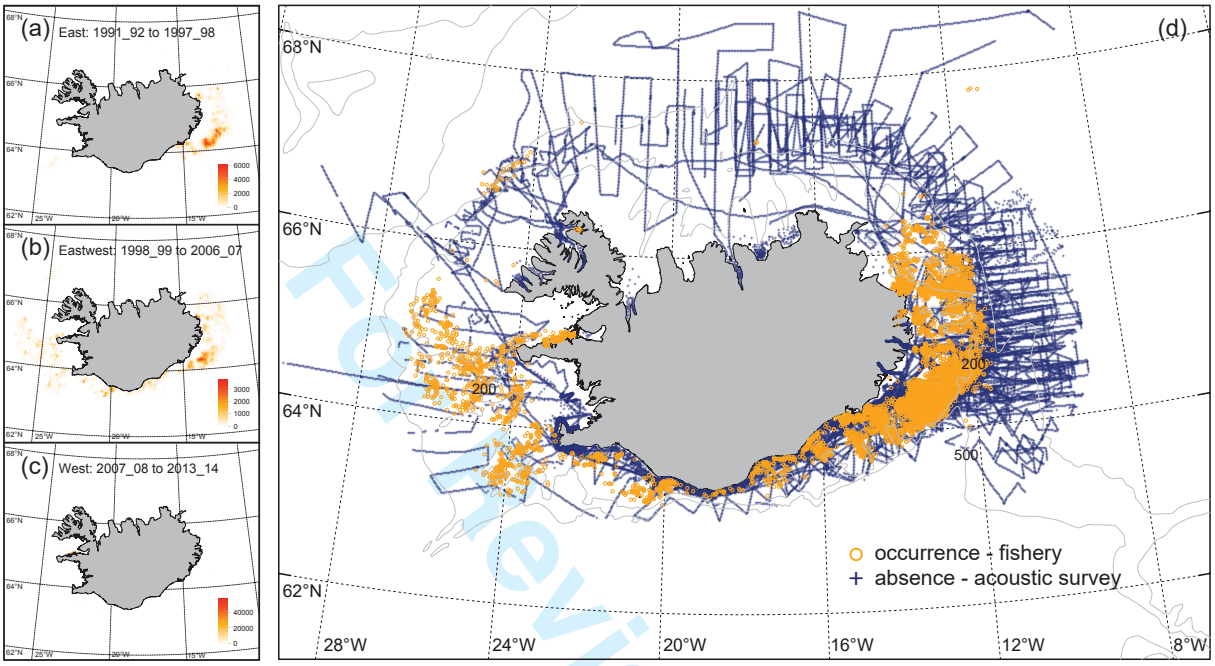

Figure 2

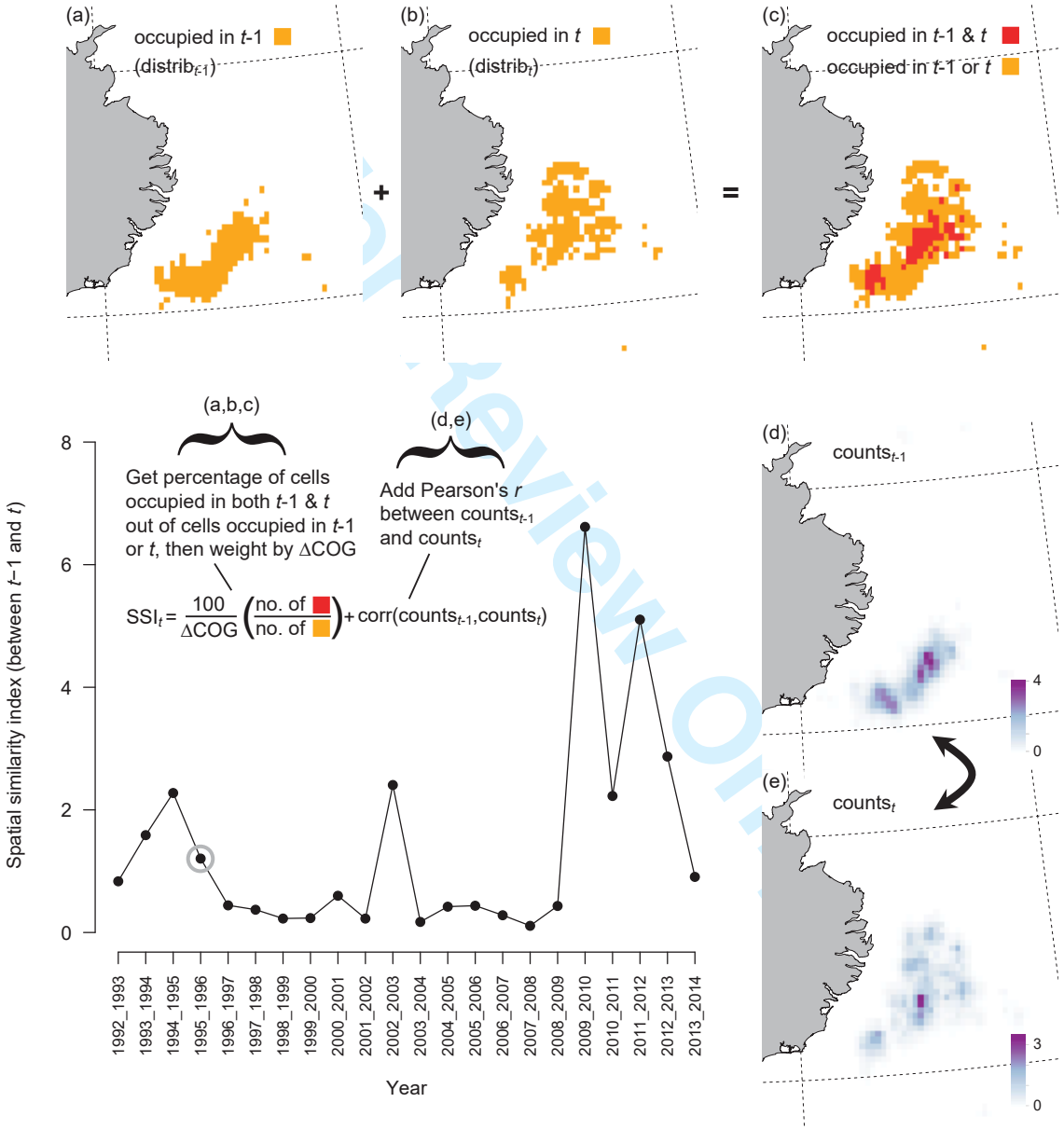
(a)
occupied in t-1
(distrib t-1)
(b)
occupied in t
(distrib t)
(c)
occupied in t-1 & t
occupied in t-1 or t
(a,b,c)
Get percentage of cells occupied in both t-1 & t out of cells occupied in t-1 or t, then weight by ΔCOG
(d,e)
Add Pearson's r between counts t-1 and counts t
SSI t = 100/ΔCOG (no. of / no. of) + corr(counts t-1, counts t)
Spatial similarity index (between t−1 and t)
Year
1992_1993
1993_1994
1994_1995
1995_1996
1996_1997
1997_1998
1998_1999
1999_2000
2000_2001
2001_2002
2002_2003
2003_2004
2004_2005
2005_2006
2006_2007
2007_2008
2008_2009
2009_2010
2010_2011
2011_2012
2012_2013
2013_2014
(d)
counts t-1
(e)
counts t

Figure 3

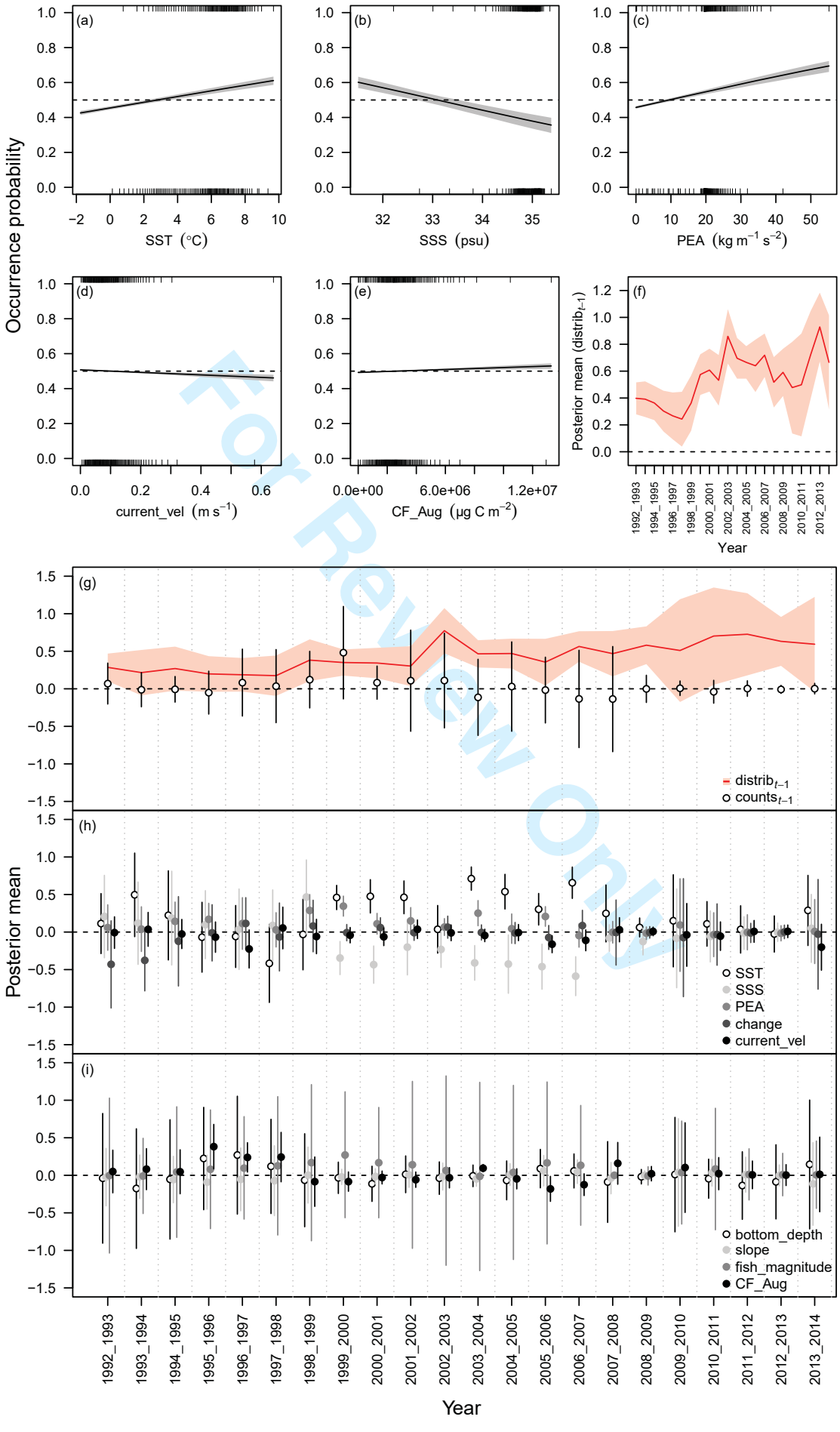

Figure 4

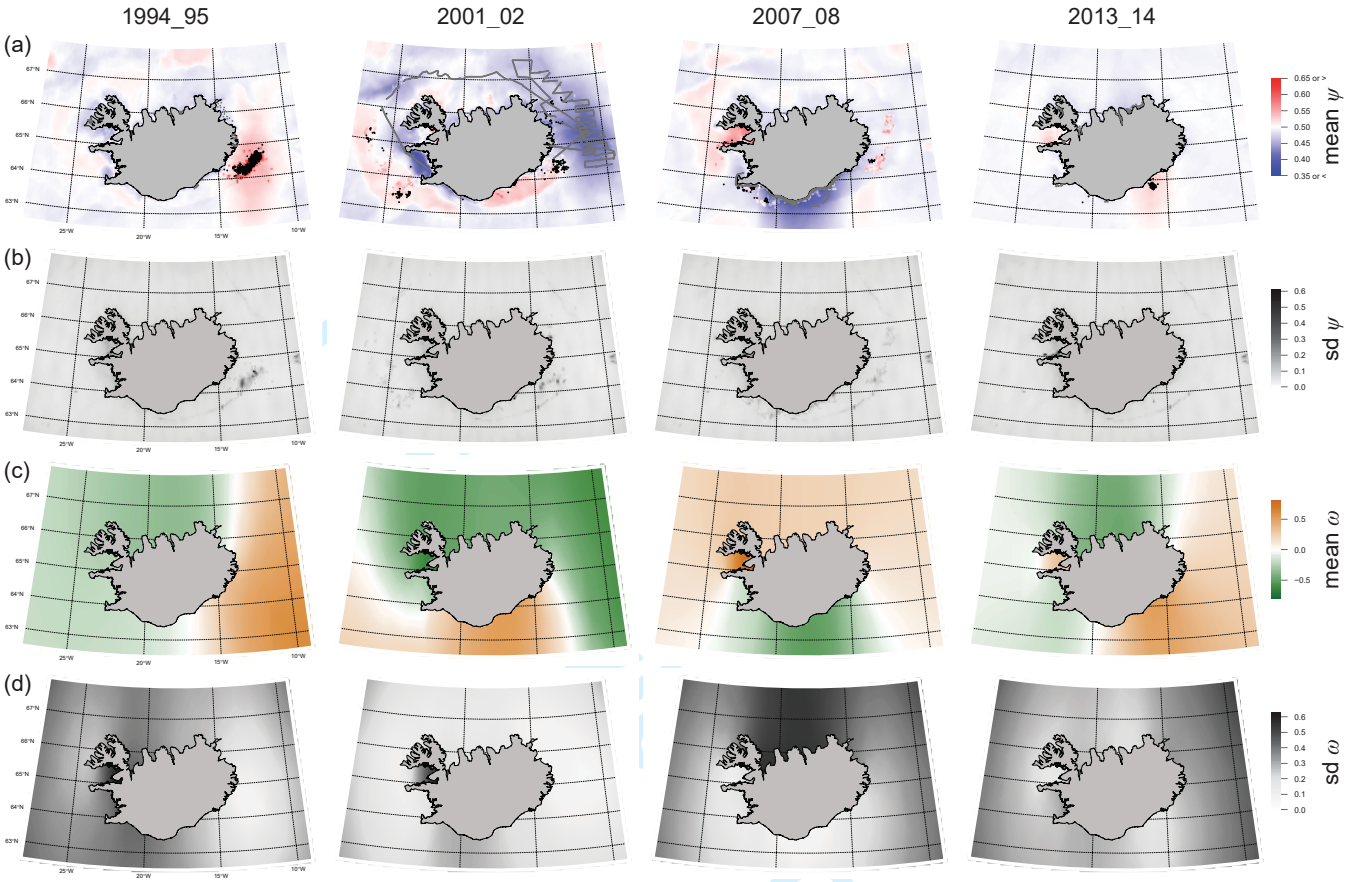

Figure 5

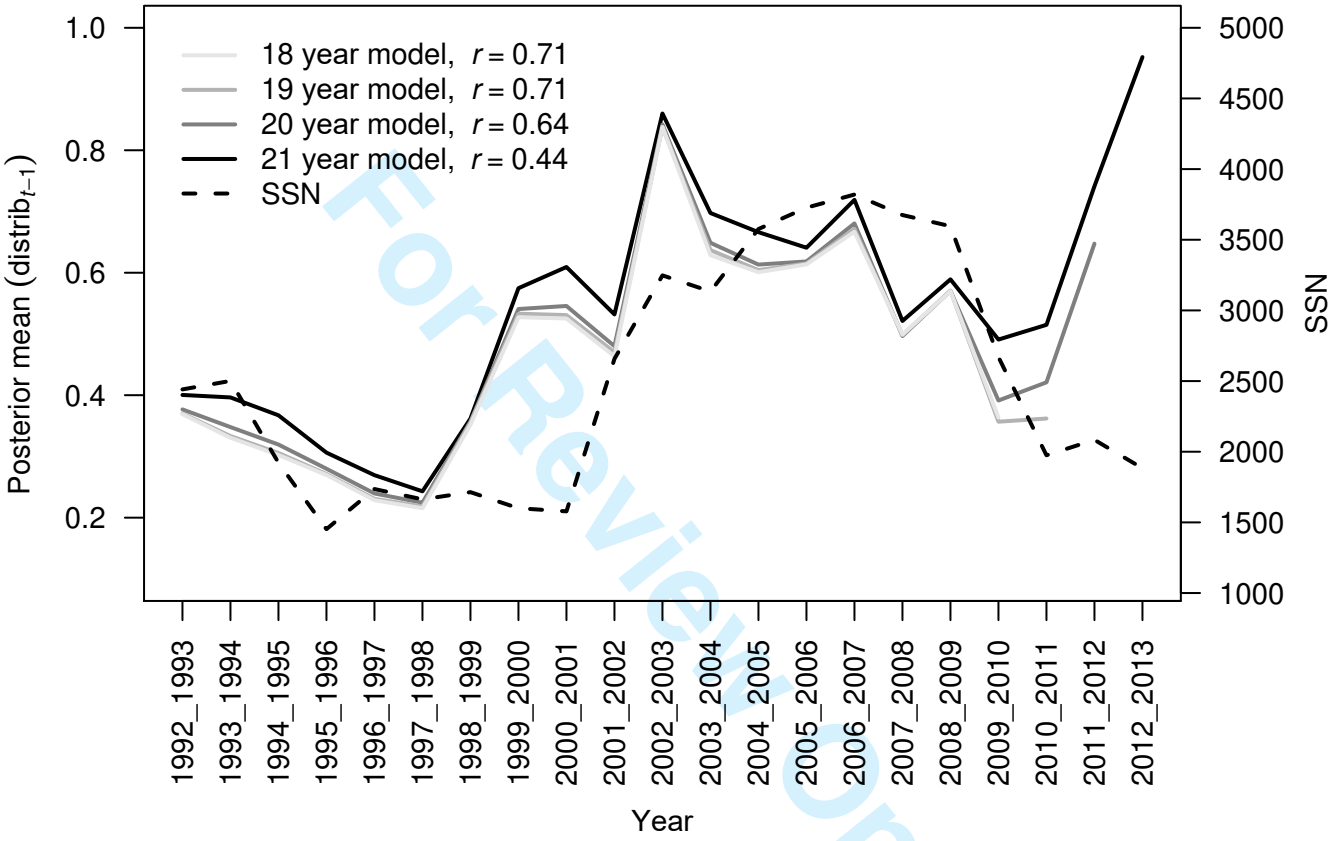

Macdonald, J. I., Logemann, K., Krainski, E. T., Sigurðsson, Þ., Beale, C. M., Huse, G., Hjøllo, S. S. and Marteinsdóttir, G. 2017. Can collective memories shape fish distributions? A test, linking space-time occurrence models and population demographics. – Ecography 000: 000–000.

**Supplementary material**

## Appendix 1: Detection and sampling coverage

*Detection*

Detection probability for our datasets is essentially = 1, notwithstanding potential recording errors. Occurrence records were included only if $c > 0$ tonnes, and the acoustic output enables accurate identification of herring schools based on area backscatter strength (Jakobsson et al. 1993, Guðmundsdóttir et al. 2007), making false absences highly unlikely. The spatiotemporal distribution of fishing effort in the Icelandic winter purse seine herring fishery is not random however, and has varied markedly over the time series considered here (ICES 2015). Early in the season, fishing locations are often selected based upon knowledge of previous overwintering areas. As the season progresses, information on recent landings, reports from other fishing vessels and input from the MRI acoustic surveys (which typically coincide with the beginning of the fishing season), drive fishing behaviour. Similarly, the location of the acoustic survey tracks is not consistent among years (Guðmundsdóttir et al. 2007, ICES 2015), with the level of survey effort reflecting funding, time availability, weather conditions as well as information exchange between MRI and active fishing vessels (Óskarsson and Pálsson 2015). This situation likely resulted in some level of sampling bias, although given the searching capacity of the purse seine fleet (Guðmundsdóttir and Sigurðsson 2004, Óskarsson et al. 2009), and the wide spatial coverage of the acoustic surveys, we consider this bias to be minimal (see below). Additionally, such bias is generally of lower concern for binomial occurrence models with near perfect detection, as it only acts to reduce precision of the estimation in less-sampled regions, rather than biasing the estimation process itself (Phillips et al. 2009, Guillera-Arroita et al. 2015).

*Sampling coverage*

It could be argued that the fishery and survey data used here may be biased and may not reflect the true extent of the herring distribution in a given season. We contend that such bias would be minimal for three reasons. First, the fishing fleet for Icelandic herring, which currently consists of 15 large vessels, conducts extensive searches for wintering herring schools each season, covering a substantial portion of the stock's distributional range which is fully captured within the Icelandic exclusive economic zone (EEZ) (Óskarsson et al. 2009, author's personal observation). Second, the annual acoustic surveys, although varying in sampling intensity each year, have covered a large region of the Icelandic EEZ in all years from the mid-1990s onwards. Thirdly, the close working relationship between MRI and the fishing companies results in constant information exchange regarding the distribution of the herring schools during the autumn/winter fishing period. Hence, we contend that although the full extent of the realized distribution may not be captured by the fishery and survey data, it does reflect the major trends in overwintering distribution over the 1991_92 to 2013_14 period. Furthermore, given the near perfect detection in our dataset, there is no need to make assumptions about capturing the full realized niche during the overwintering period. Rather, we use the data we have to build the models.



**References**

Guðmundsdóttir, A. and Sigurðsson, Þ. 2004. The autumn and winter fishery and distribution of the Icelandic summer-spawning herring during 1978–2003. Report 104, Marine Research Institute, Reykjavík, Iceland.

Guðmundsdóttir, A. et al. 2007. Estimating year-class strength of Icelandic summer-spawning herring on the basis of two survey methods. – ICES J. Mar. Sci. 64: 1182–1190.

Guillera-Arroita, G. et al. 2015. Is my species distribution model fit for purpose? Matching data and models to applications. – Global Ecol. Biogeogr. 24: 276–292.

ICES. 2015. Report of the North Western Working Group, 28 April - 5 May 2015. ICES CM 2015/ACOM:07, Copenhagen, Denmark.

Jakobsson, J. et al. 1993. Stock-related changes in biological parameters of the Icelandic summer-spawning herring. – Fish. Oceanogr. 2: 260–277.

Óskarsson, G. J. and Pálsson. J. 2015. Estimation on number-at-age of the catch of Icelandic summer-spawning herring in 2014/2015 fishing season and the development of *Ichthyophonus hoferi* infection in the stock. Working Document No. 2, ICES North Western Working Group, 28 April - 5 May 2015, Copenhagen, Denmark.

Óskarsson, G. J. et al. 2009. Variation in spatial distribution and migration of Icelandic summer-spawning herring. – ICES J. Mar. Sci. 66: 1762–1767.

Phillips, S. J. et al. 2009. Sample selection bias and presence-only distribution models: implications for background and pseudo-absence data. – Ecol. Appl. 19: 181–197.

## Appendix 2: Details and R code for constructing the distrib$_t$ and counts$_t$ variables and calculating the spatial similarity index (SSI)

### Appendix 2.1: Construction of distrib$_t$ and counts$_t$ layers

To construct the distrib$_t$ layers, we defined an area of interest that encompassed all records in our dataset, then divided this region into 0.1° longitude × 0.05° latitude (i.e. ~ 5 × 5 km) grid cells. Next, for each of the 23 years $t = 1, 2, \ldots, T$, we summed the number of occurrence records in each cell $k$, denoted $r_{k,t}$. If $r_{k,t} > 0$, then distrib$_{k,t}$ was coded as 1, otherwise 0. We used these results to produce annual gridded maps of occurrence (distrib$_t$) across our study region (Fig. 2a–c).

Using the same spatial grid, we then computed the counts$_t$ variable which reflects the number of occurrence records (i.e. successful fishing events) in each cell in each year, whilst also accounting for potential joining/splitting interactions among herring schools occupying nearby cells (Mackinson et al. 1999, Nøttestad and Axelsen 1999). For each grid cell $k$, in year $t$, counts$_{k,t}$ is the sum of $r_{k,t}$ and the mean number of occurrence records in all 1$^{st}$ order neighbouring cells $n_{k,t,j}$ ($j = 1, 2, \ldots, 8$), excluding the central cell (Eq. A1) (see Appendix 2.3 for R code). To allow for comparisons among years, we converted counts$_{k,t}$ to a percentage of the total number of occurrences recorded across the whole study region in each year, denoted $occ_t$.

$$\text{counts}_{k,t} = \frac{100}{occ_t}\left(r_{k,t} + \frac{\sum_{j=1}^{8} n_{k,t,j}}{8}\right) \qquad \text{(A1)}$$

Like distrib$_t$, we created annual gridded maps of counts$_t$ for each year of the time series (Fig. 2d,e). The counts$_t$ variable can be considered a proxy for herring abundance that is less prone

to error than using landings data directly, as catch rates by vessels using purse seine gears are inherently variable (Hilborn and Ledbetter 1985, Ruttan and Tyedmers 2007, Vázquez-Rowe and Tyedmers 2013).

**Appendix 2.2:** Calculation of the SSI

For year $t = 2, 3, \ldots, T$, we sum the grid cell values from the gridded occurrence map from the previous year ($distrib_{t-1}$) and those from the current year ($distrib_t$). Where grid cell counts = 2, this cell has been occupied in year $t$-1 and year $t$. We then divide this number by the total number of occupied cells in $t$-1 or $t$, and convert to a percentage. This last step captures the degree of expansion and contraction in the area occupied from year to year. Next, we calculate the distance change (km) in the centre of gravity (ΔCOG) of the stock between $t$-1 and $t$. The COG for fishing year $t$ can be defined as the mean location of the population for that year (Wolliez et al. 2007), and was estimated here by weighting each fishing location by the catch recorded from that location in that year, giving all fishing evenets equal weight (see Eq. A2). For each year $t$,

$$\mathrm{COG} = \frac{\sum_{i=1}^{M} x_i c_i}{\sum_{i=1}^{M} c_i} \qquad \text{(A2)}$$

where $M$ is the total number of catch locations, $x_i$ is the geographic position (i.e., longitude and latitude) of location $i$ and $c_i$ is the catch (tonnes) at location $i$.

Dividing by ΔCOG down weights the SSI when the distributional centroid has changed dramatically between one year and the next. This calculation generates an 'SSI_overlap' value (see R code in Appendix 2.3). Next, we calculate Pearson's $r$ between the $counts_{t-1}$ and

$counts_t$ layers across all grid cells. This captures the change in density of occurrence records from year to year, and generates the 'SSI_pearson' value. Finally, we sum the 'SSI_overlap' and 'SSI_pearson' value to create an 'SSI_estimate' for each year (see R code in Appendix 2.3).

*Why use 1st order neighbours?*

The decision to use only 1st order neighbouring cells in the calculation for $counts_t$, rather than an autoregressive model, can justified for two reasons. First, this way we have direct control over the distance considered, which can then be tuned to relevant ecological processes. The maximum distance from the outer edge of one of our grid cells to the outer edge of a neighbouring cell is ~ 10 km – a distance representative of the scale at which school joining and splitting behaviour often operates (Mackinson et al. 1999). Second, allowing more flexibility in the numbers of neighbouring cells included in the calculations makes more assumptions outside the spatial range of the occurrence records. In effect, our approach can be viewed as quite conservative, as it only estimates values one-cell removed from where the data actually are. We stress however, that the distance considered in the calculation of $counts_t$ can be easily adjusted if there are reasons to believe that ecological processes are acting at finer or coarser scales.

*Excluding catch biomass in the calculation of* $counts_t$

Catch biomass ($c$) for each fishing event can vary based on vessel-, skipper-, gear- and weather-related factors in addition to the actual amount of herring present at a particular location (Branch et al. 2006, Vázquez-Rowe and Tyedmers 2013). Given that we did not explicitly measure the first four of these sources of variability in this study, in addition to the inherent difficulties in accurately capturing these effects in any case (see Squires and Kirkley

1999), we chose to take a conservative approach in computing $counts_t$ – i.e. based on the number of occurrences per grid cell, per year. We also gave equal weight to occurrence records with $0 < c < 1$ tonne and all $c \geq 1$ tonne, as differences in $c$ may arise through interactions among the aforementioned factors that are unrelated to the point abundance of herring *per-se*. Through this approach we hoped to minimize bias associated with these unquantified sources of variability.

**Appendix 2.3:** The folder 'Macdonald et al._R code and data.zip' (deposited in the Dryad Digital Repository <http://datadryad.org/>) contains R code and data for constructing the $counts_t$ variable and for calculating the spatial similarity index (SSI) using the Icelandic summer spawning herring dataset for illustration.

| | |
|---|---|
| Folder name: | 'Macdonald et al._R code and data.zip' |
| Relevant files: | i) 'Create counts(t) rasters.R' (R code) |
| | ii) 'Spatial similarity index calculation.R' (R code) |
| | iii) 'SSI_calc_stats.csv' (.csv data file) |



**References**

Branch, T. A. et al. 2006. Fleet dynamics and fishermen behavior: lessons for fisheries managers. – Can. J. Fish. Aquat. Sci. 63: 1647–1668.

Hilborn, R. and Ledbetter, M. 1985. Determinants of catching power in the British Columbia salmon purse seine fleet. – Can. J. Fish. Aquat. Sci. 42: 51–56.

Mackinson, S. et al. 1999. Cross-scale observations on distribution and behavioural dynamics of ocean feeding Norwegian spring-spawning herring (*Clupea harengus* L.). – ICES J. Mar. Sci. 56: 613–626.

Nøttestad, L. and Axelsen, B. E. 1999. Herring schooling manoeuvres in response to killer whale attacks. – Can. J. Fish. Aquat. Sci. 77: 1540–1546.

Ruttan, L. M. and Tyedmers, P. H. 2007. Skippers, spotters and seiners : analysis of the " skipper effect " in US menhaden (*Brevoortia* spp.) purse-seine fisheries. – Fish. Res. 83: 73–80.

Squires, D. and Kirkley, J. 1999. Skipper skill and panel data in fishing industries. – Can. J. Fish. Aquat. Sci. 56: 2011–2018.

Vázquez-Rowe, I. and Tyedmers, P. 2013. Identifying the importance of the "skipper effect" within sources of measured inefficiency in fisheries through data envelopment analysis (DEA). – Mar. Policy 38: 387–396.

Woillez, M. et al. 2007. Indices for capturing spatial patterns and their evolution in time, with application to European hake (*Merluccius merluccius*) in the Bay of Biscay. – ICES J. Mar. Sci. 64: 537–550.

## Appendix 3. Additional information on covariates for the space-time models

*Spatial memory*

Our aim was to capture the main features represented in the SSI (Fig. 2, Appendix 2) in covariates that could be used for input into spatially-explicit models to predict seasonally-varying occurrence patterns. We employed the $distrib_t$ and $counts_t$ variables described in the Methods under '*Capturing shifting distributions: a spatial similarity index*' for this purpose (see also Appendix 2 for calculation details). By using the layers created for the previous year (i.e. $t$-1), we defined two covariates that represent the occurrence pattern (i.e. $distrib_{t-1}$) and density of occurrence records (i.e. $counts_{t-1}$) one-year earlier (see Fig. A1 for examples of rasters for 2001_02). These two covariates are able to test the following two hypotheses. 1) Does the occurrence of herring at a particular location in year $t$-1 (represented by the $distrib_{t-1}$ covariate) influence the probability of occurrence in year $t$? 2) Does the relative density of occurrences at a particular location in year $t$-1 (represented by the $counts_{t-1}$ covariate) influence the probability of occurrence in $t$? That is, are herring here in $t$ because they were here in numbers in $t$-1 – akin, to a density-dependent effect with one-year lag?

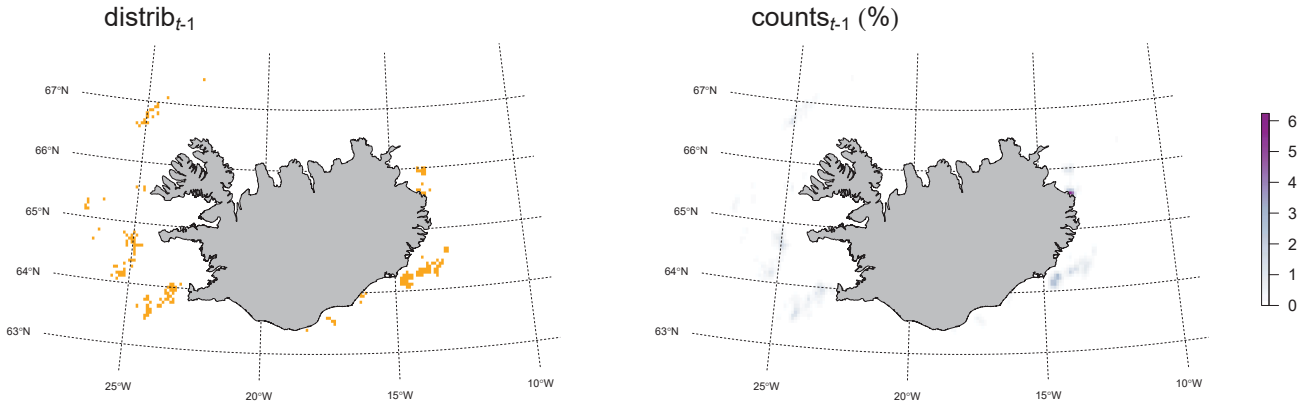


Fig. A1. Rasters of spatial memory covariates for 2001_2002. In distrib$_{t-1}$, orange cells indicate those occupied the previous year (i.e. 2000_2001). See Table 1 in main text for units and derivation for these covariates.

*Dynamic environmental variables*

As temperature, salinity and flow velocity can impact strongly on herring distribution during several phases of the species' life history (Sinclair and Iles 1985, Maravelias et al. 2000a,b and references therein, Toresen and Østvedt 2000, Lindegren et al. 2011, Bartolino et al. 2014), information on sea surface temperature – SST (°C), sea surface salinity – SSS (psu), and the east-west (U-component) and north-south (V-component) flow vectors (m $s^{-1}$) were extracted from the CODE model (Logemann et al. 2013) at three spatial scales (i.e. 1 × 1 km, 4 × 4 km and 8 × 8 km buffer distances around each fishing/survey record) and two temporal scales (i.e. day of record, mean of the preceding 7 days) (Fig. A2). From these data, three new variables were created (at the same scales) to capture mixing processes through the water column that may influence the behaviour of wintering herring: the potential energy anomaly – PEA (kg $m^{-1}$ $s^{-2}$) a proxy for stratification, and defined as the energy required to vertically mix the water column so that the density is uniform from surface to bottom (Planque et al. 2006, Huret et al. 2013), the temperature gradient between surface and bottom waters – change (°C), and the mean absolute values of the U and V flow vectors in surface waters – current_vel (m $s^{-1}$) (Fig. A2). The highest resolution data obtainable from the CODE (i.e. 1 × 1 km grid, day of record) most closely matched both the area sampled by, and the timing of each fishing or survey record, providing the most realistic representation possible of the ambient environment

experienced by the school at that time and place. In light of this, in conjunction with the high collinearity found among the spatial and temporal scales considered for each covariate (Pearson's $r > 0.8$ in all cases), we decided to extract data at 1 × 1 km on the day of the record.

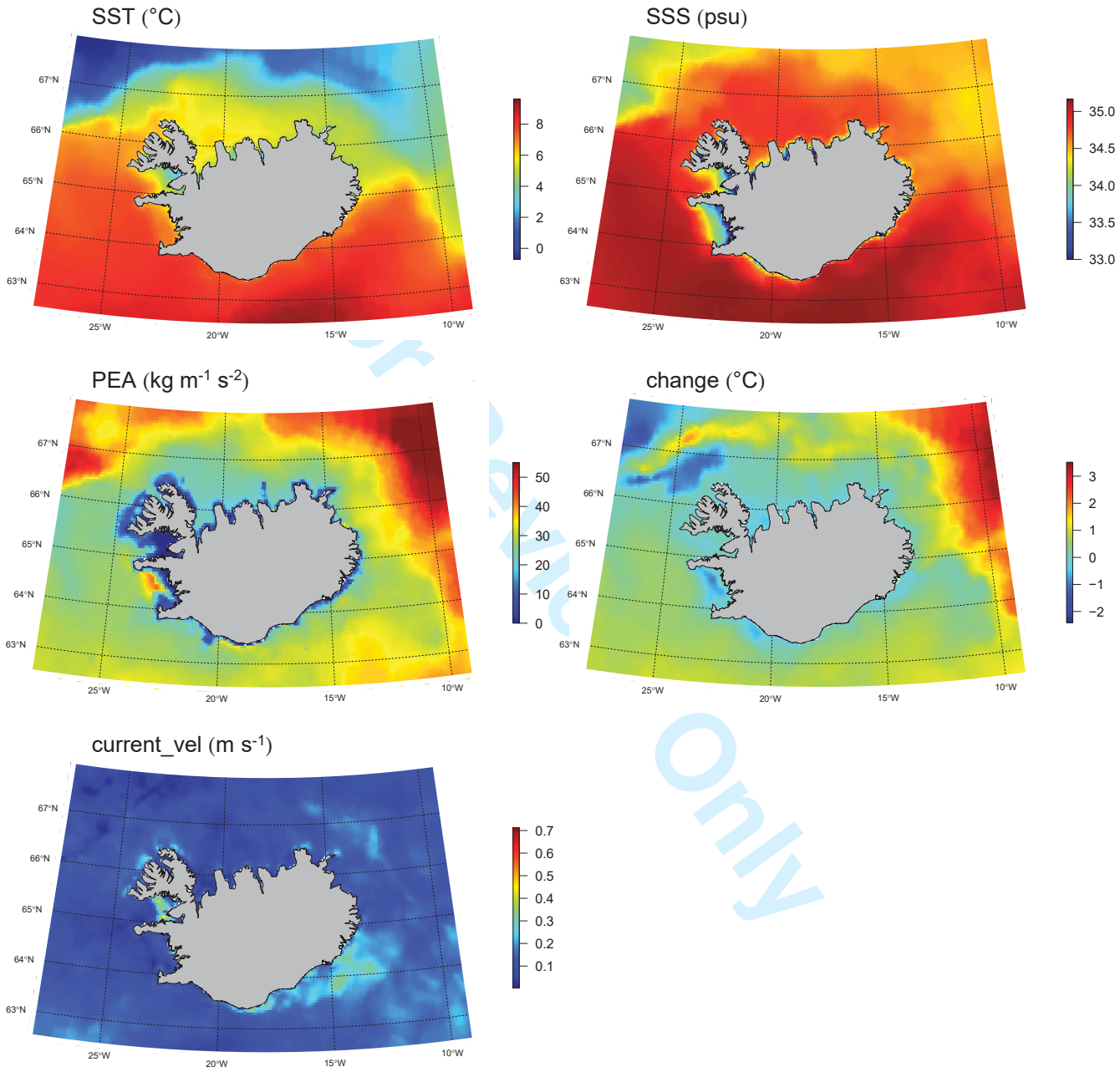


Fig. A2. Rasters of dynamic environmental covariates for 2001_2002. See Table 1 in main text for derivation. For model fitting, these covariates were extracted from the CODE ocean model (Logemann et al. 2013) at 1 × 1 km resolution on the day of each catch or survey record (see text above). However, rasters presented here are at 0.1° longitude × 0.05° latitude resolution and represent mean grid cell values across the 2001_2002 season. This is the common scale used for spatial prediction for all covariates (see *Spatial prediction* in the Material and methods for further details).

The CODE model assimilates observational data from CTD (conductivity, temperature, depth) profiles and river discharge data from 46 Icelandic watersheds into its simulation, and excellent concordance was found between modelled and observed temperature, salinity and flow fields across our study region (see Table 1 in Logemann et al. 2013).

*Static environmental variables*

As both previous work and visual examination of our dataset suggest that herring may favour specific bottom topography during pre-spawning (Maravelias et al. 2000b) and wintering phases (MRI, unpublished data), we extracted information on depth - bottom_depth (m) and slope - slope (degrees) of the sea-floor from the GEBCO website. These data were available at 30 arcsecond resolution around each fishing/survey record. As wintering ISS herring have been often been found close to the coast over the past three decades (Óskarsson et al. 2009), we calculated distance to shore - dist_to_shore (km) from each record using the 'gDistance' function in the 'rgeos' package in R (Fig. A3).



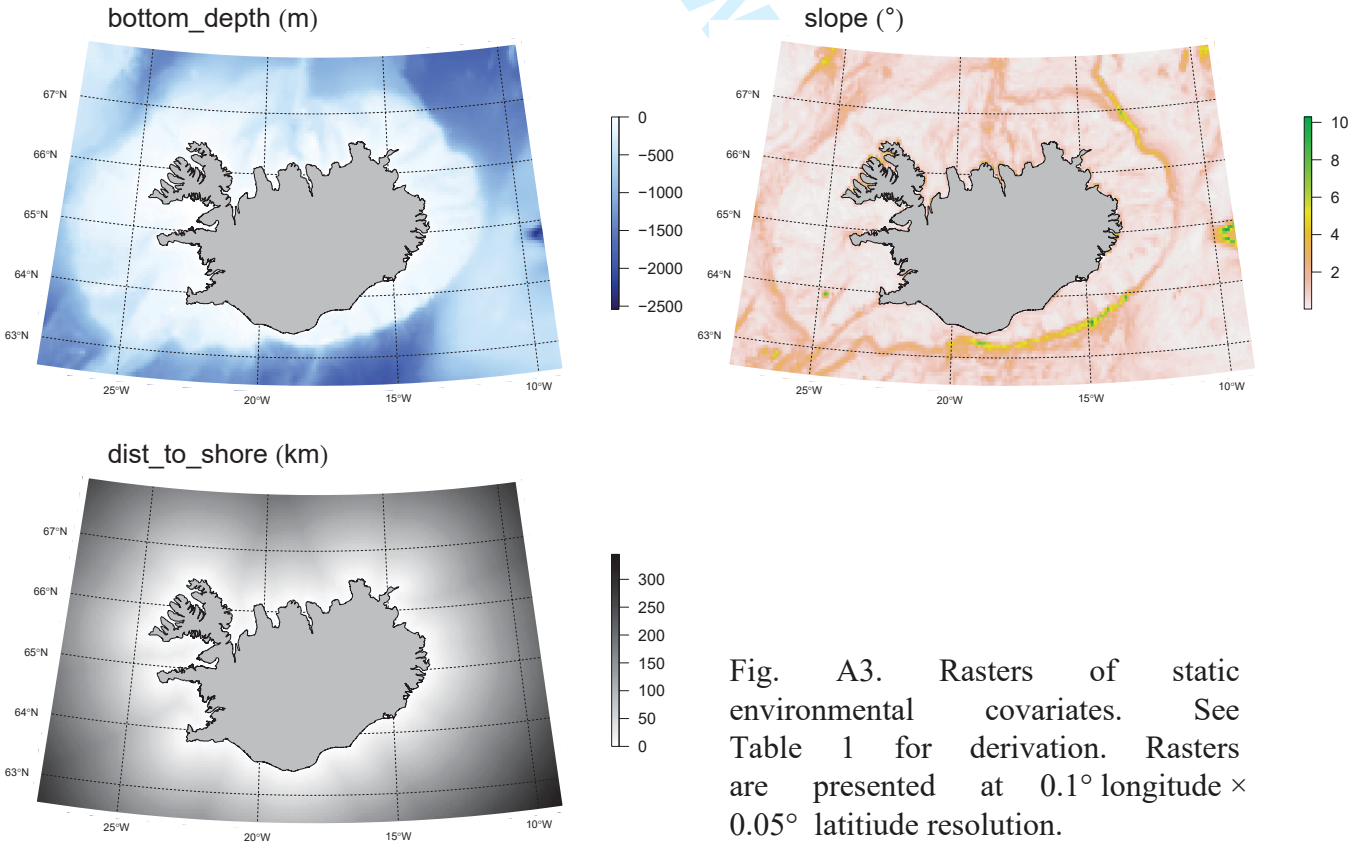


Fig. A3. Rasters of static environmental covariates. See Table 1 for derivation. Rasters are presented at 0.1° longitude × 0.05° latitiude resolution.

*Zooplankton biomass in August*

Although herring hardly feed during the winter (Slotte 1999), adult stages of the zooplankter *Calanus finmarchicus* are a major prey item for herring in the North Atlantic during summer (Holst et al. 1997, Dalpadado et al. 2000, Gislason and Astthorsson 2002, Prokopchuk and Sentyabov 2006). Hence, we suggest that regions of high summer *C. finmarchicus* biomass is likely be a feeding hotspot for pre-wintering ISS. Further, we propose that selection of wintering areas may be geographically close to where these hotspots are located. To test this, we extracted georeferenced mean August biomass estimates for adult *C. finmarchicus* (i.e. C4, C5, C6 stages), integrated in the upper 400 m of the water column at 20 × 20 km horizontal resolution, from the output of a *C. finmarchicus* IBM – CF_Aug (µg C $m^{-2}$) (Hjøllo et al. 2012) (Fig. A4). We used this dataset as a proxy for late summer ISS feeding distribution, in lieu of spatially-referenced fishing or survey data that were not available for that time of year during the time series. Temporal coverage of Hjøllo et al.'s simulation spanned 1995 to 2007, and missing values for other years in our dataset were imputed using predictive mean matching in an approximate Bayesian framework in the 'mi' package in R (see below for further details).

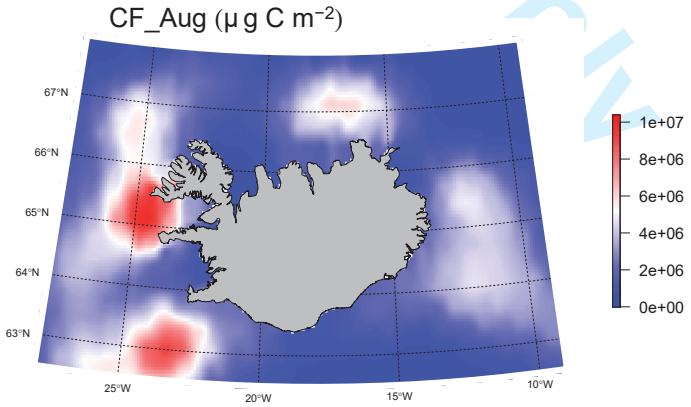


Fig. A4. Raster of mean *C. finmarchicus* biomass for August 2001. See Table 1 for derivation. Layers were available at 20 × 20 km resolution, and we used this resolution for data extraction and model fitting. Prediction was made to the 0.1° longitude × 0.05° latitude grid presented here, with data resampled using a bilinear interpolation.

*Imputation of CF_Aug using the 'mi' package*

The 'mi' R package uses a chained equation approach to multiple imputation for datasets with missing values (Su et al. 2011). In our case, we had missing values only for CF_Aug in the years 1992-1994 and 2008-2013. The 'mi' function approximates a Bayesian approach and draws imputed values from the conditional distribution for CF_Aug given the observed values of the other covariates. With Student-*t* priors (mean = 0, df = 1, scale = 2.5) placed on the regression coefficients, we ran four independent chains initialized with different starting values and assessed convergence after 30 (the default), 50 and 80 iterations via $\hat{R}$ statistics. We found acceptable convergence after 80 iterations (CF_Aug: mean = 1.01, sd = 1.02) and diagnostic plots (produced by the 'plot' function in 'mi') revealed good congruence between observed and imputed data. Our procedure generated four multiply imputed datasets (one per chain), and we took the mean imputed values for each across these datasets as our new values for CF_Aug.

*Fishing magnitude*

Given the known disruptive effects of fishing and vessel activity on the behaviour of pelagic schooling species like herring (e.g. Olsen 1971, Fréon et al. 1992, Vabø et al. 2002, Ona et al. 2007, Lindegren et al. 2011) we aggregated data on numbers of successful fishing events ($succ_k$) and total landings in tonnes ($c_k$) in each 0.1° longitude × 0.05° latitude grid cell $k$ for each week of winter. We then constructed a measure of local fishing magnitude – fish_magnitude (tonnes) = $succ_k \times c_k$, for each grid cell in each week, month and year across the time series (Fig. A5). Finally, for each fishing/survey event, we calculated a fish_magnitude value in the week prior to that particular observation. Our hypothesis was that a high fishing magnitude would disperse the herring schools in that area, making the probability of capture at that location in the following week less likely.

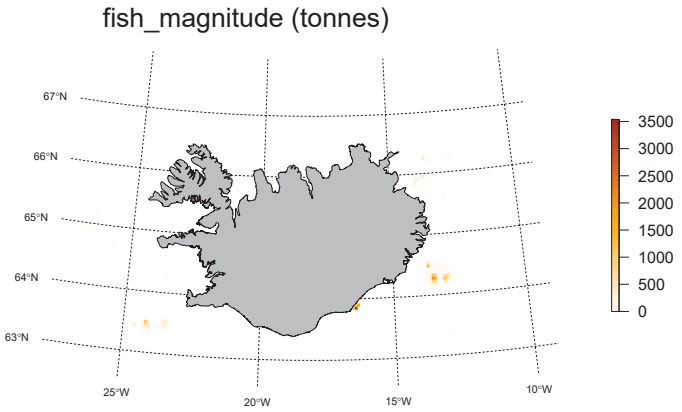


Fig. A5. Raster of mean fishing magnitude for 2001_2002. See Table 1 in main text for derivation. Model fitting was conducted using data extracted at a weekly resolution, but grid cell values (0.1° l ongitude × 0.05° latitude resolution) were summed across the entire year for spatial predictions.

**References** (including references cited in Table 1)

Bainbridge, V. and Forsyth, D. C. T. 1972. An ecological survey of a Scottish herring fishery. Part V: The plankton of the northwestern North Sea in relation to the physical environment and the distribution of the herring. – Bull. Mar. Ecol. 8: 21–52.

Bartolino, V. et al. 2014. Forecasting fish stock dynamics under climate change: Baltic herring (*Clupea harengus*) as a case study. – Fish. Oceanogr. 23: 258–269.

Blaxter, H. S. 1985. The herring: a successful species? – Can. J. Fish. Aquat. Sci. 42: 21–30.

de Boer, G. J. et al. 2008. Using the potential energy anomaly equation to investigate tidal straining and advection of stratification in a region of freshwater influence. – Ocean Model. 22: 1–11.

Burchard, H. and Hofmeister, R. 2008. A dynamic equation for the potential energy anomaly for analysing mixing and stratification in estuaries and coastal seas. – Estuar. Coast. Shelf Sci. 77: 679–687.

Corten, A. 1993. Learning processes in herring migrations. ICES C.M. 1993/H:18 Pelagic Fish Committee, Copenhagen, Denmark.

Corten, A. 1999a. A proposed mechanism for the Bohuslan herring periods. – ICES J. Mar. Sci. 56: 207–220.

Corten, A. 1999b. The reappearance of spawning Atlantic herring (*Clupea harengus*) on Aberdeen Bank (North Sea) in 1983 and its relationship to environmental conditions. – Can. J. Fish. Aquat. Sci. 56: 2051–2061.

Corten, A. 2000. A possible adaptation of herring feeding migrations to a change in timing of the *Calanus finmarchicus* season in the eastern North Sea. – ICES J. Mar. Sci. 57: 1270.

Corten, A. 2001. Northern distribution of North Sea herring as a response to high water temperatures and/or low food abundance. – Fish. Res. 50 :189–204.

Corten, A. 2002. The role of “conservatism” in herring migrations. – Rev. Fish Biol. Fisher.

11: 339–361.

Corten, A. and Van de Kamp, G. 1992. Natural changes in pelagic fish stocks of the North Sea in the 1980s. – ICES Mar. Sc. 195: 402–417.

Dalpadado, P. et al. 2000. Food and feeding conditions of Norwegian spring-spawning herring (*Clupea harengus*) through its feeding migrations. – ICES J. Mar. Sci. 57: 843–857.

Doksæter, L. et al. 2009. Behavioral responses of herring (*Clupea harengus*) to 1-2 and 6-7 kHz sonar signals and killer whale feeding sounds. – J. Acoust. Soc. Am. 125: 554–564.

Fernö, A. et al. 1998. The challenge of the herring in the Norwegian Sea: making optimal collective spatial decisions. – Sarsia 83: 149–167.

Fréon, P. et al. 1992. Changes in school structure according to external stimuli: description and influence on acoustic assessment. – Fish. Res. 15: 45–66.

Gislason, A. and Astthorsson, O. S. 2002. The food of Norwegian spring-spawning herring in the western Norwegian Sea in relation to the annual cycle of zooplankton. – Sarsia 87: 236–247.

Hjøllo, S. S. et al. 2012. Modelling secondary production in the Norwegian Sea with a fully coupled physical/primary production/individual-based *Calanus finmarchicus* model system. – Mar. Biol. Res. 6: 508–526.

Holst, J. C. et al. 1997. Feeding, *Ichthyophonus* sp. infection, distribution and growth history of Norwegian spring-spawning herring in summer. – J. Fish Biol. 50: 652–664.

Huret, M. et al. 2013. A multi-decadal hindcast of a physical–biogeochemical model and derived oceanographic indices in the Bay of Biscay. – J. Mar. Syst. 109-110: S77–S94.

Huse, G. et al. 2010. Establishment of new wintering areas in herring co-occurs with peaks in the "first time/repeat spawner" ratio. – Mar. Ecol. Prog. Ser. 409: 189–198.

Huse, G. et al. 2002. Modelling changes in migration pattern of herring: collective behaviour and numerical domination. – J. Fish Biol. 60: 571–582.

Huse, I. and Korneliussen, R. 2000. Diel variation in acoustic density measurements of overwintering herring (*Clupea harengus* L.). – ICES J. Mar. Sci. 57: 903–910.

Jakobsson, J. 1969. Síld og sjávarhiti. – In Einarsson, M. Á. (ed.), Hafásinn. Reykjavík, Iceland, pp. 497–511.

Lindegren, M. et al. 2011. Interacting trophic forcing and the population dynamics of herring. – Ecology 92: 1407–1413.

Logemann, K. et al. 2013. The circulation of Icelandic waters – a modelling study. – Ocean Sci. 9: 931–955.

Maravelias, C. D. 1997. Trends in abundance and geographic distribution of North Sea herring in relation to environmental factors. – Mar. Ecol. Prog. Ser. 159: 151–164.

Maravelias, C. D. and Reid, D. 1995. Relationship between herring (*Clupea harengus*, L.) distribution and sea surface salinity and temperature in the northern North Sea. – Sci. Mar. 59: 427–438.

Maravelias, C. D. and Reid, D. 1997. Identifying the effects of oceanographic features and zooplankton on prespawning herring abundance using generalized additive models. – Mar. Ecol. Prog. Ser. 147: 1–9.

Maravelias, C. D. et al. 2000a. Modelling spatio-temporal effects of environment on Atlantic herring, *Clupea harengus*. – Env. Biol. Fish 58: 157–172.

Maravelias, C. D. et al. 2000b. Seabed substrate, water depth and zooplankton as determinants of the prespawning spatial aggregation of North Atlantic herring. – Mar. Ecol. Prog. Ser. 195: 249–259.

McQuinn, I. 1997. Metapopulations and the Atlantic herring. – Rev. Fish Biol. Fisher. 7: 297–329.

Misund, O. et al. 1997. Migration behaviour of Norwegian spring spawning herring when entering the cold front in the Norwegian Sea. – Sarsia 82: 107–112.

Misund, O. et al. 1998. Distribution, migration and abundance of Norwegian spring spawning herring in relation to the temperature and zooplankton biomass in the Norwegian Sea as recorded by coordinated surveys in spring and summer 1996. – Sarsia 83: 117–127.

Nøttestad, L. et al. 2007. Herring at the Arctic front: influence of temperature and prey on their spatio-temporal distribution and migration. – Mar. Ecol. 28: 123–133.

Olsen, K. 1971. Influence of vessel noise on the behaviour of herring. – In Kristjonsson, H. (ed.), Modern fishing gear of the world. Fishing News Books, London, UK, pp. 291–293.

Ona, E. et al. 2007. Silent research vessels are not quiet. – J. Acoust. Soc. Am. 121: EL145.

Óskarsson, G. J. et al. 2009. Variation in spatial distribution and migration of Icelandic summer-spawning herring. – ICES J. Mar. Sci. 66: 1762–1767.

Planque, B. et al. 2006. Typology of hydrological structures modelled and observed over the Bay of Biscay shelf. – Sci. Mar. 70S1: 43–50.

Prokopchuk, I. and Sentyabov, E. 2006. Diets of herring, mackerel, and blue whiting in the Norwegian Sea in relation to *Calanus finmarchicus* distribution and temperature conditions. – ICES J. Mar. Sci. 63: 117–127.

Simpson, J. 1981. The shelf-sea fronts: implications of their existence and behaviour. – Philos. T. Roy. Soc. A 302: 531–546.

Sinclair, M. and Iles, T. D. 1985. Atlantic herring (*Clupea harengus*) distributions in the gulf of Maine – Scotian shelf area in relation to oceanographic features. – Can. J. Fish. Aquat. Sci. 42: 880–887.

Slotte, A. 1999. Differential utilization of energy during wintering and spawning migration in Norwegian spring-spawning herring. – J. Fish Biol. 58: 338–355.

Su, Y. et al. 2011. Multiple imputation with diagnostics (mi) in R: opening windows into the black box. – J. Stat. Softw. 45: 1–31.

Toresen, R. and Østvedt, J. 2000. Variation in abundance of Norwegian spring-spawning herring (*Clupea harengus*, Clupeidae) throughout the 20th century and the influence of climatic fluctuations. – Fish Fish. 1: 231–256.

Utne, K. R. et al. 2012. Estimating the consumption of *Calanus finmarchicus* by planktivorous fish in the Norwegian Sea using a fully coupled 3D model system. – Mar. Biol. Res. 8: 527–547.

Vabø, R. et al. 2002. The effect of vessel avoidance of wintering Norwegian spring spawning herring. – Fish. Res. 58: 59–77.

**Appendix 4: R code and data for SPDE models**

The folder 'Macdonald et al._R code and data.zip' (deposited in the Dryad Digital Repository <http://datadryad.org/>), contains R code and data to run all models described in the paper. Due to confidentially issues, the 'herring_data.csv' dataset is a modified version of that used in the paper, so results of the analyses will differ. However, to encourage further exploration of our specific results, we include the 'quadres2_sLap.Rdata', a list containing model output that allows readers to reproduce the figures and tables presented in the manuscript.

Key components of the R code include:-

(1) Preparing the data for modelling, allowing for different degrees of linearity and non-stationarity in the covariates and different specifications of the spatiotemporal random effects.
(2) Creating a triangulated mesh upon which the GMRFs can be calculated.
(3) Fitting the models, assessing model fit and predictive performance.
(4) Extracting results from the posterior distribution and plotting summaries.
(5) Making spatial predictions to an area of interest within the time series.
(6) Assessing predictive performance to seasons outside the time series.

Folder name: 'Macdonald et al._R code and data.zip'

Relevant files: i) 'Herring models_23yrs.R' (R code and functions for SPDE models)
ii) 'mesh creation.R' (R code for different mesh resolutions)
iii) 'herring_data.csv' (.csv file containing point-referenced occurrence/absence records and covariates)

iv) ‘bisland.csv’ (coordinates of Icelandic coast)

v) ‘Adult-recruit ratios_SSB_numbers.csv’ (time series of demographic parameters for Icelandic summer spawning herring)

vi) ‘space_grid.csv’ (coordinates for spatial prediction grid)

vii) ‘quadres2_sLap.Rdata’ (a four-element list containing model output for plotting Figs. 3-5, A7, reproducing Tables 2, 3, A1-A3, and summarizing key results). This list is accessed directly through the ‘Herring models_23yrs.R’ R script.

viii) ‘Final prediction rasters’ (folder containing covariate layers for making spatial predictions for a subset of seasons)

**Appendix 5: Prior specification for the space-time models**

We assigned vague Gaussian priors for all fixed effects N(0, 1000) and the intercept N(0, ∞) in the *stationary* and *partly non-stationary* models. Although information on the influence of some environmental variables on herring occurrence is available from previous work that could be used to inform prior specification, this information relates to other herring stocks at other times of year. These stocks are exposed to markedly different oceanographic conditions compared with those experienced by the ISS herring during the autumn and winter months. To this end, we chose to assign vague normal priors to all of our fixed effects, but tested the sensitivity of our results to prior choice by refitting the *stationary* 'no space' models using Cauchy priors with mean 0 and scale = 2.5 for fixed effect covariates and scale = 10 for the intercept in the 'arm' R package (Gelman et al. 2008).

For the *non-stationary* models, the rw1 models specified for the time-varying coefficients were defined by a Gaussian distribution N(0, *prec***R**), where *prec* is the precision parameter assigned a Gamma(1, 5e-05) prior, and **R** is a fixed structure matrix reflecting the model's neighbourhood structure. We also tried various ar1 models for these time-varying terms, using a range of 'Penalized Complexity' priors that control the degree of correlation among seasons (see Simpson et al. 2015 for further details). We found that the rw1 models gave essentially the same results, yet with vast computational benefits, so we used these throughout. The SPDE model is defined by hyperparameters log($\tau$) and log($\kappa$), (related to the spatial range $\rho$, and marginal variance $\sigma_{\omega}^2$) which were given normal independent priors N(0, 1), and the coefficient '$a$' that controls the degree of correlation in the spatial field between seasons, to which we assigned N(0, 0.15).

## References

Gelman, A. et al. 2008. A weakly informative default prior distribution for logistic and other regression models. – Ann. Appl. Stat. 2: 1360–1383.

Simpson, D. P. et al. 2015. Penalising model component complexity: a principled, practical approach to constructing priors. – arXiv 1403.4630 [stat.ME].

## Appendix 6: Spatial prediction

*Scaling covariates to match prediction grain size*

Where the spatial resolution of covariates used in model fitting was smaller (i.e. all dynamic environmental covariates at ~1 × 1 km), we aggregated the smaller cells to match the 0.1° longitude × 0.05° resolution of the prediction grid, and used the mean value of the aggregated cells. In the case of the *C. finmarchicus* biomass layers (CF_Aug) (extracted at 20 × 20 km resolution for model fitting), we used bilinear interpolation with the 'resample' function in the 'raster' package in R to create layers with the same extent and resolution as the prediction grid. For the fishing magnitude variable (fish_magnitude), we summed the grid cell values for each week in each fishing year (i.e. October to January inclusive), resulting in one layer reflecting total fishing magnitude for each of year.

*Prediction to* t+*1* (see Appendix 4 for R code for running all analyses)

We used the best *partly non-stationary* model (i.e. part_ns5) specification to fit models to the first 18, 19, 20 and 21 years of data. We wanted to see how well we could predict the observed occurrences and absences in the 19th, 20th, 21st and 22nd years respectively. For this, we need to be able to estimate the $distrib_{t-1}$ regression coefficient for $t$+1. We tested if we could do this by examining relationships between the time series of $distrib_{t-1}$ in the fitted models and nine demographic parameters for the ISS herring stock (see *Step 2* below). If a strong correlation existed with one or several demographic factors, we then fitted a GLM to predict the $distrib_{t-1}$ coefficient from the demographic factor. Assuming that we have data for (or can estimate) the demographic parameter in $t$+1, we can then feed this value into the GLM and estimate the $distrib_{t-1}$ coefficient in $t$+1. The steps we used are summarised as follows.

*Step 1:* Use the more general *partly non-stationary* model. In this model, all covariates are kept stationary in time, except for spatial memory covariate (i.e. $distrib_{t-1}$) which is allowed to vary by year according to rw1 dynamics. Note that the $distrib_{t-1}$ covariate represents the spatial occurrence pattern in the previous year, $t$-1.

*Step 2:* Examine correlations between the 22-year time series of $distrib_{t-1}$ coefficients from the above model and time series of the nine demographic parameters for the ISS herring stock described in main text under '*Correlation among covariates and demographic parameters*'. They are as follows:-

i) Number of age3:age4+

ii) Number of age3:age4to7

iii) Number of age3:age8to13

iv) Spawning stock biomass (SSB)

v) Spawning stock numbers (SSN)

vi) Number of experienced individuals (*n* age4+)

vii) Number of young experienced individuals (*n* age4to7)

viii) Number of old experienced individuals (*n* age8to13)

ix) Mean age of the spawning stock (mean age).

*Step 3:* If a strong correlation with one or more of these parameters is found, run a GLM to model $distrib_{t-1}$ as a function of the demographic parameter.

This analysis revealed a strong positive correlation between SSN on the regression coefficients for distrib$_{t-1}$ across the time series. We then fitted a linear model and found a significant effect of SSN on the distrib$_{t-1}$ regression coefficients. This means that we may be able to predict the distrib$_{t-1}$ coefficient in $t$+1, given SSN in $t$+1 is known or can be estimated.

*Step 4:* Subset full dataset to get first 18, 19, 20 and 21 years of observations and prepare data for model fitting.

*Step 5:* Fit models to the first 18, 19, 20 and 21 years of the dataset. These models use the same formulation as the best *partly non-stationary* model with linear and quadratic terms for environmental covariates, a rw1 model for distrib$_{t-1}$ and independent realizations of the spatiotemporal random field ($\omega$) each year.

*Step 6:* For each of the four models in turn, extract the coefficients for the distrib$_{t-1}$ time series.

*Step 7:* Correlate this time series with the equivalent time series of SSN.

*Step 8:* If strong correlation with SSN is found, fit a GLM to model the distrib$_{t-1}$ coefficients as function of SSN.

*Step 9:* Get (or predict) an estimate of SSN for $t$+1 (i.e. from stock assessment in year $t$). In our case, we already have the SSN estimates for the 19$^{th}$, 20$^{th}$, 21$^{st}$ and 22$^{nd}$ years.

*Step 10:* Feed this value into the GLM to predict the distrib$_{t-1}$ coefficient in $t$+1.

*Step 11:* Calculate a new multiplier for the $distrib_{t-1}$ covariate for the year we want to predict to. For example, for predicting 2010_11, we divide the predicted coefficient from *Step 10* by the estimated coefficient from the fitted 18-year model. This value is the new coefficient we use multiply the $distrib_{t-1}$ covariate values for 2010_11 by in the 'effects' list of the prediction stack.

*Step 12:* Validate these models on held-out observations in $t$+1, and assess predictive capacity for the next year (i.e. $t$+1). Do this by creating a validation stack with covariates referenced for $t$+1 and refitting the 18, 19, 20 and 21 year models with response = NA, using the spatiotemporal random effect estimated for year $t$. Examine model calibration and predicted outcomes versus observations (using cross-validated mean Brier scores and AUC).

*Step 13:* Finally, make spatial predictions across the entire domain for the four $t$+1 prediction years (i.e. 2010_2011, 2011_2012, 2012_2013, 2013_2014).

**Appendix 7: Additional details on wintering area characteristics, modelling output, occurrence-environment relationships in wintering ISS herring and environmental sensitivity in other herring stocks**

*Environmental characteristics of wintering areas*

By charting the hydrographic variability in wintering areas across seasons, we gain some insight into the level of environmental plasticity exhibited by wintering ISS herring. Sea surface temperatures (i.e. SST) in the wintering areas differed somewhat among seasons; however, most estimates were in the range of ~ 4 to 9°C, and rarely below 3°C (Fig. A6a). In 19 out of the 22 seasons, median SST's were higher in wintering areas than in areas where herring were absent. Marked among-year consistency was observed in both sea surface salinity (i.e. SSS) and the degree of stratification (i.e. PEA) during the early to middle part of the time series, yet conditions inshore, inside the fjords occupied during the 'West' phase were substantially more mixed and less saline (Fig. A6b, c). Wintering areas were also typified by relatively small vertical temperature gradients (Fig. A6d), low and uniform current velocities (Fig. A6e), depths ranging from ~500 m off the east coast up to ~ 20 m inshore on the west coast (Fig. A6f), and low bathymetric relief across all seasons (Fig. A6g).

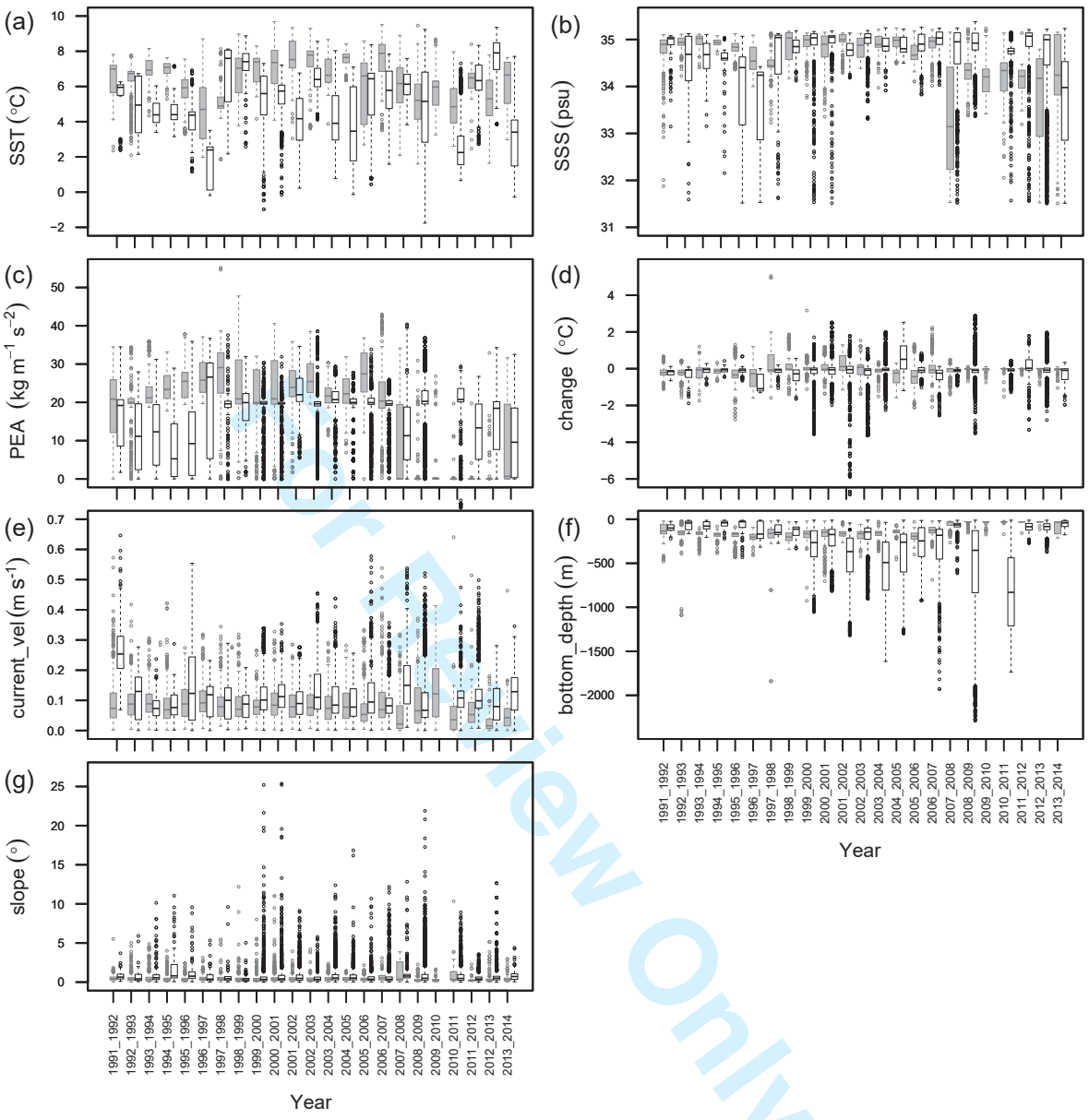


Fig. A6. Seasonal variation in environmental characteristics of wintering areas occupied by ISS herring between 1991_1992 and 2013_2014. Boxplots show the annual distributions of environmental data associated with each occurrence record (grey boxes) and absence record (white boxes) in our dataset. Data for all dynamic variables (i.e., A–E) were extracted on the day of capture at 1 × 1 km resolution around each catch location from the CODE ocean model (Logemann et al. 2013). Data for both static variables (i.e., F,G) were extracted at 30 arcsec resolution around each catch location from the GEBCO database (www.gebco.net). The median (thick horizontal line), and lower (Q1) and upper (Q3) quartiles (box limits) are shown for each year. Upper whiskers represent the smaller of the maximum value for each variable and Q3 + 1.5 × interquartile range, and lower whiskers are the larger of the minimum value and Q1 – 1.5 × interquartile range. Circles are data points outside these ranges. Note that no absence data was available for 2009_2010.

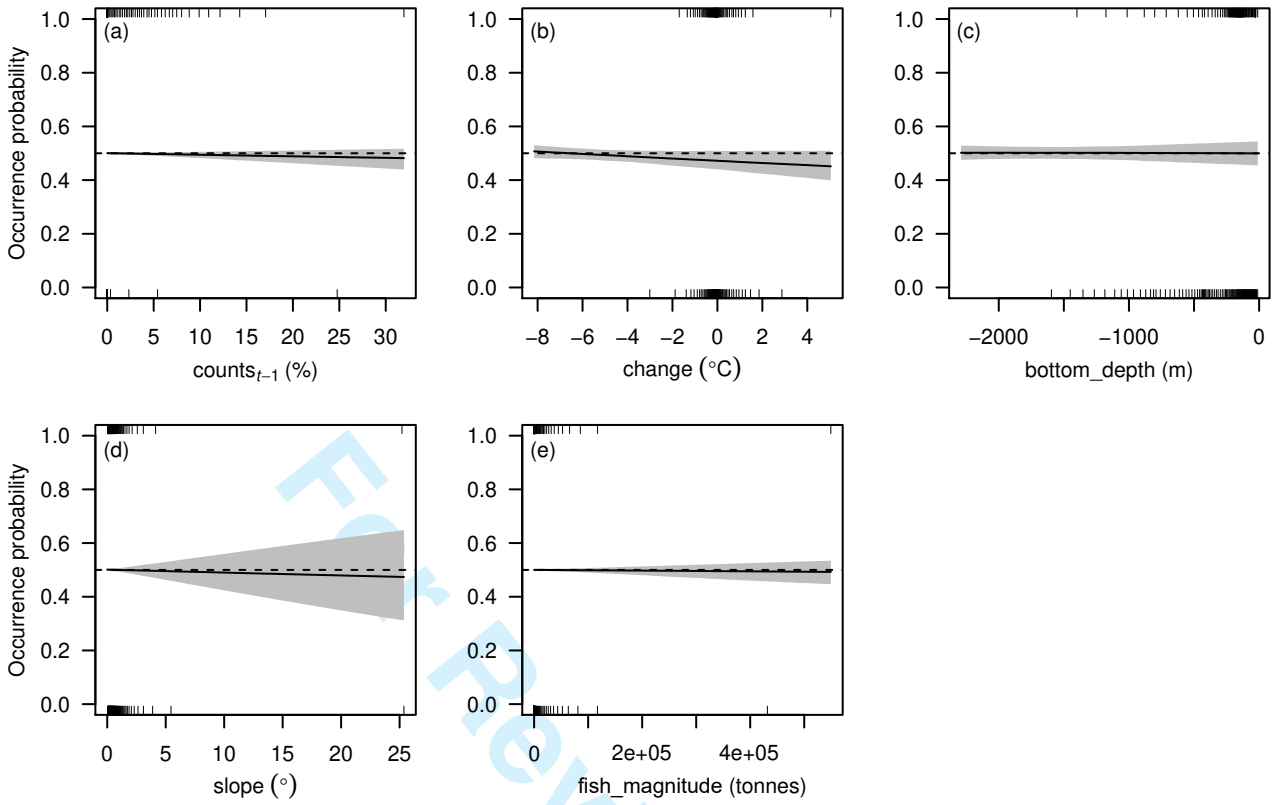


Fig. A7. Marginal effect plots for non-significant covariates in the best *partly non-stationary* model (part_ns5): (a) density of occurrence records in *t*-1 (counts$_{t-1}$), (b) vertical temperature gradient (change), (c) bottom depth, (d) bottom slope and (e) fishing intensity in the previous week (see Table 1 for detailed descriptions and derivation). Black lines represent the median estimate of 1000 draws from the posterior distribution for a sequence of 100 values across the full range of each covariate, and grey-shaded regions are 95% CIs. Tick marks denote the percentile distribution of raw data for each covariate for occurrence records (top of plots) and absence records (bottom of plots). Plots (a and e) represent the linear effect, and (b, c and d) the quadratic effect of the covariate.

Table A1. Posterior mean estimates and 95% credible intervals for fixed effects, the spatial range ($\rho$) and marginal variance ($\sigma^2_\omega$) for the best-performing *stationary*, *partly non-stationary* and *fully non-stationary* models. Estimates for random effect covariates with time-varying coefficients in the *non-stationary* models are presented graphically in Fig. 3. All models were fitted using simplified Laplace approximation.

| Parameter | *Stationary model* (s9) | | | *Partly non-stationary* model (part_ns5) | | | *Fully non-stationary* model (full_ns5) | | |
|---|---|---|---|---|---|---|---|---|---|
| | mean | $Q_{2.5\%}$ | $Q_{97.5\%}$ | mean | $Q_{2.5\%}$ | $Q_{97.5\%}$ | mean | $Q_{2.5\%}$ | $Q_{97.5\%}$ |
| $\alpha$ | -0.140 | -0.206 | -0.075 | -0.183 | -0.204 | -0.161 | -0.137 | -0.170 | -0.104 |
| $\text{distrib}_{t\text{-}1}$ | 0.487 | 0.440 | 0.534 | | | | | | |
| $\text{counts}_{t\text{-}1}$ | 0.004 | -0.021 | 0.029 | -0.010 | -0.041 | 0.020 | | | |
| SST | 0.247 | 0.205 | 0.290 | 0.170 | 0.132 | 0.209 | | | |
| $\text{SST}^2$ | 0.146 | 0.100 | 0.192 | 0.090 | 0.046 | 0.134 | | | |
| SSS | -0.168 | -0.224 | -0.113 | -0.109 | -0.162 | -0.056 | | | |
| $\text{SSS}^2$ | -0.051 | -0.070 | -0.032 | -0.037 | -0.056 | -0.018 | | | |
| PEA | 0.116 | 0.087 | 0.145 | 0.127 | 0.098 | 0.156 | | | |
| $\text{PEA}^2$ | 0.083 | 0.052 | 0.113 | 0.076 | 0.046 | 0.107 | | | |
| change | -0.001 | -0.026 | 0.024 | -0.005 | -0.029 | 0.020 | | | |
| $\text{change}^2$ | -0.005 | -0.014 | 0.004 | -0.005 | -0.014 | 0.003 | | | |
| current_vel | -0.052 | -0.078 | -0.026 | -0.039 | -0.065 | -0.014 | | | |
| $\text{current\_vel}^2$ | 0.017 | -0.007 | 0.041 | 0.014 | -0.010 | 0.038 | | | |
| bottom_depth | 0.010 | -0.044 | 0.063 | -0.003 | -0.055 | 0.049 | | | |
| $\text{bottom\_depth}^2$ | 0.009 | -0.027 | 0.044 | 0.000 | -0.035 | 0.034 | | | |
| slope | -0.009 | -0.039 | 0.020 | -0.011 | -0.041 | 0.018 | | | |
| $\text{slope}^2$ | 0.000 | -0.007 | 0.006 | 0.000 | -0.006 | 0.007 | | | |
| fish_magnitude | -0.003 | -0.023 | 0.018 | -0.003 | -0.024 | 0.019 | | | |
| CF_Aug | 0.022 | -0.004 | 0.048 | 0.036 | 0.012 | 0.060 | | | |
| $\text{year}_{9394}$ | -0.147 | -0.272 | -0.021 | | | | | | |
| $\text{year}_{9495}$ | -0.201 | -0.329 | -0.074 | | | | | | |
| $\text{year}_{9596}$ | -0.034 | -0.164 | 0.095 | | | | | | |
| $\text{year}_{9697}$ | 0.061 | -0.075 | 0.197 | | | | | | |
| $\text{year}_{9798}$ | -0.137 | -0.294 | 0.020 | | | | | | |
| $\text{year}_{9899}$ | -0.055 | -0.191 | 0.081 | | | | | | |
| $\text{year}_{9900}$ | -0.022 | -0.102 | 0.057 | | | | | | |
| $\text{year}_{0001}$ | -0.038 | -0.124 | 0.048 | | | | | | |
| $\text{year}_{0102}$ | -0.068 | -0.157 | 0.020 | | | | | | |
| $\text{year}_{0203}$ | -0.105 | -0.186 | -0.023 | | | | | | |
| $\text{year}_{0304}$ | -0.016 | -0.092 | 0.060 | | | | | | |
| $\text{year}_{0405}$ | -0.051 | -0.139 | 0.035 | | | | | | |
| $\text{year}_{0506}$ | -0.060 | -0.148 | 0.029 | | | | | | |
| $\text{year}_{0607}$ | -0.050 | -0.138 | 0.037 | | | | | | |
| $\text{year}_{0708}$ | -0.093 | -0.202 | 0.016 | | | | | | |
| $\text{year}_{0809}$ | -0.077 | -0.149 | -0.004 | | | | | | |
| $\text{year}_{0910}$ | -0.106 | -0.427 | 0.214 | | | | | | |
| $\text{year}_{1011}$ | -0.009 | -0.105 | 0.087 | | | | | | |
| $\text{year}_{1112}$ | -0.093 | -0.184 | -0.003 | | | | | | |
| $\text{year}_{1213}$ | -0.248 | -0.333 | -0.162 | | | | | | |
| $\text{year}_{1314}$ | 0.003 | -0.185 | 0.189 | | | | | | |
| $\rho$ | 9.945 | 8.190 | 11.768 | 10.395 | 8.547 | 12.314 | 11.247 | 9.212 | 13.364 |
| $\sigma^2_\omega$ | 0.107 | 0.081 | 0.135 | 0.109 | 0.081 | 0.137 | 0.086 | 0.063 | 0.110 |

Table A2. Structure and performance of candidate space-time occurrence models for wintering Atlantic herring. Each model contains all covariates (full), and results are shown for fitting using Gaussian approximation (see Table 2 in main text for results based on a simplified Laplace approximation strategy). s1-s15, *stationary* models; part_ns1-part_ns9, *partly non-stationary* models; full_ns1-full_ns9, *fully non-stationary* models. Covariate form refers to models that include linear terms only (linear), and quadratic terms (quadratic) or penalized regression spline terms for environmental covariates (spline). Structure details the form of the spatiotemporal random effect $\omega_{i,t}$, and if a fixed factor for year ($year_t$) was included; no-space/no-time, no spatially or temporally structured effects; time_indep, independent realization of the spatial random field at each $t$; time_corr, temporal correlation (ar1) is considered in the realization of the spatial random field at each $t$. The best-performing model within each stationarity class is shown in bold.

| Model | Covariate form | Structure | DIC | mean log score | Brier score | AUC |
|---|---|---|---|---|---|---|
| *Stationary* | | | | | | |
| s1 | linear | full (no-space/no-time) | 49104.4 | 0.504 | 0.157 | 0.934 |
| s2 | linear | full + $year_t$ | 48354.0 | 0.496 | 0.154 | 0.974 |
| s3 | linear | full + time_indep $\omega_{i,t}$ | 41877.0 | 0.429 | 0.123 | 0.993 |
| s4 | linear | full + $year_t$ + time_indep $\omega_{i,t}$ | 41816.8 | 0.429 | 0.123 | 0.993 |
| s5 | linear | full + time_corr $\omega_{i,t}$ | 41881.7 | 0.429 | 0.123 | 0.992 |
| s6 | quadratic | full (no-space/no-time) | 48917.4 | 0.502 | 0.156 | 0.943 |
| s7 | quadratic | full + $year_t$ | 48060.0 | 0.493 | 0.152 | 0.981 |
| s8 | quadratic | full + time_indep $\omega_{i,t}$ | 41737.1 | 0.428 | 0.122 | 0.994 |
| **s9** | **quadratic** | **full + $year_t$ + time_indep $\omega_{i,t}$** | **41634.0** | **0.427** | **0.122** | **0.995** |
| s10 | quadratic | full + time_corr $\omega_{i,t}$ | 41738.2 | 0.428 | 0.122 | 0.994 |
| s11 | spline | full (no-space/no-time) | 49232.4 | 0.505 | 0.158 | 0.917 |
| s12 | spline | full + $year_t$ | 48366.0 | 0.496 | 0.154 | 0.973 |
| s13 | spline | full + time_indep $\omega_{i,t}$ | 41912.0 | 0.430 | 0.123 | 0.993 |
| s14 | spline | full + $year_t$ + time_indep $\omega_{i,t}$ | 41838.2 | 0.429 | 0.123 | 0.993 |
| s15 | spline | full + time_corr $\omega_{i,t}$ | 41913.5 | 0.430 | 0.123 | 0.992 |
| *Partly non-stationary* | | | | | | |
| part_ns1 | linear | full (no-space/no-time) | 48953.5 | 0.502 | 0.157 | 0.952 |
| part_ns2 | linear | full + time_indep $\omega_{i,t}$ | 41738.2 | 0.428 | 0.122 | 0.993 |
| part_ns3 | linear | full + time_corr $\omega_{i,t}$ | 41746.6 | 0.428 | 0.122 | 0.992 |
| part_ns4 | quadratic | full (no-space/no-time) | 48726.0 | 0.500 | 0.155 | 0.960 |
| **part_ns5** | **quadratic** | **full + time_indep $\omega_{i,t}$** | **41626.5** | **0.427** | **0.122** | **0.994** |
| part_ns6 | quadratic | full + time_corr $\omega_{i,t}$ | 41630.6 | 0.427 | 0.122 | 0.994 |
| part_ns7 | spline | full (no-space/no-time) | 49081.0 | 0.504 | 0.157 | 0.943 |
| part_ns8 | spline | full + time_indep $\omega_{i,t}$ | 41784.9 | 0.428 | 0.122 | 0.993 |
| part_ns9 | spline | full + time_corr $\omega_{i,t}$ | 41790.5 | 0.429 | 0.122 | 0.992 |
| *Fully non-stationary* | | | | | | |
| full_ns1 | linear | full (no-space/no-time) | 47333.0 | 0.486 | 0.148 | 0.989 |
| full_ns2 | linear | full + time_indep $\omega_{i,t}$ | 41342.6 | 0.424 | 0.120 | 0.996 |
| full_ns3 | linear | full + time_corr $\omega_{i,t}$ | 41351.8 | 0.424 | 0.120 | 0.995 |
| full_ns4 | quadratic | full (no-space/no-time) | 46760.2 | 0.480 | 0.146 | 0.995 |
| **full_ns5** | **quadratic** | **full + time_indep $\omega_{i,t}$** | **41057.3** | **0.421** | **0.119** | **0.997** |
| full_ns6 | quadratic | full + time_corr $\omega_{i,t}$ | 41065.8 | 0.421 | 0.119 | 0.997 |
| full_ns7 | spline | full (no-space/no-time) | 46975.4 | 0.482 | 0.147 | 0.993 |
| full_ns8 | spline | full + time_indep $\omega_{i,t}$ | 41228.6 | 0.423 | 0.119 | 0.996 |
| full_ns9 | spline | full + time_corr $\omega_{i,t}$ | 41236.4 | 0.423 | 0.120 | 0.996 |

Table A3. Results for single-term deletions from the best *stationary* model (s9). Note that for environmental covariates, this equates to deletion of both linear and quadratic terms.

| Model | Covariate form | Structure | DIC | mean log score | mean Brier score |
|---|---|---|---|---|---|
| s9 | quadratic | full + year$_t$ + time-indep $\omega_{i,t}$ | 41629.0 | 0.427 | 0.122 |
| Deletions from s9 | | | | | |
| - distrib$_{t-1}$ | | | 42168.6 | 0.432 | 0.124 |
| - counts$_{t-1}$ | | | 41629.0 | 0.427 | 0.122 |
| - SST | | | 41858.6 | 0.429 | 0.123 |
| - SSS | | | 41680.3 | 0.427 | 0.122 |
| - PEA | | | 41725.6 | 0.428 | 0.122 |
| - change | | As above | 41631.0 | 0.427 | 0.122 |
| - current_vel | | | 41653.8 | 0.427 | 0.122 |
| - bottom_depth | | | 41629.0 | 0.427 | 0.122 |
| - slope | | | 41630.0 | 0.427 | 0.122 |
| - fish_magnitude | | | 41630.4 | 0.427 | 0.122 |
| - CF_Aug | | | 41637.9 | 0.427 | 0.122 |

*Further details on modelled occurrence-environment relationships*

Whilst extreme low temperature conditions can impact directly on physiology (see main text for details), and logic dictates that preferences for lower velocity zones may promote energy savings and compensate somewhat for any metabolic costs incurred through residing in warmer waters (see Liao et al. 2003), the search for causality in the relationships we observed between ψ, SSS and PEA (see Fig. 3b, c) is more challenging. Given herring's euryhaline nature, and ability to inhabit brackish and fresh waters down to 1 psu in the Baltic Sea (Teacher et al. 2013, Miethe et al. 2014), it is clear that the lowest salinities encountered in Icelandic surface waters (i.e. ~ 31.5 psu) would not impose high physiological demands. Likewise, the highest SSS in the region throughout the study period approached 35.4 psu – a value close to surface measurements made in Ofotfjorden, Norway, during the late 1980s and early 1990s when it harbored the majority of the wintering NSS stock (Dommasnes et al. 1994). As these bounding values are well within the known tolerance range of the species, and that the vertical salinity gradient in the upper water column (between 1 and 100 m) across our dataset never exceeded 2 psu, we argue that wintering ISS herring undertaking diurnal vertical migrations would not have been exposed to strong physiological forcing by salinity, and that any effects we see are likely indirect. With regard to our results for PEA, although it could be argued that selection of less stratified, shallower, fresher waters, as seen during the recent years of our time series (Fig. A6c) could provide energetic benefits to vertically migrating herring (Huse and Ona 1996), we see no direct fitness advantage to wintering fish of inhabiting more stratified waters.

In the absence of any clear mechanistic basis for these findings, we propose two alternatives. First, active avoidance of cold water masses could indirectly influence the population's response to salinity and stratification. The warmer waters encountered at the time and

location of the bulk of successful fishing events were also often characterized by higher PEA values (particularly during the 'East' and 'Eastwest' phases), weaker currents and lower SSS (particularly close to the coast during the inshore 'West' phase) compared with conditions associated with survey-derived absence records (Fig. A6). Such hydrographic conditions are common in coastal Icelandic waters (Appendix 3, Fig. A2, authors' unpublished data), and other regions at certain times of year (e.g. North Sea: Maravelias and Reid (1995); Bay of Biscay: Planque et al. (2006), Huret et al. (2013); Lindåspollene, Norway: Langård et al. (2014)), and residence in them during winter would shape the response to each of these covariates in the way we observe (see Fig. 3)[1]. Second, preference for moderately-stratified zones, particularly during the early and middle years of the time series (Fig. A6c) could also reflect adaptations for predator-avoidance. During this period, the locations of our occurrence records were typically quite distant from major fronts off the northwest and north coast (i.e. boundaries between strong vertical temperature gradients – see 'change' plot in Appendix 3, Fig. A2, and Pálsson and Thorsteinsson (2003)) or strongly-mixed zones offshore (i.e. those associated with lower PEA values) often rich in herring predators like adult cod (Pálsson and Thorsteinsson 2003, Pálsson and Björnsson 2011). Our results may reflect high predator densities in these years, with occupation of more stratified areas affording some release from predation pressure. Although we included recent fishing activity in our analysis as a potential top-down control, spatially-resolved data on the distribution of other non-human predators in the study region during winter are needed to allow a more explicit examination of predator

[1] We note that our PEA estimates may underestimate the true degree of stratification in very shallow zones (i.e. < 15 m deep), due to limits on the minimum vertical bin-depth of the CODE model (= 2.5 m). However, given that only 68 (0.1%) of our records were located in such shallow waters – in all cases near shore in fjords, and that these locations are generally influenced strongly by river run-off and tidal processes which enforce water-column mixing, we contend that slight inaccuracies in our estimates would have negligible effects on model estimation and prediction.

effects and their environmental interactions on herring spatial distribution patterns (see the '*Fishing and predation*' in the main text for a further discussion).

*Issues of scale*

That environmental factors contributed to the wintering patterns we observed (at least in some years) contrasts with recent work on wintering ISS herring (Óskarsson et al. 2009) and NSS herring (Huse et al. 2010). Both studies found no clear evidence for environmental signals as determinants of wintering dynamics. Huse et al. (2010) showed that the six different wintering locations used by the NSS stock over the past 50+ years, were characterized by vastly different environmental conditions. In Iceland, Óskarsson et al. (2009) found no support for a temperature effect on the ISS wintering patterns of the late 1970s up until the mid-2000s, but suggested that temperature may still play a role at finer scales. We agree with this, and posit that the inability to detect a signal in these studies may have arisen from a mismatch between the scale of the temperature data used (i.e. single CTD stations measured annually), and the scale of the process giving rise to the occurrence of herring in that area. In developing our study, we acknowledged the variable spatial and temporal scales at which stimuli may act (Levin 1992, Witman et al. 2015); shoaling species' responses to them emerging as a result of exposure to, and/or retention of specific cues experienced during early age (e.g. olfactory imprinting), the social transmission of long-standing traditions among generations (e.g. Fernö et al. 2011), or the spontaneous spread of information among individuals, that can manifest in rapid expansion in school size (Makris et al. 2009), and elicit fast, school-wide responses to environmental gradients, prey resources or predation threats (Doksæter et al. 2009, Makris et al. 2009). We deemed it crucial to capture this variability in our models. Therefore, we extracted environmental data from the CODE model (Logemann et al. 2013) at several grain sizes and temporal windows (Table 1,

Appendix 3), and, through prioritizing ecological reasoning in the trade-off between data quality and availability, selected scales for the other variables (Table 1, Appendix 3). Our goal here was to match as closely as possible the scale of processes acting on herring schools in both the pre-wintering period and during residence in the wintering areas (i.e. behavioral states 1 and 2), given the scale of the fishery purse-seine shots that comprise our occurrence data. Although the scales of our covariates likely miss several processes relevant to wintering herring, particularly the complexities of intra-school shoaling dynamics and diurnal vertical migration (Mackinson et al. 1999), the potential impact of larger-scale, non-spatial climatic indices (e.g. North Atlantic Oscillation (NAO) winter index, Atlantic Multidecadal Oscillation (AMO) – see Engelhard et al. 2011) and possibly, interactions between past environmental conditions and spatial persistence in distribution (see Corten 2002, Rindorf and Lewy 2006), we feel that the spatial and temporal resolution we chose provided a plausible linkage between processes and observations. With continuing improvements in the quality of measured and modelled data available for marine systems and the species within them, opportunities are emerging to incorporate more mechanistic information into spatial models (e.g. Teal et al. in press). Such process-based approaches allow the 'best' scale to emerge naturally from the physiological process of interest, and by their general nature, rooted in data or theory on metabolic rates, hold great promise for predicting species' distributions when observational data are limited. We anticipate rapid progress in this field in the coming years (see also Appendix 9 '*Notes on the modelling approach'*).

*Environmental sensitivity in herring*

Sensitivity to environmental forcing has also been seen in other herring stocks during winter (e.g. Corten 1999a), and at different times of the year. For example, in a series of papers focused on North Sea herring, Maravelias and colleagues demonstrated strong effects of

temperature gradients, salinity, stratification, zooplankton biomass and bottom topography in shaping pre-spawning summer distribution (e.g. Maravelias and Haralabous 1995, Maravelias and Reid 1997, Maravelias et al. 2000a, b). The direction and magnitude of these effects differed substantially from our study, a finding that was anticipated given that the ISS stock is located near the northerly range-edge for the species, and is therefore exposed to vastly different environmental conditions to those typically encountered in the North Sea. Moreover, these North Sea papers and similar studies in Nordic seas (e.g. Misund et al. 1998, Jakobsson and Østvedt 1999, Kvamme et al. 2003, Nøttestad et al. 2007, Broms et al. 2012) have often focused on distribution patterns during spring and summer, periods of high feeding activity in which adult herring can be tightly linked to prey resources either directly (e.g. Holst et al. 1997, Maravelias and Reid 1997, Olsen et al. 2007) or indirectly through hydrographic proxies. Some examples of the latter include the northwards displacement of the feeding distribution of North Sea herring in the 1980s, posited as a response to intensification of the shelf edge current leading to increased productivity off the Norwegian coast, concurrent with elevated water temperatures causing a range contraction of *C. finmarchicus* to northern waters (Corten and Van de Kamp 1992, Corten 2001). And, the reappearance of the Aberdeen Bank spawning population in 1983, suggested as a corollary of increased Atlantic inflow into the North Sea that caused a redistribution of key planktonic prey and their predators (e.g. pre-spawning herring) southwards (Corten 1999b). It has also been suggested that the quality of future spawning habitat (e.g. water depth, seabed roughness – Maravelias et al. (2000b), Langård et al. (2014a)), and distance to spawning grounds (Jech and Stroman 2012) can affect pre-spawning distribution to some extent. These examples illustrate how environmental and biotic factors can interact in complex ways to shape herring feeding and pre-spawning distributions, yet such processes are largely irrelevant during residence on wintering grounds (i.e. during behavioral state 2 – see main text for definition).

**References**

Broms, C. et al. 2012. Navigation mechanisms of herring during feeding migration : the role of ecological gradients on an oceanic scale. – Mar. Biol. Res. 8: 37–41.

Corten, A. 1999a. A proposed mechanism for the Bohuslan herring periods. – ICES J. Mar. Sci. 56: 207–220.

Corten, A. 1999b. The reappearance of spawning Atlantic herring (*Clupea harengus*) on Aberdeen Bank (North Sea) in 1983 and its relationship to environmental conditions. – Can. J. Fish. Aquat. Sci. 56: 2051–2061.

Corten, A. 2001. Northern distribution of North Sea herring as a response to high water temperatures and/or low food abundance. – Fish. Res. 50: 189–204.

Corten, A. 2002. The role of "conservatism" in herring migrations. Rev. Fish Biol. Fisher. – 11: 339–361.

Corten, A. and Van de Kamp, G. 1992. Natural changes in pelagic fish stocks of the North Sea in the 1980s. – ICES Mar. Sc. 195: 402–417.

Doksæter, L. et al. 2009. Behavioral responses of herring (*Clupea harengus*) to 1-2 and 6-7 kHz sonar signals and killer whale feeding sounds. – J. Acoust. Soc. Am. 125: 554–564.

Dommasnes, A. et al. 1994. Reduced oxygen concentrations in herring wintering areas. – ICES J. Mar. Sci. 51: 63–69.

Engelhard, G. H. et al. 2011. Nine decades of North Sea sole and plaice distribution. – ICES J. Mar. Sci. 68: 1090–1104.

Holst, J. C. et al. 1997. Feeding, *Ichthyophonus* sp. infection, distribution and growth history of Norwegian spring-spawning herring in summer. – J. Fish Biol. 50: 652–664.

Huret, M. et al. 2013. A multi-decadal hindcast of a physical–biogeochemical model and derived oceanographic indices in the Bay of Biscay. – J. Mar. Syst. 109-110: S77–

S94.

Huse, I. and Ona, E. 1996. Tilt angle distribution and swimming speed of overwintering Norwegian spring spawning herring. – ICES J. Mar. Sci. 53: 863–873.

Huse, G. et al. 2010. Establishment of new wintering areas in herring co-occurs with peaks in the "first time/repeat spawner" ratio. – Mar. Ecol. Prog. Ser. 409: 189–198.

Jakobsson, J. and Østvedt, O. J. 1999. A review of joint investigations on the distribution of herring in the Norwegian and Iceland Seas 1950-1970. – Rit Fiskideildar 16: 209–238.

Jech, J. M. and Stroman, F. 2012. Aggregative patterns of pre-spawning Atlantic herring on Georges Bank from 1999-2010. – Aquat. Living Resour. 25: 1–14.

Kvamme, C. et al. 2003. Migration patterns in Norwegian spring-spawning herring: why young fish swim away from the wintering area in late summer. – Mar. Ecol. Prog. Ser. 247: 197–210.

Langård, L. et al. 2014. Thermal stratification influences maturation and timing of spawning in a local *Clupea harengus* population. – J. Fish Biol. 84: 1202–1209.

Levin, S. 1992. The problem of pattern and scale in Ecology. – Ecology 73: 1943–1967.

Liao, J. C. et al. 2003. Fish exploiting vortices decrease muscle activity. – Science 302: 1566–1569.

Logemann, K. et al. 2013. The circulation of Icelandic waters – a modelling study. – Ocean Sci. 9: 931–955.

Mackinson, S. et al. 1999. Cross-scale observations on distribution and behavioural dynamics of ocean feeding Norwegian spring-spawning herring (*Clupea harengus* L.). – ICES J. Mar. Sci. 56: 613–626.

Makris, N. C. et al. 2009. Critical population density triggers rapid formation of vast oceanic fish shoals. – Science 323: 1734–1737.

Maravelias, C. D. and Haralabous, J. 1995. Spatial distribution of herring in the

Orkney/Shetland area (northern North Sea): a geostatistical analysis. – Neth. J. Sea. Res. 34: 319–329.

Maravelias, C. D. and Reid, D. G. 1995. Relationship between herring (*Clupea harengus*, L.) distribution and sea surface salinity and temperature in the northern North Sea. – Sci. Mar. 59: 427–438.

Maravelias, C. D. and Reid, D. G. 1997. Identifying the effects of oceanographic features and zooplankton on prespawning herring abundance using generalized additive models. – Mar. Ecol. Prog. Ser. 147: 1–9.

Maravelias, C. D. et al. 2000a. Modelling spatio-temporal effects of environment on Atlantic herring, *Clupea harengus*. – Env. Biol. Fish 58: 157–172.

Maravelias, C. D. et al. 2000b. Seabed substrate, water depth and zooplankton as determinants of the prespawning spatial aggregation of North Atlantic herring. – Mar. Ecol. Prog. Ser. 195: 249–259.

Miethe, T. et al. 2014. The effects of periodic marine inflow into the Baltic Sea on the migration patterns of Western Baltic spring-spawning herring. – ICES J. Mar. Sci. 71: 519–527.

Misund, O. et al. 1998. Distribution, migration and abundance of Norwegian spring spawning herring in relation to the temperature and zooplankton biomass in the Norwegian Sea as recorded by coordinated surveys in spring and summer 1996. – Sarsia 83: 117–127.

Nøttestad, L. et al. 2007. Herring at the Arctic front: influence of temperature and prey on their spatio-temporal distribution and migration. – Mar. Ecol. 28: 123–133

Olsen, E. M. et al. 2007. Spatially structured interactions between a migratory pelagic predator, the Norwegian spring-spawning herring *Clupea harengus* L., and its zooplankton prey. – J. Fish Biol. 70: 799–815.

Óskarsson, G. J. and Taggart, C. T. 2009. Spawning time variation in Icelandic summer-

spawning herring (*Clupea harengus*). – Can. J. Fish. Aquat. Sci. 66: 1666–1681.

Pálsson, Ó. K. and Björnsson, H. 2011. Long-term changes in trophic patterns of Iceland cod and linkages to main prey stock sizes. – ICES J. Mar. Sci. 68: 1488–1499.

Pálsson, Ó. K. and Thorsteinsson, V. 2003. Migration patterns, ambient temperature, and growth of Icelandic cod (*Gadus morhua*): evidence from storage tag data. – Can. J. Fish. Aquat. Sci. 60: 1409–1423.

Planque, B. et al. 2006. Typology of hydrological structures modelled and observed over the Bay of Biscay shelf. – Sci. Mar. 70S1: 43–50.

Rindorf, A. and Lewy, P. 2006. Warm, windy winters drive cod north and homing of spawners keeps them there. – J. Appl. Ecol. 43: 445–453.

Teacher, A. et al. 2013. Oceanographic connectivity and environmental correlates of genetic structuring in Atlantic herring in the Baltic Sea. – Evol. Appl. 6: 549–567.

Teal, L. R. et al. in press. Physiology-based modelling approaches to characterize fish habitat suitability: their usefulness and limitations. – Estuar. Coast. Shelf Sci. doi:10.1016/j.ecss.2015.11.014.

Witman, J. et al. 2015. Towards an integration of scale and complexity in marine ecology. – Ecol. Monogr. 85: 475–504.

**Appendix 8: Exploring the relationship between adult population size and occupied area.**

Although the spatial inconsistency of our fishery and survey dataset limits precise quantification of expansion or contraction in Icelandic summer spawning (ISS) herring winter distribution over time, we can consider our occurrence records, and their gridded representations in the spatial similarity index (SSI), as a minimum, yet fairly accurate estimate of the realized winter distribution, reflecting the major spatial trends over the 1991_92 to 2013_14 period (Guðmundsdóttir and Sigurðsson 2004, Óskarsson et al. 2009, and see Appendix 1 for further details). Hence, by summing the number of occupied grid cells within each year $t = 1, 2, \ldots, T$, and plotting these values against fishery-independent estimates of adult population size, represented by spawning stock numbers (SSN), we were able to examine the association between abundance and occupied area for wintering ISS herring. We found no evidence of a positive relationship for our data (Fig. A8).

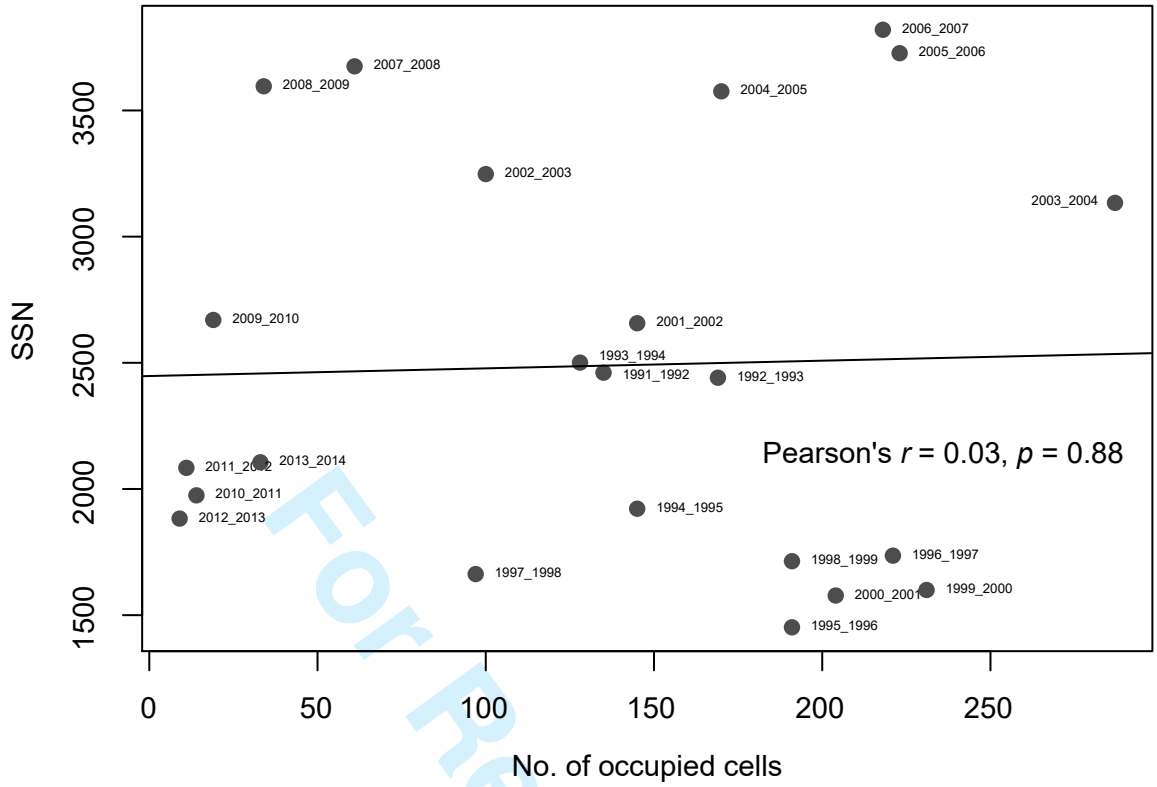


Fig. A8. Plot of adult population size in the ISS herring stock, represented by estimated spawning stock numbers (SSN), against the number of occupied 0.1 longitude × 0.05 latitude grid cells during winter (i.e. October to January) for the 23 years from 1991_92 to 2013_14. Data for the latter are drawn from the distrib$_t$ layers used in the creation of the spatial similarity index (SSI), and are considered as a minimal estimate of occupied area for each year. Estimates for SSN are derived from annual stock assessments for ISS herring conducted by the MRI, Iceland. No evidence of an abundance-occupied area relationship was found for overwintering ISS herring. The black line is the fitted curve from the non-significant linear regression of SSN against the number of occupied cells ($R^2 = 0.001$, $p = 0.885$).



## References

Guðmundsdóttir, A. and Sigurðsson, Þ. 2004. The autumn and winter fishery and distribution of the Icelandic summer-spawning herring during 1978–2003. – Hafrannsóknastofnunin Fjölrit 104: 1–42.

Óskarsson, G. J. 2009. Variation in spatial distribution and migration of Icelandic summer-spawning herring. – ICES J. Mar. Sci. 66: 1762–1767.

**Appendix 9: Notes on the modelling approach**

The mixed effects models we fit in this paper fall broadly within the class of 'empirical' statistical models as defined by Levins (1966). These types of models are in essence correlative, although they may have mechanistic underpinnings related to the fundaments of Grinnellian and Eltonian niches (Hutchinson 1957, Soberón 2007, Beale et al. 2014). In lieu of the oft-lacking, detailed physiological knowledge needed for parameterization of an exciting new family of process-based models (e.g. Freitas et al. 2010, Jørgensen et al. 2012, Teal et al. 2012, see Peck et al. in press for a review), correlative models, which tend to compromise generality for realism and precision (Levins 1966, Dickey-Collas et al. 2014), remain widely used in ecology to explore the nature of relationships between species' distributions and biotic and abiotic factors, to build hypotheses and to guide management decisions (Guisan and Thuiller 2005, Elith and Leathwick 2009, Robinson et al. 2011).

Increasing recognition of the role of demographic structure, dispersal and density-dependence in shaping fish distribution patterns has motivated recent attempts to incorporate these processes explicitly (Cheung et al. 2009, Loots et al. 2010, Planque et al. 2011, Ciannelli et al. 2012). Moreover, regression models including time-lagged covariates, which provide insights into how the past may impact the present (e.g. Rindorf and Lewy 2006), and those in which covariate coefficients can vary in space and/or time, have proved valuable in understanding the interplay between density-dependent and density-independent controls on observed distributions (Bartolino et al. 2011, Ciannelli et al. 2012). Whilst still not allowing causation to be inferred directly, this class of models implicitly integrate mechanistic processes in their formulation, and hence occupy a space between environmental envelope and process-based models (Beale and Lennon 2012, Peck et al. in press).

We built our models in line with these ideas. By linking measures of distribution history, output from a spatially-explicit, individual-based model of zooplankton biomass, fine scale environmental fields and estimates of local fishing intensity, we fitted stationary and time-varying coefficient GLMMs for ISS herring occurrence across a 23-year time series. Correlations between the relative influence of these factors across years and time series of demographic parameters were then examined *post-hoc*, providing a basis for model validation to held-out observations one-year ahead. Our models were fitted in a Bayesian framework in R-INLA, using the SPDE approach to capture spatial and temporal dependence in the data (Rue et al. 2009, Lindgren et al. 2011). The merits of the Bayesian approach for this type of hierarchical model are many (Gelfand et al. 2006, Gelman and Hill 2007, Royle et al. 2007). Without reviewing these exhaustively here (see Elderd and Miller 2016 for a comprehensive appraisal), we highlight the inherent way in which random effects are handled as parameters of interest, resulting in fully specified probability distributions from which information on the intensity and uncertainty of the effects can be drawn; the option to incorporate prior knowledge based on empirical data or theory; and the ability to robustly quantify and propagate uncertainty through all modelling stages. Model fitting using INLA is computationally efficient, and provides accurate approximations of the posterior marginal distributions of model parameters that show high concordance with Markov chain Monte Carlo (MCMC) simulations (Rue and Martino 2007, Rue et al. 2009, Held et al. 2010). Since Lindgren and colleagues proved that a continuously indexed Gaussian field described by a Matérn covariance function can be represented as a discretely indexed GMRF (Rue and Held 2005, Lindgren et al. 2011), rapid development of the SPDE approach within R-INLA has facilitated fitting of an expanding suite of hierarchical spatial and spatiotemporal models to spatial point patterns (Krainski et al. 2016). This approach has recently proven useful in

analyses of georeferenced fisheries datasets, which are often data-rich and where inference at the scale of point locations, rather than grids, is required (e.g. Cosandey-Godin et al. 2015, Ward et al. 2015, Ono et al. 2016).

One of the well-noted criticisms of correlative species distribution models (Elith and Leathwick (2009) for a review of different methods) has been their inability to adequately account for residual autocorrelation in space and/or time. This situation that can violate independence assumptions in regression models, leading to inference errors and/or misrepresentation of covariate importance (Legendre 1993, Dormann 2007, Beale et al. 2010). The SPDE approach considers these correlation structures directly, and allows great flexibility in their specification (e.g. Cosandey-Godin et al. 2015). In our space-time models for example, we specified temporally-independent (time-indep), or temporally-evolving (time-corr) annual realizations of spatially-structured error terms. As wintering herring displayed varying persistence in their spatial distribution from year to year (Fig. 2), our aim was to gain insight into if, and how $\omega_{i,t-1}$ might influence $\omega_{i,t}$. Although model performance did not alter greatly (Table 2), the time-indep structure was preferred for all models. This is most likely due to inclusion of time-lagged covariates (i.e. $\text{distrib}_{t-1}$, $\text{counts}_{t-1}$), the former of which was highly significant in all cases, and captured well the occurrence pattern of the previous year.

We specified covariates as additive effects only in these models, but did allow for varying degrees of non-linearity and temporal non-stationarity in occurrence-covariate relationships. Whilst acknowledging that important interactions among predictors (e.g. environment and fishing intensity – Planque et al. (2010)) may have been overlooked, our decision reflects an attempt to balance model complexity with meaningful ecological inference (Merow et al.

2014). Hence, we placed priority on deriving biologically-realistic functional forms that could also vary in time. We found that including quadratic terms for the environmental covariates improved model fit compared with linear specifications alone, or where covariates were represented by penalized regression splines (Table 2), although most relationships approached linearity (Fig. 3). As the wintering stock was often clustered tightly in space, we also did not consider models with spatially-varying coefficients (e.g. Bacheler et al. 2009, Bartolino et al. 2011, Ciannelli et al. 2012). At the spatial scales of our observations, we assumed that any effect of a particular covariate would be imparted roughly equally across the space encompassing all herring schools encountered. This assumption is unlikely to hold if the occupied range expands, for example, during the spring feeding period, or if various ontogenetic stages, inhabiting geographically or environmentally disparate areas, are included in the models (see Bartolino et al. 2011 for an example). In these cases, inclusion of spatially non-stationary terms would likely provide important new insights.

A key limitation of our analysis relates to the lack of age-disaggregated or spatially-standardized catch or survey data available during our temporal window. Because of this, we were forced to consider demographic factors in a non-spatial, correlative context (i.e., estimates across the entire stock for each year), and were unable to incorporate the singular or interactive effects of density-dependence and age-structure directly within the model formulation. Although our results suggest that density-dependence is unlikely to play a major role in governing winter occurrence in herring (see Appendix 8, Fig. A8), and that population size may influence spatial persistence in wintering area use, georeferenced data on age-structure of each fishing event or survey record would have allowed direct tests of hypotheses around age-related differences in environmental preference, susceptibility to fishing pressure and the tendency to follow traditions and return to previously-used wintering sites. This type

of data is available for many other herring stocks, and ongoing work is focused on exploring these ideas.

Our models were specific to wintering ISS herring, limiting their generality. However, the approach used, and the covariates created, are easily adaptable to other herring stocks and species for which questions on the drivers and scales of conservatism or homing remain open. Bolstered by the strong congruence between modelled and observed temperature, salinity and flow fields in Icelandic waters (Logemann et al. 2013), the 23-year dataset we analyzed represents a substantial compilation of georeferenced records on the environmental conditions experienced by wintering ISS herring. The model outputs therefore provide a basis for identifying physiological thresholds that can be used to develop more informative priors and guide variable selection in future regression models (Simpson et al. 2015, Authier et al. 2017), or to aid parameterization of mechanistic models (Teal et al. in press). We agree with Rochette et al. (2013) who advocate a hierarchical Bayesian framework as an appealing platform upon which to meld different types of data and models together, making it possible to assimilate the processes acting on different life-history phases within the one 'full life cycle' model. Such a model in under development for NSS herring in the Norwegian and Barents Seas (Utne and Huse 2012, Huse 2016) and we see potential for the types of models developed here to contribute to it.



**References**

Authier, M. et al. 2017. Variable selection and accurate predictions in habitat modelling: a shrinkage approach. – Ecography 40: 549–560.

Bacheler, N. M. et al. 2009. Density-dependent, landscape, and climate effects on spawning distribution of walleye pollock *Theragra chalcogramma*. – Mar. Ecol. Prog. Ser. 391: 1–

12.

Bartolino, V. et al. 2011. Ontogenetic and sex-specific differences in density-dependent habitat selection of a marine fish population. – Ecology 92: 189–200.

Beale, C. M. and Lennon, J. J. 2012. Incorporating uncertainty in predictive species distribution modelling. – Phil. Trans. R. Soc. B 367: 247–258.

Beale, C. M. et al. 2010. Regression analysis of spatial data. – Ecol. Lett. 13: 246–264.

Beale, C. M. et al. 2014. A new statistical framework for the quantification of covariate associations with species distributions. – Methods Ecol. Evol. 5: 421–432.

Cheung, W. W. L. et al. 2009. Projecting global marine biodiversity impacts under climate change scenarios. – Fish Fish. 10: 235–251.

Ciannelli, L. et al. 2012. Non-additive and non-stationary properties in the spatial distribution of a large marine fish population. – Proc. R. Soc. B 279: 3635–3642.

Cosandey-Godin, A. et al. 2015. Applying Bayesian spatiotemporal models to fisheries bycatch in the Canadian Arctic. – Can. J. Fish. Aquat. Sci. 12: 1–12.

Dickey-Collas, M. et al. 2014. Hazard warning: model misuse ahead. – ICES J. Mar. Sci. 71: 2300–2306.

Dormann, C. F. 2007. Effects of incorporating spatial autocorrelation into the analysis of species distribution data. – Global Ecol. Biogeogr. 16: 129–138.

Elderd, B. D. and Miller, T. E. X. 2016. Quantifying demographic uncertainty: Bayesian methods for integral projection models. – Ecol. Monogr. 86: 125–144.

Elith, J. and Leathwick, J. 2009. Species distribution models: ecological explanation and prediction across space and time. – Annu. Rev. Ecol. Evol. Syst. 40: 677–697.

Freitas, V., et al. 2010. Temperature tolerance and energetics: a dynamic energy budget-based comparison of North Atlantic marine species. – Phil. Trans. R. Soc. B 365: 3553–65.

Gelfand, A. E. et al. 2006. Explaining species distribution patterns through hierarchical modeling. – Bayesian Anal. 1: 41–92.

Gelman, A. and Hill, J. 2007. Data analysis using regression and multilevel/hierarchical models. – Cambridge University Press.

Guisan, A. and Thuiller, W. 2005. Predicting species distribution: offering more than simple habitat models. – Ecol. Lett. 8: 993–1009.

Held, L. et al. 2010. Posterior and cross-validatory predictive checks: A comparison of MCMC and INLA. – In: Kneib, T. and Tutz, G. (eds), Statistical modelling and regression structures. Physica-Verlag, pp. 91–110.

Hutchinson, G. E. 1957. Concluding remarks. – Cold Spring Harbor Symposium on Quantitative Biology 22: 415–427.

Jørgensen, C. et al. 2012. Conservation physiology of marine fishes: advancing the predictive capacity of models. – Biol. Lett. 8: 900–903.

Krainski, E. T. et al. 2016. The R-INLA tutorial on SPDE models. – Norwegian University of Science and Technology, Trondheim, Norway.

Legendre, P. 1993. Spatial autocorrelation: trouble or new paradigm? – Ecology 74: 1659–1673.

Levins, R. 1966. The strategy of model building in population biology. – Am. Sci. 54: 421–431.

Lindgren, F. et al. 2011. An explicit link between Gaussian fields and Gaussian Markov random fields: the stochastic partial differential equation approach. – J. R. Stat. Soc. 73: 423–498.

Logemann, K. et al. 2013. The circulation of Icelandic waters – a modelling study. – Ocean Sci. 9: 931–955.

Loots, C. et al. 2010. What controls the spatial distribution of the North Sea plaice spawning

population? Confronting ecological hypotheses through a model selection framework. – ICES J. Mar. Sci. 67: 244–257.

Merow, C. et al. 2014. What do we gain from simplicity versus complexity in species distribution models? – Ecography 37: 1267–1281.

Ono, K. et al. 2016. Space-time investigation of the effects of fishing on fish populations. – Ecol. Appl. 26: 392–406.

Peck, M. A. et al. in press. Projecting changes in the distribution and productivity of living marine resources: a critical review of the suite of modelling approaches used in the large European project VECTORS. – Estuar. Coast. Shelf Sci. doi:10.1016/j.ecss.2016.05.019.

Planque, B. et al. 2010. How does fishing alter marine populations and ecosystems sensitivity to climate? – J. Mar. Syst. 79: 403–417.

Planque, B. et al. 2011. Uncertainties in projecting spatial distributions of marine populations. – ICES J. Mar. Sci. 68: 1045–1050.

Rindorf, A. and Lewy, P. 2006. Warm, windy winters drive cod north and homing of spawners keeps them there. – J. Appl. Ecol. 43: 445–453.

Robinson, L. M. et al. 2011. Pushing the limits in marine species distribution modelling: lessons from the land present challenges and opportunities. – Global Ecol. Biogeogr. 20: 789–802.

Rochette, S. et al. 2013. A hierarchical Bayesian model for embedding larval drift and habitat models in integrated life cycles for exploited fish. – Ecol. Appl. 23: 1659–1676.

Royle, J. et al. 2007. Hierarchical spatial models of abundance and occurrence from imperfect survey data. – Ecol. Monogr. 77: 465–481.

Rue, H. and Held, L. 2005. Gaussian Markov random fields: theory and applications. Monographs on statistics and applied probability volume 104. – Chapman & Hall.

Rue, H. and Martino, S. 2007. Approximate Bayesian inference for hierarchical Gaussian Markov random fields models. – J. Stat. Plan. Inference 137: 3177–3192.

Rue, H. et al. 2009. Approximate Bayesian inference for latent Gaussian models by using integrated nested Laplace approximations. – J. R. Stat. Soc. B 71: 319–392.

Simpson, D. P. et al. 2015. Penalising model component complexity: a principled, practical approach to constructing priors. – arXiv 1403.4630.

Soberón, J. 2007. Grinnellian and Eltonian niches and geographic distributions of species. – Ecol. Lett. 10: 1115–1123.

Teal, L. R. et al. 2012. Bio-energetics underpins the spatial response of North Sea plaice (*Pleuronectes platessa* L.) and sole (*Solea solea* L.) to climate change. – Glob. Change Biol. 18: 3291–3305.

Teal, L. R. et al. in press. Physiology-based modelling approaches to characterize fish habitat suitability: their usefulness and limitations. – Estuar. Coast. Shelf Sci. doi:10.1016/j.ecss.2015.11.014.

Ward, E. J. et al. 2015. Using spatiotemporal species distribution models to identify temporally evolving hotspots of species co-occurrence. – Ecol. Appl. 25: 2198–2209.

**Appendix 10: Fish and mammal predation on herring**

Humans are but one of herring's many predators. Across their distributional range, herring aggregations are targeted by demersal and pelagic fishes, in addition to several species of seals, whales and seabirds (Read and Brownstein 2003, Pitcher et al. 1996, Similä et al. 1996, Nøttestad and Axelsen 1999, Overholtz and Link 2007, Guse et al. 2009, Víkingsson et al. 2014). Herring have developed complex behavioral strategies to combat this; classic examples including diurnal vertical migration (Dommasnes et al. 1994) and extended residence in deep waters, that whilst potentially energetically expensive (Huse and Ona 1996) are suggested as an adaptive response to visual predators like Atlantic cod (*Gadus morhua*) (Langård et al. 2014), surface-feeding fin whales (*Balaenoptera physalus*) (Nøttestad et al. 2002) and killer whales (*Orcinus orca*) (Similä 1997). *In-situ* observations of killer whale-herring interactions on wintering grounds in Norway have shed further light on the diversity of predator-evasion responses employed by herring schools (Nøttestad 1998, Nøttestad and Axelsen 1999), and the cooperative tactics used by killer whales to overcome such responses (Similä 1997, Domenici et al. 2000).

In Icelandic waters, killer whales specialize on wintering ISS herring, and large numbers of these whales are often present on the wintering grounds between December and March (Samarra and Foote 2015). The ability of killer whales to influence herring schooling behaviour is very real (Nøttestad and Axelsen 1999). However, as herring are typically established on wintering grounds by early October (pre-dating killer whale arrival – Samarra and Foote 2015), and wintering areas are not vacated once colonized (ICES 2014, authors' personal observation), we propose that any displacement by killer whale foraging would occur mainly at localized scales. For these reasons, and due to data scarcity, we did not

include killer whale occurrence or density in our analysis. We stress however, that information on arrival times may help expose the evolutionary and contemporary risks herring face in following traditions and returning to the same, predator-rich, wintering grounds.

**References**

Domenici, P. et al. 2000. Killer whales (*Orcinus orca*) feeding on schooling herring (*Clupea harengus*) using underwater tail-slaps: kinematic analyses of field observations. – J. Exp. Biol. 203: 283–294.

Dommasnes, A. et al. 1994. Reduced oxygen concentrations in herring wintering areas. – ICES J. Mar. Sci. 51: 63–69.

Guse, N. et al. 2009. Diet of red-throated divers *Gavia stellata* reflects the seasonal availability of Atlantic herring *Clupea harengus* in the southwestern Baltic Sea. – J. Sea Res. 62: 268–275.

Huse, I. and Ona, E. 1996. Tilt angle distribution and swimming speed of overwintering Norwegian spring spawning herring. – ICES J. Mar. Sci. 53: 863–873.

ICES. 2014. Advice for 2014/2015 Herring in Division Va (Icelandic summer-spawning herring). ICES Advice 2014, Book 2:1–7, Copenhagen, Denmark.

Langård, L. et al. 2014. State-dependent spatial and intra-school dynamics in pre-spawning herring *Clupea harengus* in a semi-enclosed ecosystem. – Mar. Ecol. Prog. Ser. 501: 251–263.

Nøttestad, L. 1998. Extensive gas bubble release in Norwegian spring-spawning herring (*Clupea harengus*) during predator avoidance. – ICES J. Mar. Sci. 55: 1133–1140.

Nøttestad, L. and Axelsen, B. E. 1999. Herring schooling manoeuvres in response to killer whale attacks. – Can. J. Fish. Aquat. Sci. 77: 1540–1546.

Nøttestad, L. et al. 2002. How whales influence herring school dynamics in a cold-front area of the Norwegian Sea. – ICES J. Mar. Sci. 59: 393–400.

Overholtz, W. J. and Link, J. S. 2007. Consumption impacts by marine mammals, fish, and seabirds on the Gulf of Maine – Georges Bank Atlantic herring (*Clupea harengus*) complex during the years 1977-2002. – ICES J. Mar. Sci. 64: 83–96.

Pitcher, T. J. et al. 1996. Adaptive behaviour of herring schools in the Norwegian Sea as revealed by high-resolution sonar. – ICES J. Mar. Sci. 53: 449–452.

Read, A. J. and Brownstein, C. R. 2003. Considering other consumers: fisheries, predators, and Atlantic herring in the Gulf of Maine. – Conserv. Ecol. 7: 1–12.

Samarra, F. I. P. and Foote, A. D. 2015. Seasonal movements of killer whales between Iceland and Scotland. – Aquat. Biol. 24: 75–79.

Similä, T. 1997. Sonar observations of killer whales (*Orcinus orca*) feeding on herring schools. – Aquat. Mamm. 23.3: 119–126.

Similä, T. et al. 1996. Occurrence and diet of killer whales in northern Norway: seasonal patterns relative to the distribution and abundance of Norwegian spring-spawning herring. – Can. J. Fish. Aquat. Sci. 53: 769–779.

Víkingsson, G. A. et al. 2014. Recent changes in the diet composition of common minke whales (*Balaenoptera acutorostrata*) in Icelandic waters. A consequence of climate change? – Mar. Biol. Res. 10: 138–152.